

**“Combined targeting of the Menin-MLL chromatin  
regulatory complex and the FLT3 tyrosine kinase as a  
novel therapeutic approach against *NPM1*<sup>mut</sup> and *MLL-r*  
leukemia with concurrent *FLT3* mutation”**

Dissertation

zur Erlangung des Grades

Doktor der Naturwissenschaften

Am Fachbereich Biologie

der Johannes Gutenberg-Universität

in Mainz

vorgelegt von

**Margarita Dzama**

geb. am 03.11.1992 in Dubna (Russland)

Mainz, 2021



## Abstract

Acute myeloid leukemia (AML) is a heterogeneous clonal disorder characterized by aberrant proliferation and blocked differentiation of immature myeloid cells eventually causing bone marrow failure. *NPM1* mutant (*NPM1<sup>mut</sup>*) and *MLL*-rearranged (*MLL-r*) acute myeloid leukemia subtypes, characterized by aberrant expression of *HOX* and *MEIS1* transcription factors, commonly harbor concurrent activating mutations in the FMS-like tyrosine kinase receptor (*FLT3*). It has been previously demonstrated that the interaction of Menin and MLL (*MLL1*, *KMT2A*) proteins represents a dependency in *NPM1<sup>mut</sup>* and *MLL-r* AML, and therefore a potential therapeutic opportunity against these leukemias. The aim of this study was to investigate the effect of pharmacological inhibition of Menin-MLL complex on *FLT3* expression and *FLT3* mutant signaling as well as to assess the therapeutic potential of combined Menin-MLL and *FLT3* targeting.

In order to explore transcriptional changes associated with disruption of the Menin-MLL complex, RNA-sequencing (RNA-seq) of *NPM1<sup>mut</sup>* OCI-AML3 and *MLL-r* MOLM13 and MV411 leukemia cells following inhibition with the small-inhibitory molecule MI-503 was performed. *MEIS1* and its target gene *FLT3* were found among the most significantly downregulated genes. I confirmed these results in various human *NPM1<sup>mut</sup>* or *MLL-r* cell lines and in primary murine *Npm1<sup>mut/+</sup>Flt3<sup>mut/+</sup>* leukemia cells. Moreover, I found a profound suppression of the *FLT3* mutant allele following MI-503 treatment in the *MLL-r* MV411 and MOLM13 cells using specific primers followed by quantitative PCR (qPCR). I also observed a significant decrease in *FLT3* protein expression upon MI-503 treatment in all tested *NPM1<sup>mut</sup>* and *MLL-r* AMLs as assessed by FACS. Using chromatin immunoprecipitation followed by qPCR (ChIP-qPCR) I could demonstrate that inhibition of Menin and MLL interaction significantly reduces the binding of both proteins to the *MEIS1* gene.

Next, I evaluated the therapeutic potential of combined Menin-MLL and *FLT3* inhibition in the *FLT3*-ITD positive *MLL-r* and *NPM1<sup>mut</sup>* leukemias. I found synergistic anti-proliferative activity accompanied by enhanced apoptosis upon combined treatment with MI-503 and the specific *FLT3* inhibitor Quizartinib compared to single-drug treatment or vehicle control in human MV411 and MOLM13 cells. For murine *Npm1<sup>mut/+</sup>Flt3<sup>mut/+</sup>* leukemia cells, I used the multi-tyrosine kinase inhibitor Ponatinib as a combination partner for MI-503 in these cells as these cells harbor the F692L gatekeeper mutation that conveys drug resistance to most *FLT3* inhibitors, including Quizartinib. Again, similar synergistic suppression of proliferation and

colony formation as well as significantly enhanced apoptosis were observed. Similar results were obtained when MI-503 was combined with another FLT3 inhibitor - Gilteritinib, which was recently approved by U.S. Food and Drug Administration (FDA) and European Medicines Agency (EMA). Human HL-60 and NB4 cells, or the murine *Hoxa9-Meis1*-transformed cells that served as negative controls (all wildtype for *NPM1*, *MLL*, *FLT3*) were not affected by single drug or combinatorial treatment.

To investigate the mechanism of drug synergy I then evaluated the level of phosphorylated (activated) FLT3 (pFLT3) by immunoblotting and flow cytometry. As expected, I observed reduced pFLT3 upon direct FLT3 inhibition and found decreased total FLT3 and pFLT3 with MI-503 monotreatment. The most pronounced pFLT3 reduction was observed with combined Menin-MLL and FLT3 inhibition, most likely reflecting the joint effect of direct pFLT3 inhibition with Quizartinib or Ponatinib treatment and transcriptional suppression of total FLT3 with MI-503 treatment. The observed anti-leukemic effects were confirmed by combining a recently developed second-generation Menin-MLL inhibitor, VTP-50469, that is under first clinical investigation (NCT04065399), with FLT3 inhibition as well as by performing knockdown of Menin using short hairpin RNAs, followed with Quizartinib treatment.

The phosphorylation of FLT3 downstream signaling proteins such as STAT5 (pSTAT5) and ERK1/2 (pERK1/2) was also more affected by combined Menin-MLL and FLT3 inhibition compared to the single-drug treatment. Moreover, transcriptional profiling revealed a dramatic downregulation of STAT5A-dependent genes upon combinatorial treatment compared to single-drug or vehicle controls in MV411.

Ectopic expression of *Meis1* alone or together with *Hoxa9* in the *Npm1<sup>mut/+</sup>Flt3<sup>ITD/+</sup>* cells resulted in upregulation of *Flt3* gene expression and partially rescued the anti-proliferative effect of both Menin-MLL inhibition alone and combined Menin-MLL and FLT3 inhibition.

Primary AML cells harvested from patients with *NPM1<sup>mut</sup> FLT3<sup>mut</sup>* AML showed significantly better responses to combined Menin-MLL and FLT3 inhibition than to single-drug or vehicle control treatment while AML cells with wildtype *NPM1*, *MLL*, and *FLT3* were not affected by any of the two drugs. The blast-colony formation of primary human leukemia cells, as well as murine *Npm1<sup>mut/+</sup>Flt3<sup>ITD/+</sup>*, was also most significantly abrogated with the drug combination versus all other treatment groups.

Next, I evaluated the therapeutic effect of combined Menin-MLL and FLT3 inhibition in an MV411-derived leukemic xenograft murine model *in vivo*. I detected a significantly reduced

leukemia burden defined by bone marrow engraftment after 14 days of treatment in mice treated with the combination of both inhibitors versus single-drug or vehicle treated animals. In a separate experiment, animals that had been treated with the combination of drugs also showed a significant survival advantage compared to the groups treated with a single drug or vehicle.

In summary, combined Menin-MLL and FLT3 inhibition has synergistic on target activity against mutant FLT3 signaling in *NPM1<sup>mut</sup>* or *MLL-r* leukemias *in vitro* and *in vivo*. This concept may represent a novel therapeutic opportunity against these AMLs harboring a prognostically adverse *FLT3-ITD*, and is already available for clinical testing.

## Table of contents

1.1. Acute myeloid leukemia (AML).....	9
1.2. AML classification .....	9
1.3. Genetic risk stratification by genetics of AML.....	11
1.4. Current treatment concept.....	13
1.5. The Menin-MLL complex in normal hematopoiesis .....	14
1.6. The role of the Menin-MLL complex in <i>MLL</i> -rearranged and <i>NPM1</i> <sup>mut</sup> leukemia .....	15
1.7. Role of FLT3 in normal hematopoiesis and AML .....	17
1.8. Aim of the study.....	20
2. Materials and Methods .....	21
2.1. Materials .....	21
2.1.1. Laboratory equipment .....	21
2.1.2. Laboratory consumables .....	22
2.1.3. Chemical and biological reagents.....	23
2.1.4. Commercial kits.....	26
2.1.5. Antibodies .....	26
2.1.6. Cell lines.....	27
2.1.7. Cell culture media and supplements.....	28
2.1.8. Buffers .....	28
2.1.9. Primers .....	30
2.2. Methods.....	31
2.2.1. Preparation of small molecule inhibitor solutions.....	31
2.2.2. Cell Culture and Cell Lines .....	31
2.2.3. Primary AML blast cells, co-culture assay, and colony-formation assay .....	31
2.2.4. <i>In vitro</i> cell viability assay and calculation of drug synergism .....	32
2.2.5. Chromatin immunoprecipitation (ChIP).....	33
2.2.6. Analysis of apoptotic cell death by Annexin V staining .....	34
2.2.7. Cytologic staining .....	34
2.2.8. RNA purification, cDNA synthesis, and quantitative real-time PCR (qRT-PCR) .....	34
2.2.9. Western blotting .....	35

2.2.10. Intra-cellular antibody staining followed by flow cytometry.....	36
2.2.11. Extra-cellular antibody staining followed by flow cytometry.....	36
2.2.12. Colony-forming assay .....	37
2.2.13. RNA sequencing .....	37
2.2.14. Gene Set Enrichment Analysis (GSEA).....	38
2.2.15. Retroviral overexpression of <i>Meis1</i> and <i>Meis1/Hoxa9</i> .....	38
2.2.16. Knockdown using shRNAs .....	39
2.2.17. AML Xenograft Model .....	39
2.2.18. Data Analysis and Statistical Methods .....	40
3. Results.....	42
3.1. Menin-MLL inhibition exerts anti-proliferative effects in <i>MLL</i> -rearranged and <i>NPM1</i> <sup>mut</sup> leukemia cells.....	42
3.2. <i>MEIS1</i> and <i>FLT3</i> transcription is uniformly suppressed upon Menin-MLL inhibition in <i>MLL</i> -rearranged and <i>NPM1</i> <sup>mut</sup> leukemia .....	44
3.3. Pharmaceutical disruption of the Menin-MLL complex decreases its binding to the <i>MEIS1</i> gene locus and is associated with downregulation of FLT3 protein expression .....	46
3.4. FLT3 inhibitors have anti-leukemic activity against <i>MLL</i> -r or <i>NPM1</i> <sup>mut</sup> leukemias that harbor a concurrent <i>FLT3</i> -ITD.....	48
3.5. Combined Menin-MLL and FLT3 inhibition has synergistic activity against <i>MLL</i> -r or <i>NPM1</i> <sup>mut</sup> leukemias that harbor a concurrent <i>FLT3</i> -ITD .....	50
3.6. Menin-MLL inhibition enhances FLT3 inhibitor mediated abrogation of phosphorylated FLT3 .....	53
3.7. Combined Menin-MLL and FLT3 inhibition suppress pFLT3 downstream signaling pathways.....	56
3.8. Ectopic <i>Meis1</i> and <i>Hoxa9</i> expression partially rescues the anti-proliferative effect of Menin-MLL and FLT3 inhibition .....	59
3.9. Synergistic anti-leukemic activity of combined Menin/FLT3 inhibition is confirmed with the more selective next-generation Menin-MLL inhibitor VTP50496.....	63
3.10. Combinatorial treatment suppresses primary <i>NPM1</i> <sup>mut</sup> <i>FLT3</i> <sup>ITD</sup> AML patient cells <i>in vitro</i> .....	67

3.11. Combined <i>in vivo</i> treatment significantly prolongs survival of <i>MLL-r FLT3</i> -ITD positive leukemic mice .....	69
4. Discussion .....	71
4.1. A necessity of combined treatment against AML.....	71
4.2. Potential and limitations of combined Menin-MLL and FLT3 inhibition .....	73
4.3. Regulation of <i>FLT3</i> gene transcription.....	75
4.4. FLT3 targeting as the main mechanism behind Menin-MLL and FLT3 synergism.....	75
4.5. Role of STAT5 and ERK1/2 in AML .....	76
4.6. The relation of Menin-MLL inhibition and <i>HOX</i> gene expression .....	78
4.7. Model of combined Menin-MLL and FLT3 inhibition .....	80
5. References .....	81
7. Appendix.....	94
7.1. List of Abbreviations .....	94
7.2. Table of common downregulated genes in MV411, MOLM13 and OCI-AML3.....	99

# 1. Introduction

## 1.1. Acute myeloid leukemia (AML)

Acute myeloid leukemia represents a heterogeneous group of neoplastic diseases characterized by increased proliferation and reduced differentiation of immature progenitor cells of the myeloid lineage (myeloid blasts)<sup>1,2</sup>. These leukemic blasts accumulate in bone marrow and peripheral blood and overgrow healthy and functional cells, leading to severe infections, anemia, leukopenia, thrombocytopenia, and hemorrhage. According to the World Health Organization (WHO) classification system, AML is defined by the presence of 20% or more of bone marrow or peripheral blood cells<sup>3,4</sup>. Acute myeloid leukemia is the most common acute leukemia in the Western world with a median age at diagnosis of 69 years<sup>5</sup> and with a relatively unsatisfactory survival rate<sup>2,6,7</sup>. Currently, only 35-40% of the younger and 5-15% of elderly patients (> 60 years) can be cured<sup>2</sup>. AML can arise *de novo* or secondary to previous cytotoxic or radiation treatment (therapy-related AML), after hematopoietic disorder (secondary AML), or because of rare genetic disorders, that may predispose AML, such as Down syndrome, Ataxia-telangiectasia, Shwachman-Diamond syndrome, Fanconi anemia, and others.

## 1.2. AML classification

The first classification of different types of AML, named French-American-British (FAB) classification, was developed in 1976. It distinguished clinically and biologically different 8 subtypes, M0 through M7, based on integrated evaluation of histomorphological, molecular, and cytochemical characteristics of the leukemic cells<sup>8</sup>. Later, in 2001, the World Health Organization (WHO) presented a new classification system taking into account the genetic abnormalities along with morphologic, cytochemical, immunophenotypic, and clinical aspects. This classification was revised in 2008 and 2016 considering new scientific and clinical information<sup>3,4</sup>. The most recent 2016 WHO classification identifies 6 main categories of AML containing several distinct entities and subtypes (Table 1.1).

WHO acute leukemia and related neoplasms classification		
1	AML with recurrent genetic abnormalities	<ul style="list-style-type: none"> <li>- AML with <i>RUNX1-RUNX1T1</i></li> <li>- AML with <i>CBFB-MYH11</i></li> <li>- APL with PML-RARA</li> <li>- AML with <i>MLLT3-KMT2A</i></li> <li>- AML with <i>DEK-NUP214</i></li> <li>- AML with <i>GATA2, MECOM</i></li> <li>- AML (megakaryoblastic) with <i>RBM15-MKL1</i></li> <li>- Provisional entity: AML with <i>BCR-ABL1</i></li> <li>- AML with mutated <i>NPM1</i></li> <li>- AML with biallelic mutations of <i>CEBPA</i></li> <li>- Provisional entity: AML with mutated <i>RUNX1</i></li> </ul>
2	AML with myelodysplasia-related changes	
3	Therapy-related myeloid neoplasms	
4	AML not otherwise specified (NOS)	<ul style="list-style-type: none"> <li>- AML with minimal differentiation</li> <li>- AML without maturation</li> <li>- AML with maturation</li> <li>- Acute myelomonocytic leukemia</li> <li>- Acute monoblastic/monocytic leukemia</li> <li>- Pure erythroid leukemia</li> <li>- Acute megakaryoblastic leukemia</li> <li>- Acute basophilic leukemia</li> <li>- Acute panmyelosis with myelofibrosis</li> </ul>
5	Myeloid sarcoma	
6	Myeloid proliferations related to Down syndrome	<ul style="list-style-type: none"> <li>- Transient abnormal myelopoiesis</li> <li>- Myeloid leukemia associated with Down syndrome</li> </ul>

Table 1.1. Classification of acute leukemia and related neoplasms proposed by WHO in 2016<sup>4</sup>.

### 1.3. Genetic risk stratification by genetics of AML

Within the last decades, comprehensive next-generation sequencing (NGS) studies have significantly improved the understanding of the molecular pathogenesis of AML. Identification of genetic abnormalities was important for improving the classification and outcome prediction of AML and developing novel therapeutic approaches<sup>4,9</sup>. These studies have provided a broad list of recurrent cytogenetic and mutational abnormalities that are now considered potential driver events of AML pathogenesis<sup>10-13</sup>. The Cancer Genome Atlas (TCGA) Research Network completed the sequencing of the genomes of 200 patients with *de novo* AML and systematized the commonly mutated genes in 9 functional groups<sup>10,14</sup> (Figure 1.1). Deep sequencing efforts identified a total of 23 genes being significantly mutated and a median number of 5 and at least 2 genetic driver events to be present per AML case<sup>10,12,14,15</sup>. About 50% of AML patients displayed a normal karyotype with a lack of chromosomal abnormalities.

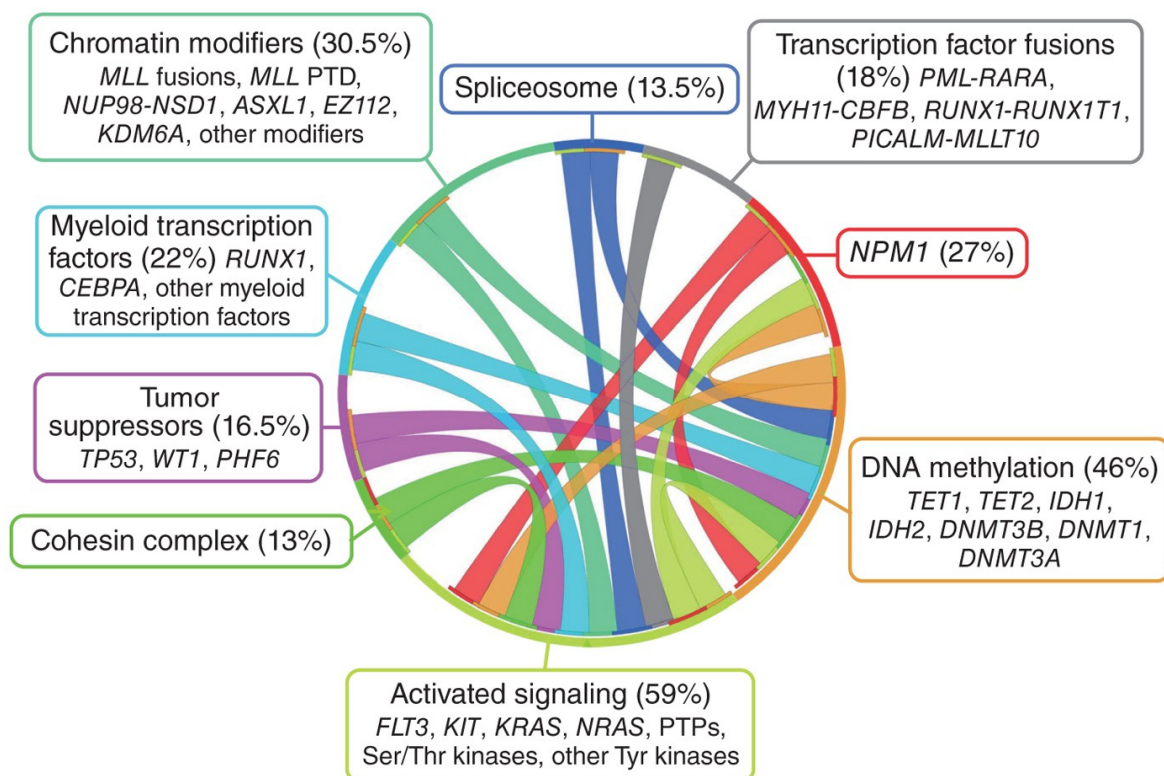


Figure 1.1. Scheme of functional categories of genes commonly affected in AML (according to the TCGA data set) from Chen et al., Nature Genetics 2013<sup>14</sup>. Colorful lines indicate correlation of mutations in different categories.

These studies also found nucleophosmin (*NPM1*) and the FMS-like tyrosine kinase 3 (*FLT3*) as the most commonly mutated genes in AML, each being affected in about one-third of

AML cases. Moreover, genetic abnormalities in genes encoding epigenetic regulators of transcription were detected in about two-thirds of AML cases<sup>10,15</sup>.

A more recent and comprehensive sequencing study of bone marrow samples from 1540 *de novo* AML patients identified driver mutations in 76 genes or genomic regions<sup>12</sup>. Similar to the previous study, the presence of at least 2 driver mutations per AML case in 86% of cases was detected. As personalized prognostication depends not only on the presence or absence of one specific mutation but also on the presence of concomitant mutations, this study assessed patterns of associated mutations. As a result, 11 mutually exclusive subgroups of AML were defined. The largest AML subgroup carried *NPM1* mutation, which was highly associated with some other mutations, for example, in *IDH2*, *DNMT3A* and *FLT3* genes. The presence of *FLT3*-ITD in patients with *NPM1* mutation showed a worse effect on survival<sup>12</sup>.

Treatment recommendations proposed by the European LeukemiaNet (ELN) initially in 2010 and later revised in 2017 integrated the prognostic value of genetic markers in AML<sup>9,16</sup>. The ELN categorizes AML patients into 3 groups: favorable, intermediate, and adverse risk categories. According to ELN, *NPM1* mutations are associated with a favorable prognosis<sup>9,17</sup>. However, the prognostic predicate of *NPM1* mutation is affected by additional mutations such as *DNMT3A*<sup>mut</sup>, *FLT3*-ITD, *NRAS*<sup>G12/G13</sup>, *IDH1*<sup>mut</sup> and *IDH2*<sup>R140</sup>, with *FLT3*-ITD being of particular interest as similar to the previous study its co-appearance alters the clinical outcome from a favorable to an intermediate group of risk<sup>9,12,18</sup> (Figure 1.2).

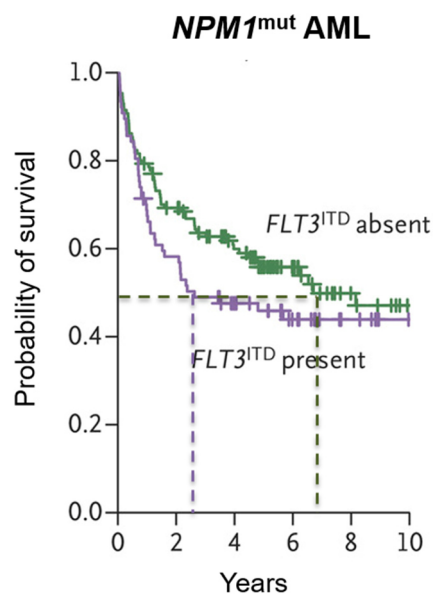


Figure 1.2. Kaplan-Maier curves for overall survival of patients in the presence or absence of *FLT3*-ITD in *NPM1*<sup>mut</sup> AML, adapted from Papaemmanuil et al., *NEJM*, 2016<sup>12</sup>. Dashed lines indicate survival of 50% patients.

#### 1.4. Current treatment concept

Despite our growing understanding of its pathogenesis, AML remains a therapeutic challenge. Curative treatment efforts still rely on intensive chemotherapy as a backbone which has been the standard approach for several decades<sup>9</sup>. Patients fit for intensive chemotherapy undergo induction therapy, including a standard combination of the so-called 7+3 regimen combining 7 days of continuous infusion of cytarabine (AraC) with short infusions of an anthracycline drug, mainly daunorubicin or idarubicin, on each of the first 3 days (intensive chemotherapy). Daunorubicin and idarubicin are both DNA topoisomerase II (Top II) inhibitors that inhibit the catalytic enzyme reaction needed for inducing and releasing DNA coils, which leads to DNA strand breaks and eventually to apoptosis of leukemia cells<sup>19</sup>. Cytarabine is a pyrimidine analog that intercalates DNA during S-phase with subsequent arrest of the replication fork and induction of DNA double-strand break<sup>20</sup>.

Patients achieving complete remission (CR), when the bone marrow presents less than 5% of blast cells and normal blood cell maturation is restored, will receive standard post-remission (consolidation) therapy in order to eliminate any remaining leukemia cells. This includes 2-4 cycles of intermediate cytarabine or allogeneic hematopoietic stem cell transplantation (allo-HSCT) for fit patients of the intermediate or high-risk ELN subgroups<sup>21,22</sup>. In general, current treatment options are predicated on clinical studies mostly performed on younger patients (<60 years) eligible for intensive chemotherapy, while median age of diagnosis is 69 years<sup>5</sup> with a survival rate of the elderly patients (> 60 years) being just 5-15%<sup>2</sup>. In addition, the lower performance status, the comorbidities arising with age and less tolerance to intensive chemotherapy put a bound to the intensive treatment options, or even make it not applicable at all for some patients<sup>5</sup>. For these reasons, finding less toxic treatment options is pivotal.

Hope arises from the introduction of mechanism-based targeted agents that utilize AML specific genetic abnormalities or epigenetic vulnerabilities<sup>23,24</sup>. Since 2017, 8 novel drugs were approved by the FDA for the treatment of AML<sup>25,26</sup>. One example is FLT3 inhibitors (details are described in chapter 1.7). For patients with *de novo* FLT3 mutated (*FLT3<sup>mut</sup>*) AML, the targeted therapy drug Midostaurin, a first-generation multi-targeted inhibitor of FLT3 phosphorylation, is given along with induction chemotherapy as it has been shown to improve survival rates<sup>27</sup>.

Moreover, various novel agents are currently undergoing clinical testing and many of them target epigenetic mechanisms. One promising therapeutic opportunity tackling an epigenetic vulnerability in AML is to inhibit the interaction between the histone

methyltransferase MLL (MLL1, KMT2A) and the chromatin-associated oncogenic co-factor Menin<sup>28-34</sup>.

### 1.5. The Menin-MLL complex in normal hematopoiesis

*MLL* (Myeloid/Lymphoid or Mixed-Lineage Leukemia Protein), the human homolog of the *Drosophila melanogaster* gene *trithorax*, encodes a histone-3-lysine-4 (H3K4) N-methyltransferase, a member of the methyltransferase SET/MLL family. In mammals, the members of SET/MLL family are presented by MLL (MLL1, KMT2A), MLL2 (KMT2D), MLL3 (KMT2C), MLL4 (KMT2B), SET1A (KMT2F), and SET1B (KMT2G) proteins. All 6 members contain a conserved C-terminal SET domain – a catalytic domain, which is important for H3K4 methyltransferase activity<sup>35-37</sup>. H3K4 mono-, di- and trimethylations (H3K4me1, H3K4me2 and H3K4me3, respectively) show slightly different genome-wide distribution patterns. H3K4me1 is mostly enriched at enhancers, H3K4me2 is more generally distributed throughout active genes, including transcription start sites (TSS), gene bodies and enhancers, and H3K4me3 predominantly marks TSS regions and promoters of actively transcribed genes<sup>35,36,38</sup>. MLL and MLL2 both write H3K4me3 marks, however, *Mll2* knockdown showed a reduction in H3K4me3 levels mainly at bivalent genes (H3K4me3 is present along with repressive H3K27me3 mark), suggesting its major role in maintaining H3K4me3 promoter enrichment in order to repel repression complexes at target genes<sup>38</sup>.

All MLL1-4 and SET1A-B methyltransferases form complexes with common protein partners, such as WDR5, RbBP5, ASH2L and DPY30. However, MLL and MLL2 can also uniquely interact with Menin and LEDGF proteins, where Menin plays the role of a molecular adaptor that tethers the MLL with chromatin-associated LEDGF<sup>39,40</sup>. Interestingly, loss of Menin or LEDGF decreases binding of MLL to target genes<sup>39,41-44</sup>.

Although MLL and MLL2 proteins are orthologues and have similar structures, deletion of murine *Mll* was shown to impede normal hematopoiesis, while *Mll2* knockdown did not reveal any effect on hematopoietic development<sup>45</sup>. In early hematopoietic progenitor cells, the MLL complex induces H3K4me3 at *HOX* genes, particularly *HOXA* genes<sup>45,46</sup> (Figure 1.4).

## 1.6. The role of the Menin-MLL complex in *MLL*-rearranged and *NPM1*<sup>mut</sup> leukemia

The *MLL* gene is a common target for chromosomal translocations, which are found in approximately 10% of AML cases in adults<sup>47,48</sup>. Chromosomal rearrangements at the *MLL* locus (11q23 chromosomal location) result in the fusion of the N-terminal part of MLL to one of more than 80 different partners forming direct fusion oncoproteins<sup>48,49</sup>. The fusion with one of nine common partners – AF4 (~36%), AF9 (~19%), ENL (~13%), AF10 (~8%), PTD (~5%), ELL (~4%), AF6 (~4%), EPS15 (~2%), and AF1Q (~1%) – comprises the majority of *MLL*-r leukemias in adult patients<sup>48,50,51</sup>. Of note, no chromosome translocations of the *MLL2* gene in leukemia have been detected to date<sup>45</sup>. MLL-fusion proteins play a role in the activation of leukemogenic gene expression that includes *MEIS1*, *PBX3*, and *MEF2C* transcription factors, that drive the leukemic transformation of hematopoietic stem or progenitor cells<sup>52-55</sup>, resulting in enhanced proliferation (Figure 1.4). The chromatin-modifying ability associated with MLL-fusion is different from the one promoted by wildtype (wt) MLL<sup>56</sup>. AF4, AF9, ENL and ELL fusion partners of MLL are also subunits of the super elongation complex (SEC), which plays an important role in transcriptional elongation. Recruitment of SEC by MLL-fusion proteins results in aberrant gene expression<sup>56</sup>. Moreover, SEC can engage with the H3K79 histone methyltransferase DOT1L<sup>57,58</sup>, which is solely catalyzing me1, me2 and me3 of H3K79, where me2 and me3 were shown to be associated with active gene transcription<sup>59,60</sup>.

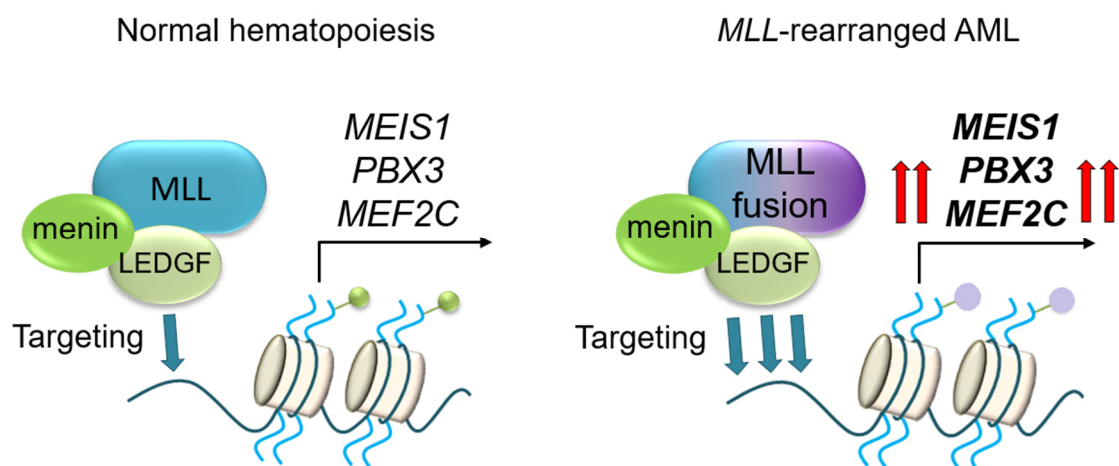


Figure 1.4. The Menin-MLL complex in normal hematopoiesis and AML. Green and purple pins represent different histone marks.

In *MLL*-r leukemia, the other intact wt *MLL* allele is usually preserved and expressed<sup>61</sup>. It has been assumed that WT MLL protein plays an important role in maintaining *MLL*-r leukemia

as MLL-fusion proteins lack the C-terminal SET domain of MLL protein and therefore unable to write H3K4me3, and yet target genes of MLL-fusion stayed methylated at H3K4. However, in rare cases, some patients still might have *MLL*-rearranged AML even though there is no MLL WT allele<sup>62</sup>. It has been also shown that the genetic deletion of the SET domain in MLL does not affect leukemogenesis, suggesting that histone-modifying activity of the MLL protein is dispensable for *MLL*-rearranged leukemia<sup>63</sup>. Moreover, knockdown of endogenous murine *Mll* did not have a significant impact on the survival of mice transduced with both *MLL-AF9* and *MLL-AF6* cells<sup>61</sup>.

The chromatin binding capability of both wildtype and the fusion MLL protein depends on the transcription co-factor Menin, which binds to the N-terminal end of MLL, retained in all MLL fusion proteins, and to the LEDGF protein, as mentioned earlier<sup>39,40</sup>. Pharmacological inhibition of the Menin-MLL interaction showed an anti-leukemic effect in *MLL-r* AML<sup>28-33,64</sup>, and two small-molecule inhibitory agents recently entered clinical trials (NCT04067336 and NCT04065399).

It has been demonstrated that the Menin-MLL interaction is also a dependency in a different leukemia subtype – *NPM1*<sup>mut</sup> leukemias. This group of leukemias represents the most common AML subtype in adults. *NPM1* is a multifunctional protein, which is mostly localized in the nucleolus and is thought to function as a molecular chaperone of proteins<sup>65,66</sup>. It is associated with regulation of mRNA processing<sup>67</sup>, ribosome biogenesis and transport to the cytoplasm<sup>68</sup>, participates in chromatin remodeling, centrosome duplication<sup>69</sup>, and maintenance of genomic stability<sup>70,71</sup>. Mutations in the *NPM1* gene are heterogeneous, however, the most common variant of mutation is represented by the insertion of four nucleotides at exon 12, which cause aberrant cytoplasmic dislocation of the *NPM1* mutant protein<sup>65,72</sup>.

Although *NPM1*<sup>mut</sup> leukemias lack an MLL-fusion protein, they still show aberrant expression of a leukemogenic gene program that resembles *MLL-r* leukemias, including *MEIS1*, *HOX*, *PBX3*, and *FLT3*<sup>73-75</sup>. Using CRISPR/Cas9 screening, our lab has previously demonstrated that Menin binding motif in MLL is required for *NPM1*<sup>mut</sup> AML<sup>75</sup>. Pharmacological disruption of Menin-MLL interaction using small-molecule inhibitors MI-2-2 and MI-503 displayed a dose-dependent reduction in cell proliferation of human and murine *NPM1*<sup>mut</sup> AML models similar to *MLL-r* leukemia. Menin-MLL inhibition also induced differentiation of leukemic cells and reversed the expression of *MEIS1*, *FLT3* and *HOX* genes in *NPM1*<sup>mut</sup> leukemia models (Figure 1.5). Moreover, our group has also previously demonstrated a significant survival advantage of

mice transplanted with *Npm1*<sup>mut</sup> cells upon MI-503 treatment compared to vehicle control group<sup>75</sup>. These findings were recently endorsed by another group that developed next-generation Menin-MLL inhibitors with better drug-like properties<sup>33,34</sup>.

Of note, our group has also shown that *FLT3*, a putative transcriptional MEIS1 target, is among the most dramatically downregulated genes upon Menin-MLL inhibition in *NPM1*<sup>mut</sup> AML<sup>75</sup> (Figure 1.5). This discovery is of particular interest as activating mutations within *FLT3* gene are important leukemic drivers.

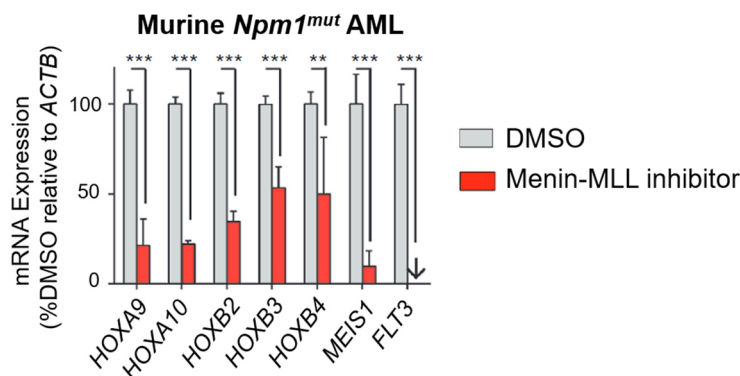


Figure 1.5. Gene expression in murine *Npm1*<sup>mut</sup> cells assessed on day 4 of Menin-MLL inhibition (MI-503, 2.5  $\mu$ mol/L) from Kühn et al., Cancer Discovery 2016<sup>75</sup>.

### 1.7. Role of FLT3 in normal hematopoiesis and AML

FLT3 receptor is a transmembrane protein, that plays an important role in cell proliferation during normal hematopoiesis<sup>76</sup>. FLT3 is a member of the class III receptor tyrosine kinase family that also includes platelet-derived growth factor receptor (PDGFR  $\alpha/\beta$ ), stem cell factor receptor (c-KIT), and macrophage colony-stimulating factor receptor (CSF1R)<sup>77</sup>. All have similar structural features, such as five immunoglobulin-like domains in the extracellular region, a transmembrane domain, an intracellular short juxtamembrane domain followed by the kinase domain, and a C-terminal domain<sup>78</sup> (Figure 1.6).

Upon binding of the FLT3 ligand to the extracellular domain, FLT3 undergoes conformational changes that promote and stabilize receptor dimerization causing the concomitant proximity of the kinase domains with eventual receptor autophosphorylation<sup>78,79</sup>. The autophosphorylation of the receptor enables the docking sites for signal-transducing effector molecules and activates multiple signaling pathways, including STAT5, PI3K/AKT, and RAS/ERK, promoting cell proliferation, differentiation or survival<sup>79,80</sup> (Figure 1.6).

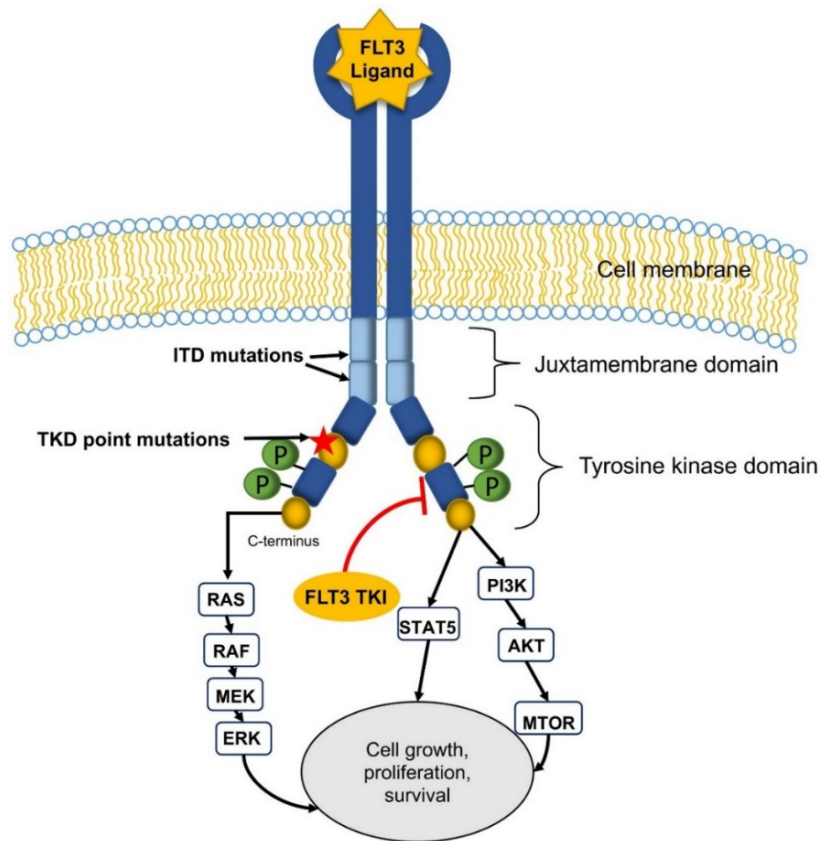


Figure 1.6. Schematic depiction of FLT3 receptor with indication of mutation sites and downstream pathways from Weis et al., *Critical Reviews in Oncology / Hematology* 2019<sup>81</sup>. “TKI” = “tyrosine kinase inhibitor”.

Activating mutations in the *FLT3* gene occur in approximately 30% of AML cases<sup>82,83</sup>. These mutations cause a continuous proliferation of blasts as the FLT3 receptor stays constitutively phosphorylated, and therefore activated<sup>79,82,83</sup>. The most common mutations are represented by the internal tandem duplication (ITD), arising in the juxtamembrane domain of FLT3 in approximately 20-30% of all AML cases, and point mutations in the tyrosine kinase domain (TKD), occurring in approximately 7-10% of all AML cases<sup>10,84-88</sup> (Figure 1.6). The location of ITD, as well as the size of the repetitive sequence, may vary starting from 3 bp up to hundreds of bp, but it never causes a frame-shift<sup>86,89</sup>.

It has been demonstrated that the FLT3 wild type (WT) and FLT3-ITD receptors regulate the RAS/ERK and PI3K/AKT downstream pathways in a similar way but the activation of STAT5 differs. In cells with FLT3 WT receptor, phosphorylated STAT5 does not bind to the DNA, while cells harboring FLT3-ITD showed elevated phosphorylation of STAT5 and its DNA-binding<sup>90,91</sup>. Both FLT3-ITD and FLT3-TKD result in constitutive activation of FLT3 signaling, however, there is a difference in signaling pathways they trigger. While FLT3-ITD activates downstream STAT5

pathway, including STAT5A<sup>92</sup>, PI3K/AKT and RAS/ERK pathways, FLT3-TKD mutations activate FLT3 signaling through AKT and ERK, but not STAT5<sup>79,93</sup>. However, activation of all these pathways causes cell proliferation and inhibition of apoptosis<sup>80,82,94-96</sup>.

Regulation of *FLT3* transcription in AML was shown to be regulated by several transcription factors, including HOXA9, PBX3 and their co-factor MEIS1, which are all highly expressed in both *MLL*-r and *NPM1*<sup>mut</sup> AML<sup>74,97,98</sup>.

*FLT3* is an important prognostic marker. *FLT3* mutations occur across all AML subtypes, but particularly enriched in *NPM1*<sup>mut</sup> AML (60%) and occur in *MLL*-r leukemias (10%)<sup>99-102</sup>. Along with detecting the presence of *FLT3* mutations in patients, it is also crucial to evaluate its allelic ratio (AR) to *FLT3* WT as it is modulating the prognostic impact of the mutation. Several studies have shown that the presence of a *FLT3*-ITD at a high AR (>0.5) is associated with lower complete remission (CR) rates and adverse overall treatment outcome<sup>103,104</sup>. Furthermore, it alters the relatively favorable *NPM1*<sup>mut</sup> AML subtype into an intermediate prognostic category<sup>16,89,103-105</sup>. While the prognostic impact of *FLT3*-TKD mutations has not been proven as negative as well as significantly beneficial on the overall survival of patients with *NPM1*<sup>mut</sup> AML<sup>84,96</sup>.

Importantly, FLT3 serves as a therapeutic target in AML, and two generations of FLT3 inhibitors targeting the FLT3 phosphorylation have been developed. The mechanism of action for FLT3 inhibitors is based on competition for the ATP binding site in the tyrosine kinase domain, what prevents phosphorylation of the receptor, and eventually, its activation<sup>106</sup>. The first-generation FLT3 inhibitors are less specific and potent and target a broad range of kinases, including c-KIT and PDGFR<sup>106,107</sup>. Most of the first-generation FLT3 inhibitors showed a limited anti-leukemic effect in monotherapy with suboptimal efficiency and unfavorable toxicity in patients with *de novo* AML<sup>107-109</sup>. However, one of them – Midostaurin (PKC412) – was shown to improve overall survival rates of patients with *de novo* *FLT3*<sup>mut</sup> AML when given in combination with intensive chemotherapy<sup>27</sup>. Second-generation FLT3 inhibitors that are more potent and selective, such as Quizartinib, Gilteritinib, and Crenolanib, showed high remission rates in relapsed/refractory *FLT3*-ITD-positive AML patients as single agents<sup>110-112</sup>. One of them, Gilteritinib, was recently approved for its treatment in the U.S. and Europe, however, none of the currently used FLT3 inhibitors showed long-term remissions as a single agent<sup>110,111</sup>. Therefore, the development of a curative treatment is mostly focused on combining these compounds with other treatment regimens<sup>109</sup>.

## 1.8. Aim of the study

Despite the expanding knowledge of disease mechanisms and the recent development of new treatment approaches, AML remains an unsolved medical problem associated with significant morbidity and high mortality in the affected patients. The presence of a *FLT3*-ITD at high AR alone or as a concomitant mutation indicates an intermediate to adverse clinical outcome. Considering that *FLT3* transcription has been previously shown to be consistently downregulated upon Menin-MLL inhibition in *NPM1*<sup>mut</sup> and *MLL-r* AML, I hypothesized that transcriptional targeting of *FLT3* via the pharmacological disruption of the Menin-MLL complex combined with inhibition of the *FLT3* receptor phosphorylation might have synergistic anti-leukemic activity in both leukemia subtypes having a concomitant *FLT3*-ITD. For this, I aimed to evaluate the effect of single and combined drug treatment of Menin-MLL and *FLT3* inhibitors *in vitro* and *in vivo*, as well as establish the mechanism of the observed synergy of combinatorial treatment.

## 2. Materials and Methods

### 2.1. Materials

#### 2.1.1. Laboratory equipment

Category	Model	Manufacturer
Centrifuges	5810R	Eppendorf, DE
	5415R	Eppendorf, DE
Electrophoresis	Power Supply PS 3002	Biometra, DE
Flow Cytometry	FACSCanto II	BD Biosciences, USA
Incubators	HeraCell 240 CO2 incubator	Thermo Fisher, USA
	HeraCell 240i CO2 incubator	Thermo Fisher, USA
Laminar Flow Cabinet	HeraSafe	Thermo Fisher, USA
	Tecnoflow 2F180-II GS	Integra Biosciences, USA
Microscope	CKX-41	VWR, USA
	EVOS M5000 imaging system	Thermo Fisher, USA
Nanodrop	Nanodrop One	Thermo Fisher, USA
PCR System	C1000 Thermal cycler	BIO-RAD, USA
	QuantStudio 3	Thermo Fisher, USA
	LightCycler 480	Roche, Switzerland
Pipette	Single-channel micropipette Transferpette	BRAND, DE
	Research Plus ES10, ES20, ES200, ES1000	Eppendorf, DE
	PipetBoy	Integra, DE
Sonicator	Bioruptor Plus	Diagenode, BE
Western Blotting	iBlot2 Gel Transfer device	Thermo Fisher, USA
	iBrightCL1000	Thermo Fisher, USA
	XCell SureLock Mini-Cell	Thermo Fisher, USA
Other equipment	FLUOstar OMEGA fluometer	BMG Labtech, DE
	A120S scale	Sartorius, DE
	AS scale	Kern, DE
	Biometra OV2 thermostat	Labetec, DE

	RS-RRS shaker	Phoenix instrument, DE
	3017 shaker	GFL, DE
	TXU vortex	VELP, USA
	ZX3 vortex	VELP, USA
	Surgical instruments	Roth, DE
	Waterbath Certomat WR	B. Braun, DE
	GeneQuant 100 spectrophotometer	General Electric, USA

### 2.1.2. Laboratory consumables

Category	Consumables	Manufacturer
Cell culture	Blunt end needles	StemCell, USA
	Non-treated culture dishes (35 mm)	Corning
	TC plate 96-well suspension	Greiner, DE
	TC plate 24-well suspension	Greiner, DE
	TC plate 12-well suspension	Greiner, DE
	TC plate 6-well suspension	Greiner, DE
	TC flask T75 standard	Greiner, DE
	TC flask T175 standard	Greiner, DE
	Sterile pipette 5 mL, 10 mL, 25 mL, 50 mL	Greiner, DE
	Square BioAssay Dish with Handles	Corning
Gels and transfer membranes	Bolt™ 10% Bis-Tris Plus Gels, 12-well	Thermo Fisher, USA
	Bolt™ 8% Bis-Tris Plus Gels, 12-well	Thermo Fisher, USA
	iBlot™ 2 Transfer Stacks, nitrocellulose, mini	Thermo Fisher, USA
Mouse handling	Mouse restrainer Tailveiner TV-150	MediLumine, USA
	Microvette with Lithium-Heparin 200 µl	Sarstedt, DE
	Syringes 30Gx1/2"	B. Braun, DE
	Tubes for injections 1mL	B. Braun, DE
	Feeding tube for oral gavage, 20 ga x 38 mm	Instech Laboratories, USA

PCR	MicroAmp Fast 96-well reaction	Life Technologies, USA
	MicroAmp Optical Adhesive Film	Life Technologies, USA
Pipette tips	Filter tips 10 $\mu$ L, 100 $\mu$ L, 300 $\mu$ L, 1000 $\mu$ L	Star Lab, DE
	Tip Stack Pack Filter tips 10 $\mu$ L, 200 $\mu$ L, 1000 $\mu$ L	Sarstedt, DE
Strainer and filters	Cell strainer 100 $\mu$ M	Falcon, USA
	Cell strainer 40 $\mu$ M, 70 $\mu$ M	Corning, USA
	Filter 0.22 $\mu$ m, 0.45 $\mu$ m	VWR, USA
Tubes	Eppendorf Safe-Lock Tubes 1.5 mL, 2 mL	Eppendorf, DE
	15 mL, 50 mL	Sarstedt, DE

### 2.1.3. Chemical and biological reagents

Product	Manufacturer
2-mercaptoethanol	Sigma, DE
(2-Hydroxypropyl)- $\beta$ -cyclodextrin	Sigma, DE
4',6-diamidino-2-phenylindole (DAPI)	Sigma, DE
A/G beads (50% slurry immunoglobulin (Ig) binding domains of both protein A and protein G coupled to sepharose)	Merck, DE
Bovine Serum Albumin (BSA) Fraction V	Pan-Biotech, DE
Cell Dissociation Buffer, enzyme-free, PBS	Gibco, USA
Cell Lysis Buffer (10x)	Cell Signaling
Complete (Protease inhibitor, 25x)	Sigma, DE
Deoxycholic acid	Sigma, DE
DEPC-Treated Water	Thermo Fisher, USA
Dimethyl sulfoxide (DMSO)	Sigma, DE
DMEM + GlutaMAX	Gibco, USA
dNTP Mix (10 mM each)	Biozym, DE
Dual color protein Standard	BIO-RAD, USA
Dulbecco's Phosphate Buffer Saline	Sigma, DE

ECL Prime Western Blotting Detection Reagent	Amersham Biosciences
ECL Western Blotting Detection Reagent	Amersham Biosciences
EDTA (0.5 M), pH 8.0	Thermo Fisher, USA
ERCC RNA Spike-In Mix	Thermo Fisher, USA
Ethanol absolute (99,8%)	Sigma, DE
FACS Flow	BD Biosciences, USA
Fetal bovine serum (FBS)	Thermo Fisher, USA
G 418-BC liquid (ready-to-use solution), sterile	Merck, DE
Gilteritinib (ASP2215)	Selleckchem, USA
Glycerol 87%	Roth, DE
Human G-CSF	Peprotech, USA
Human GM-CSF	Peprotech, USA
Human FLT3L (FLT3 ligand)	Peprotech, USA
Human IL3	Peprotech, USA
Human SCF	Peprotech, USA
IMDM	Gibco, USA
L-Glutamine (200mM)	Sigma, DE
MEM-alpha + Glutamax	Gibco, USA
Methanol 99,8%	Apoware, DE
Methocult M3234	StemCell, Canada
MethoCult™ H4435 Enriched	StemCell, Canada
MI-503 (menin-MLL inhibitor)	Selleckchem, USA
Milk powder	Roth, DE
Nonidet P40	Sigma, DE
NuPAGE™ MES SDS Running Buffer (20X)	Thermo Fisher, USA
NuPAGE™ MOPS SDS Running Buffer (20X)	Thermo Fisher, USA
Opti-MEM reduced serum medium 100mL	Thermo Fisher, USA
PEG400	Roth, DE
Penicillin/Streptomycin (P/S)	Sigma, DE
Paraformaldehyde (PFA, 37%)	Sigma, DE
Ponatinib (FLT3 inhibitor)	LC Laboratories, USA

Potassium chloride (KCl)	Roth, DE
Potassium dihydrogenphosphate (KH <sub>2</sub> PO <sub>4</sub> )	Roth, DE
PowerUp™ SYBR™ Green Master Mix	Thermo Fisher, USA
Precision Plus Protein™ WesternC™ Blotting Standards	BIO-RAD, USA
Protein assay dye reagent for Bradford assay	BIO-RAD, USA
Puromycin Dihydrochlorid	Roth, DE
Quizartinib (AC220, FLT3 inhibitor)	LC Laboratories, USA
Recombinant murine SCF	Peprotech, USA
Recombinant murine IL-3	Peprotech, USA
Recombinant murine IL-6	Peprotech, USA
Red Blood Cells lysis buffer	Qiagen, DE
Restore Western Blot Stripping Buffer	Thermo Fisher, USA
Retronectin (recombinant human fibronectin fragment)	Takara, Japan
RPMI 1640 + L-Glutamin	Gibco, USA
Sodium chloride (NaCl)	Roth, DE
Sodium dodecyl sulfate (SDS)	Roth, DE
Sodium hydroxide (NaOH)	Roth, DE
Sodium hydrogenphosphate (Na <sub>2</sub> HPO <sub>4</sub> )	Roth, DE
StemRegenin 1	StemCell, Canada
StemSpan™ SFEM	StemCell, Canada
SYBR Green 1 MasterMix	Roche, Switzerland
TaqMan™ Fast Advanced Master Mix	Thermo Fisher, USA
Xtreme Gene-9 Transfection reagent	Sigma, DE
Tris base	Roth, DE
Trypan Blue Solution, 0,4%	Gibco, USA
Trypsin/EDTA 0,05/0,02%	Sigma, DE
TWEEN-20	Sigma, DE
VTP-50469	Syndax, USA
Xtreme Gene-9 Transfection reagent	Sigma, DE

#### 2.1.4. Commercial kits

Product	Manufacturer
Annexin V Apoptosis Detection kit APC	eBioscience, USA
DNeasy Tissue Kit	Qiagen, DE
Mix2Seq Kit	Eurofins, DE
PCR-Purification Kit	Qiagen, DE
RevertAid H Minus First Strand cDNA Synthesis Kit	Thermo Fisher, USA
RNeasy Mini Kit + QIAshredder	Qiagen, DE
RNase-Free DNase Set	Qiagen, DE
Quant-iT™ RiboGreen™ RNA Assay Kit	Thermo Fisher, USA
QIAquick Gel Extraction Kit	Qiagen, DE

#### 2.1.5. Antibodies

##### 2.1.5.1. Antibodies for flow cytometry

Target	Clone	Dilution	Manufacturer
Annexin V Apoptosis APC-conjugated	-	1:25	eBioscience, USA
Human CD135 (FLT3) APC-conjugated	BV10A4H2	1:25	BioLegend, UK
Human CD45 FITC-conjugated	HI30	1:25	BioLegend, UK
Phospho(Thr202/Tyr204)-ERK1/2 APC-conjugated	MILAN8R	1:25	eBioscience, USA
Phospho(Tyr591)-FLT3 FITC-conjugated	-	1:25	Biorbyt, USA
Phospho(Tyr694)-STAT5 APC-conjugated	SRBCZX	1:25	Thermo Fisher, USA

##### 2.1.5.2. Primary antibodies for immunoblotting

Target	Clone	Dilution	Manufacturer
Actin	2A3	1:5000	EMD Millipore, DE
ERK1/2	9102	1:800	Cell Signaling, USA
FLT3	S-18	1:200	Santa Cruz, DE
STAT5	A-9	1:200	Santa Cruz, DE

Phospho(Thr202/Tyr204)-ERK1/2	9101	1:500	Cell Signaling, USA
Phospho(Tyr591)-FLT3	54H1	1:800	Cell Signaling, USA
Phospho(Tyr694)-STAT5	9351	1:100	Cell Signaling, USA

### 2.1.5.3. Secondary antibodies for immunoblotting

Target	Clone	Dilution	Manufacturer
Rabbit IgG, HRP-linked	NA934-1ML	1:2000	Thermo Fisher, USA
Mouse IgG, HRP-linked	7076	1:2000	Cell Signaling, USA

### 2.1.5.3. Antibodies for ChIP

Target	Clone	Dilution	Manufacturer
Rabbit IgG	12-370	1:100	EMD Millipore, DE
Menin	A300-105A	1:100	Bethyl, DE
MLL	A300-086A	1:100	Bethyl, DE

### 2.1.6. Cell lines

Human cell lines	<i>MLL/NPM1</i> status	<i>FLT3</i> status
MV411	<i>MLL-AF4</i>	<i>FLT3</i> -ITD
MOLM13	<i>MLL-AF9</i>	<i>FLT3</i> -ITD
OCI-AML3	<i>NPM1</i> <sup>mut</sup>	<i>FLT3</i> wildtype
OCI-AML2	<i>MLL-AF6</i>	<i>FLT3</i> wildtype
HL-60	Wildtype for <i>NPM1</i> , <i>MLL</i> and <i>FLT3</i>	
NB4	Wildtype for <i>NPM1</i> , <i>MLL</i> and <i>FLT3</i>	

Murine cells	<i>Mll/Npm1</i> status	<i>Flt3</i> status
<i>Npm1</i> <sup>CA/+</sup> <i>Flt3</i> <sup>ITD/+</sup>	<i>Npm1</i> <sup>mut</sup>	<i>Flt3</i> -ITD
<i>Mll-Af9</i>	<i>Mll-Af9</i>	<i>Flt3</i> wildtype
<i>Hoxa9-Meis1</i>	Wildtype for <i>Npm1</i> , <i>Mll</i> and <i>Flt3</i>	

### 2.1.7. Cell culture media and supplements

Usage	Formulation
Human cell lines (MV411, MOLM13, OCI-AML3, OCI-AML2, NB4, and HL-60)	RPMI or $\alpha$ MEM 10% FBS 1% P/S 1% L-Glutamine
Murine cells ( <i>Npm1</i> <sup>CA/+</sup> <i>Flt3</i> <sup>ITD/+</sup> murine cells and retrovirally transformed <i>Hoxa9-Meis1</i> - and <i>Mll-Af9</i> -leukemia cells)	DMEM 15% FBS 1% P/S 100 ng/mL SCF 20 ng/mL IL-3 20 ng/mL IL-6
HEK293T and HS27 cells	DMEM 10% FBS 1% P/S 1% L-Glutamine
Primary AML patient cells	StemSpan 1% P/S 1 $\mu$ M StemRegenin 1 0.1 mM 2- $\beta$ -mercaptoethanol 100 ng/mL SCF 20 ng/mL IL-3 20 ng/mL G-SCF 50 ng/mL FLT3L
Freezing medium	90% FBS 10% DMSO

### 2.1.8. Buffers

Buffer	Formulation
RIPA extraction buffer	50 mM Tris-HCl pH 7.5 150 mM NaCl 1 mM EDTA 0.1% Na-deoxycholate, 1% NP-40 dH <sub>2</sub> O up to 1L
2x Laemmli sample buffer	20% Glycerol 125 mM Tris-HCl pH 6.8 4% SDS

	0.02% bromophenol blue 10% 2-β-mercaptoethanol
PBS-T buffer	137 mM NaCl 2.7 mM KCl 10 mM Na <sub>2</sub> HPO <sub>4</sub> 1.8 mM KH <sub>2</sub> PO <sub>4</sub> 0.05% Tween-20 dH <sub>2</sub> O up to 1L
Net-G blocking buffer	50 mM Tris base 150 mM NaCl 5 mM EDTA 0.04% Gelatine 0.05% Tween-20 dH <sub>2</sub> O up to 1L
SDS lysis buffer	50 mM Tris-HCl pH 8.1 1% SDS 10 mM EDTA Complete protease inhibitors (1:100)
Dilution buffer	16.7 mM Tris-HCl pH 8.1 167 mM NaCl 0.01% SDS 1.2 mM EDTA 1.1% Triton-X100
Low salt wash buffer	20 mM Tris-HCl pH 8.1 150 mM NaCl 2 mM EDTA 0.1% SDS 1% Triton-X100
High salt wash buffer	20 mM Tris-HCl pH 8.1 500 mM NaCl 2 mM EDTA 0.1% SDS 1% Triton-X100
LiCl wash buffer	10 mM Tris-HCl pH 8.1 0.25 M LiCl 1 mM EDTA 1% IGEPAL-CH 630 1% deoxycholic acid
TE buffer	10 mM Tris-HCl pH 8.1 1 mM EDTA
A/G beads	50% slurry protein A/G-Sepharose

	0.05% sodium azide 0.05% BSA TE buffer up to 50mL
Elution buffer	0.21 g sodium bicarbonate 2.5 mL 10% SDS dH <sub>2</sub> O up to 25 ml

## 2.1.9. Primers

### 2.1.9.1. ChIP primers

Human ChIP-qPCR primers:		
<i>MEIS1</i>	F: CCGCACACAGCTCATACCAA	R: AAGAGGGAAGCGTTGAGTCT
<i>MEIS1</i> prom	F: CCTTAGCAGAGGCTTTCCCA	R: TATTGGGGTCTGCCAGTGTT
<i>MEIS1</i> TSS	F: CCGGGTTCTAGCATTCTGGT	R: TGCTGCACTGGAAGGAGATTAG
<i>SOX2</i>	F: CAGGAGTTGTCAAGGCAGAGA	R: CCGCCGCCGATGATTGTTA
Murine ChIP-qPCR primers:		
<i>Meis1</i>	F: TGCAAGGGCTTGGGAAAT	R: CCTCGGTCAATGACGCTTTA
<i>Meis1</i> prom	F: GCGTGTGTAAAGTGTGTGTTG	R: TGTAAGACGCGACCTGTTATG
<i>Meis1</i> TSS	F: CCTCAGACCCAACTACCAAATC	R: GACAGAACGGACGATCATTCA
<i>Sox2</i>	F: CCCTGAGCAGCGTGAATAA	R: TCTGATTGGCGCAGTATCTC

### 2.1.9.2. qRT-PCR primers

Human primer sequences:		
<i>B2M</i>	F: CCAGCAGAGAATGGAAAGTC	R: GATGCTGCTTACATGTCTCG
<i>FLT3</i>	F: TCAAGTGCTGTGCATACAATTCCC	R: CACCTGTACCATCTGTAGCTGGCT
<i>MEIS1</i>	F: TCGCGCAGAAAAACCTCTAT	R: CCAAGAGGGCTGGTCAGTTA

For performing qRT-PCR on murine cells, we used commercially available primers from Thermo Fisher, USA:

Murine primers:	
<i>Gapdh</i>	Mm99999915_g1
<i>Flt3</i>	Mm00439000_m1

## 2.2. Methods

### 2.2.1. Preparation of small molecule inhibitor solutions

For *in vitro* studies, MI-503, VTP-50469 and FLT3 inhibitors were dissolved in DMSO, aliquoted and stored at -20°C. For *in vivo* applications, MI-503 was dissolved in DMSO and added freshly to 50% PBS / 25% PEG400 prior to intraperitoneal injections. Quizartinib was dissolved in 22% 2-hydroxyl-beta-cyclodextrin (freshly prepared every 7 days) and applied via oral gavage.

### 2.2.2. Cell Culture and Cell Lines

All human AML cell lines used in this study were authenticated using Multiplex Cell Authentication by Multiplexion<sup>113</sup> (Heidelberg, Germany). The human MV411, MOLM13, OCI-AML3, NB4, and HL-60 cell lines were cultured in RPMI-1640 media and OCI-AML2 in alpha-MEM media, all supplemented with 10% fetal bovine serum, 1% Penicillin/Streptomycin and 1% L-Glutamine. HEK293T and HS27 cells were cultured in DMEM with 10% FBS, 1% PS and 1% L-Glu. Murine *Npm1*<sup>CA/+</sup>*Flt3*<sup>ITD/+</sup> murine cells and retrovirally transformed *Hoxa9-Meis1*- and *Mll-Af9*-cells leukemia cells were cultured in DMEM supplemented with 15% FBS, 1% PS, and cytokines, as indicated in Materials section. All cells were kept in culture no longer than 2 months. Cells were thawed in a water bath at 37°C for 1 min, transferred to 50 mL tube containing medium, kept in it for 10 min at room temperature, centrifuged for 5 min at 1500 rpm, resuspended in fresh medium and put in a flask in the incubator at 37°C for expanding.

### 2.2.3. Primary AML blast cells, co-culture assay, and colony-formation assay

Primary human *NPM1*<sup>mut</sup>*FLT3*<sup>ITD</sup> AML samples were obtained under Institutional Review Board approved protocols, in accordance with the Declaration of Helsinki, from patients treated at the University Medical Center, Mainz. Treatment of primary human *NPM1*<sup>mut</sup>*FLT3*<sup>ITD</sup> and *NPM1*<sup>WT</sup>*FLT3*<sup>WT</sup> AML samples was performed in co-culture with irradiated HS27 human stromal cells for 7 days for cell viability assay. HS27 cells were irradiated with 4000 cGy 24 hours before

adding the media containing primary patient samples and plated at density 200000 cells/well in 6-well plate. Co-culture was maintained in StemSpan media with supplements (see 2.1.7. Materials). Cells were plated at density 350000 cells/well in 6-well plate on top of HS27 cells and were treated with single drug (2  $\mu$ M MI-503 or 6 nM Quizartinib), their combination (2  $\mu$ M MI-503 and 6 nM Quizartinib) or vehicle (DMSO) for 7 days. Treatment of each individual AML sample was performed in three replicates.

To exclude HS27 contamination, primary AML blast cells were stained with anti-human CD45-FITC antibody and cell number was determined by flow cytometry. For colony-forming assay primary AML cells were plated in methylcellulose MethoCult H4435 Enriched media at density of  $1 \times 10^5$  cells per culture dish. Cells were treated with a single drug (2.5  $\mu$ M MI-503 or 3 nM Quizartinib), their combination (2.5  $\mu$ M MI-503 and 3 nM Quizartinib) or vehicle (DMSO) for 12 days. Treatment of each individual AML sample was performed in three replicates.

#### **2.2.4. *In vitro* cell viability assay and calculation of drug synergism**

Trypan-excluding cells were plated at a density of 20,000 cells per well in 150  $\mu$ L media in 96 well plates. Cells were split and replated in fresh media with volume corresponding to 20,000 cells treated with DMSO per well every 3-4 days if they were treated for longer than 4 days. For  $IC_{50}$  determination, cells were treated with Menin-MLL inhibitors and FLT3 inhibitors sequentially diluted 2-fold for a total of 9 concentrations plus vehicle control (DMSO). Combinatorial treatment of serial dilutions of MI-503 and Quizartinib, Ponatinib and Gilteritinib were performed using constant ratios of 833:1, 25:1 and 6.25:1, respectively. VTP-50469 was combined with Quizartinib, Ponatinib or Gilteritinib using constant ratios of 33:1, 1:1 or 1:0.25, respectively. The highest concentration of MI-503, VTP-50469, Quizartinib, Ponatinib and Gilteritinib was 2.5  $\mu$ M, 100 nM, 3 nM, 100 nM and 400 nM, respectively. Cell viability was assessed by flow cytometry using DAPI (1  $\mu$ g/mL) staining. Drug synergism was assessed using the CompuSyn software tool for Chou-Talalay method-based calculations<sup>114</sup> (Figure 2.1).

## Algorithms for Computerized Simulation of Synergism, Additivism and Antagonism of the Effect of Multiple Drugs

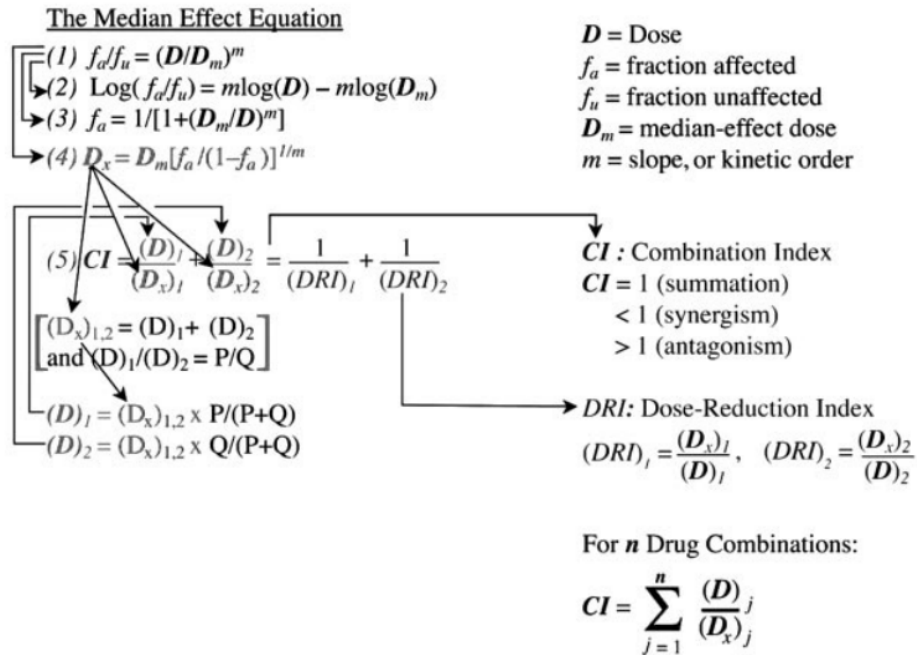


Figure 2.1. Chou-Talalay method-based calculations for defining the Combination Index (CI) and Dose-Reduction Index (DRI) for evaluation of synergy of combined treatment<sup>114</sup>.

### 2.2.5. Chromatin immunoprecipitation (ChIP)

AML cells were treated with DMSO or MI-503 (2.5  $\mu$ M) for 4 days. Paraformaldehyde was added to the culture medium containing  $2.5 \times 10^6$  cells to a final concentration of 1%. Cross-linking was allowed to proceed for 10 min at room temperature and stopped by addition of glycine at a final concentration of 125 mM (pH 8.0), followed by an additional incubation for 5 min. Cells were lysed in 100  $\mu$ L of SDS buffer and sonicated for 15 min (30 sec – active sonication, 30 sec – no sonication), yielding genomic DNA fragments with a bulk size of 100–400 bp. The lysate was then diluted with Dilution buffer to a final volume of 1 mL. Diluted lysates were precleared by addition of 20  $\mu$ L of blocked protein A/G beads. For blocking A/G beads, they were resuspended in cold blocking TE buffer, containing 0.05% Azide, 0.05% BSA, mixed O/N at 4°C, washed once with 10 ml cold blocking TE buffer and resuspended in TE blocking buffer. 50  $\mu$ L of each sample was frozen as an input control. The rest of the sample was divided into tubes and immunoprecipitated overnight at 4°C with polyclonal antibodies specific for either Menin or MLL and normal rabbit IgG as negative control. Immune complexes were recovered by adding 20  $\mu$ L of blocked protein A/G beads and incubated for 1-2 h at 4°C. Beads were washed, using

successive washes in 1 mL of Low Salt Wash Buffer, High Salt Wash Buffer, LiCl Wash Buffer and TE Buffer, all repeated twice. DNA fragments were eluted by adding 200 µL of Elution Buffer and rotating samples for 15 min at room temperature. Reverse cross-linking reaction was performed by adding NaCl to a final concentration of 0.2 M to each of the immunoprecipitated samples and to the input control samples followed by incubation overnight (O/N) at 65°C. DNA was purified using PCR Purification Kit. Eluted DNA fragments were analyzed by qPCR using the following primers:

#### **2.2.6. Analysis of apoptotic cell death by Annexin V staining**

AML cells treated with small molecule inhibitors MI-503 (2.5 µM), Quizartinib (3 nM), Ponatinib (100 nM) and Gilteritinib (400 nM) or vehicle control (DMSO) were stained with Annexin V antibody and DAPI (1 µg/mL) according to the manufacturer's instructions. The number of apoptotic cells, defined as the sum of Annexin V-positive/DAPI-negative and Annexin V-positive/DAPI-positive cells, was determined by flow cytometry.

#### **2.2.7. Cytologic staining**

100,000 cells were harvested in 150 µL PBS. Cytospins and Giemsa staining were performed by the Cytology laboratory within the Department of Hematology and Medical Oncology of the University Medical Center Mainz. Images were captured on an EVOS M5000 imaging system at 100x amplification.

#### **2.2.8. RNA purification, cDNA synthesis, and quantitative real-time PCR (qRT-PCR)**

RNA of  $1 \times 10^6$  trypan-excluding cells was isolated using the RNeasy Mini Kit according to the manufacturer's instructions and cDNA synthesis was performed using the RevertAid H Minus First Strand cDNA Synthesis Kit according to the manufacturer's instructions. Quantitative real-time polymerase chain reactions (qRT-PCR) were carried out using SYBR Green 1 Mastermix for human sequences or TaqMan MasterMix for murine sequences, and run on LightCycler®480 or QuantStudio3 cyclers, respectively. For performing qRT-PCR the following reaction mix has been prepared:

Reaction mix per well	Volume
10 pmol/μl of forward primer (F)	1 μl
10 pmol/μl of reverse primer (R)	1 μl
cDNA template 25-100 ng per reaction	5 μl
H2O	3 μl
SYBR Green 1 Mastermix or TaqMan MasterMix	10 μl

Relative gene expression was determined by the  $\Delta/\Delta C_t$  value method<sup>115</sup> and normalized to the reference gene, *β-2 Microglobulin (B2M)* or *GAPDH*. Relative expression (R) was calculated by the following equation assuming optimal doubling of the target cDNA in each qPCR cycle:  $R = 2^{\Delta C_t} = 2^{(C_{t\text{sample}} - C_{t\text{reference gene}})}$ .

Expression of our genes of interest (*FLT3* and *MEIS1*) was calculated relative to *B2M* (reference gene).

### 2.2.9. Western blotting

MOLM13 and MV411 cells were treated with MI-503 (2.5 μM) or VTP-50469 (100 nM) compounds for 4 or 3 days, respectively, AC220 (3 nM) for 24h or their combination (MI-503 and AC220 or VTP-50469 and AC220) for 4 days/24h or 3 days/24h, correspondingly. Same number of cells were washed once with ice-cold Phosphate-buffered saline (PBS), centrifuged and re-suspended in RIPA extraction buffer (5x10<sup>6</sup> cells/40 μl lysis buffer), vortexed and incubated on ice for 20 minutes. Cells were then centrifuged for 25 minutes at 13,200 rpm. Supernatants, containing whole cell lysates, were transferred to clean microcentrifuge tubes.

The protein content was quantified by Bradford assay. Identical amounts of protein of each sample (60-80 μg) were mixed with 2x Sample buffer, heated at 95°C for 5 min, loaded on a 8% Bis-Tris gel, electrophoretically separated at ~70-80V until the samples had entered the gel, then for 1-2h at 120-140V. Each lysate was loaded twice to detect total and phospho-proteins in parallel without stripping and re-probing the membrane. Separated proteins were transferred to Nitrocellulose membranes using an iBlot 2 Transfer machine according to the manufacturer's protocol.

For blocking, membranes were incubated for 30 min in 5% milk re-suspended in PBS-T and additionally in Net-G blocking buffer for 1-2h at room temperature.

Membranes were cut to allow independent incubation with antibodies O/N at 4°C. Following antibodies were used: anti-ACTIN, anti-ERK1/2, anti-phospho-ERK1/2, anti-FLT3, anti-phospho-FLT3, anti-STAT5 and anti-phospho-STAT5. Then, membranes were washed 3 times with PBS-T for 5 min at room temperature and incubated with secondary antibodies coupled with Horse-Radish Peroxidase (HRP) for 1h. The same washing steps as described before were performed followed by incubation with the ECL substrate for the Horse-Radish Peroxidase enzyme. Chemiluminescence signals were assessed using imaging machine iBrightCL1000.

The results for FLT3/pFLT3 detection were confirmed in separate experiments using a stripping and reprobing protocol: Anti-pFLT3-probed membranes were incubated with Restore Western Blot Stripping Buffer according to the manufacturer's instructions and reblocked and re-probed with FLT3 antibody. Western blot signals were quantified by densitometry using the ImageJ software tool.

#### **2.2.10. Intra-cellular antibody staining followed by flow cytometry**

MOLM13 and MV411 cells treated with MI-503 (2.5 µM) compounds for 4 or 3 days, respectively, AC220 (3 nM) for 24h or their combination (MI-503 and AC220) for 4 days/24h or 3 days/24h, correspondingly, were centrifuged, re-suspended with 1 mL of cold PBS and fixed with 100µL of 37% Paraformaldehyde for 15 min at room temperature. Cells were washed twice with 2 mL of PBS and centrifuged at 2,500 rpm for 5 min. Then, cells were re-suspended in 500 µL of PBS and 4.5 mL of 100% Methanol and incubated on ice for 30 min. After this cells were washed with 5 mL of PBS, centrifuged and stained with phosphorylated protein-specific antibodies anti-phospho(Thr202/Tyr204)-ERK1/2-APC, anti-phospho(Tyr591)-FLT3-FITC and anti-phospho(Tyr694)-STAT5-APC for 1h at room temperature in the dark. Stained cells were washed with 1 mL of PBS and stained with DAPI (1 µg/mL). As a positive control for pFLT3 staining, cells were stimulated with FLT3 ligand (100 ng/ml) for 15 min. Flow cytometry was performed on a FACSCanto II Flow Cytometer. Data were analyzed using FlowJo Version 10 software.

#### **2.2.11. Extra-cellular antibody staining followed by flow cytometry**

MOLM13 and MV411 cells treated with MI-503 (2.5 µM) compounds for 4 or 3 days, respectively, AC220 (3 nM) for 24h or their combination (MI-503 and AC220) for 4 days/24h or

3 days/24h, correspondingly, were washed twice with 1 mL of cold PBS. Cells were stained with anti-FLT3 APC-conjugated antibody for 30 min at 4°C in the dark. Stained cells were washed with 1 mL of PBS and stained with DAPI (Roth, 1 µg/mL). Flow cytometry was performed on a FACSCanto II Flow Cytometer. Data were analyzed using FlowJo Version 10 software.

### **2.2.12. Colony-forming assay**

Murine leukemia cells were plated at a density of 20,000 cells/1 mL in MethoCult with additionally added mouse cytokines (10 ng/mL IL-3, 10 ng/mL IL-6 and 50 ng/mL SCF). Cells were cultured for 7 days at 37°C and 5% CO<sub>2</sub> and colonies (defined as a collection of > 10 cells) were counted. Cells were replated and cultured for another 7 days under the same conditions in secondary plating experiments. Colonies were captured using an EVOS M5000 imaging system at 20x amplification.

### **2.2.13. RNA sequencing**

For gene expression analysis, OCI-AML3, MOLM13, and MV411 were treated in three independent experiments. OCI-AML3 and MOLM13 cells were treated with MI-503 (2.5 µM) and DMSO for 4 days. MV411 cells were treated with MI-503 (2.5 µM) for 3 days, AC220 (3 nM) for 24h, their combination (MI-503 and AC220) and vehicle control (DMSO). To control the results from the RNA-sequencing analysis for potential bias from standard normalization in the context of global transcriptional changes, 1x10<sup>6</sup> cells were harvested and 2 µL of 1:100 External RNA Controls Consortium (ERCC) RNA Spike-in mix were added to the cell lysis buffer of each sample for normalization<sup>116</sup>. ERCC is a set of 92 polyadenylated (poly-A) transcripts, 250–2000 nucleotides in length and having GC-contents between 5% and 51%, that mimic natural eukaryotic mRNAs.

RNA was isolated using the RNeasy Mini Kit including on column DNase digestion. RNA was quantified on a FLUOstar OMEGA fluorometer using the Quant-IT RiboGreen RNA Assay Kit. mRNA library construction using poly-A selection was prepared using TruSeq RNA Library Prep Kit v2 (Illumina). Sequencing of mRNA was performed on an Illumina HiSeq 4000 Next Generation machine by IMB Genomics Core Facility. For gene expression analysis 50 base pair paired-end sequencing was performed using a sequencing depth of 30-40 Million reads.

For gene expression analysis, the online analysis tool *Basepair* has been used. For this, files of FASTQ format were uploaded to the Basepair platform and the following characteristics were applied: reads were mapped to the human genome (hg19) using TopHat (version 2). Prior to analysis of differential gene expression, read counts were normalized to ERCC spike-in controls in order to remove unwanted variation. Differentially expressed genes between the treatment groups were calculated using DESeq version 2. RNA-seq data are publicly available at Gene Expression Omnibus (GSE144759).

#### **2.2.14. Gene Set Enrichment Analysis (GSEA)**

Gene Set Enrichment Analysis (GSEA) is a computational method that compares a pre-defined set of genes with all genes from performed RNA sequencing, taking in account significance and level of gene expression upon 2 biological states (e.g. drug treatment)<sup>117</sup>. The Java-based GSEA was performed using publically available software (<http://software.broadinstitute.org/gsea/index.jsp>) and pre-defined gene sets from the Broad Institute data base.

#### **2.2.15. Retroviral overexpression of *Meis1* and *Meis1/Hoxa9***

For production of retroviral particles, 50-70% confluent HEK293T cells were co-transfected with 10 µg of packaging gag-pol<sup>3</sup> plasmid, 3 µg of envelope pHCMV-EcoEnv<sup>4</sup> plasmid and 8 µg of MSCVneo\_*Meis1* or MSCVneo\_*Meis1/Hoxa9*<sup>5</sup> plasmids per 10 cm cell culture dish. The Xtreme Gene-9 Transfection reagent (18 µl per plate) was diluted with RPMI-1640 medium (270 µl per plate) and incubated for 5 minutes at room temperature. The packaging, envelope and expression plasmids were mixed together and added to Xtreme gene 9 dilution mix, re-suspended and incubated for 25 minutes at room temperature. Then, the transfection mix was added to the culturing plate with HEK293T cells covered with 6 ml of DMEM medium and incubated for 16 h at 37°C. The next day, the medium was refreshed by 5 mL of DMEM media supplemented with 20% FBS and incubated for 24 h. Retroviral particles were harvested 24 h and 48 h post-transfection, filtered (0.45-micron filter) and concentrated by adding 1:5 v/v 50% PEG in PBS (Sigma P3640). After overnight incubation, the viral precipitate was centrifuged at 2,500 rpm for 20 min at 4°C and the pellet was resuspended in 500 µL of ice-cold PBS, aliquoted and kept at -80°C.

For transduction, 6-well plates were coated with 25 µg/mL Retronectin for 2h at room temperature and subsequently blocked with 2% bovine serum albumine for 30 min. Retroviral particles were mixed with polybrene (final concentration 8 µg/mL) and added to  $1 \times 10^6$  cells in 2 mL of media per well of a retronectin-coated 6-well plate. Spin infection was performed at 2,500 rpm and 37°C for 1.5 h, followed by 3-4 h of incubation at 37°C and 5% CO<sub>2</sub>. Afterward, cells were replated in fresh media in non-treated 6-well plates. Successfully transduced cells were selected in neomycin-containing media (G-418, 1 µg/mL) for 14 days.

#### **2.2.16. Knockdown using shRNAs**

Stable cell lines with knockdown of *MEN1* were created using shRNA directed against *MEN1* and control shRNA directed against *LUC*. shRNAs cloned into hairpin pLKO.1 lentiviral vector (TRCN0000040141, TRCN0000338331, MFCD07785395) were purchased from Sigma Aldrich. Cells were co-transfected with 9 µg of lentiviral expression vectors (pLKO.1), 9 µg of gag-pol viral packaging (Addgene) and 0.9 µg of pMD2.G envelope (Addgene) plasmids. Virus was concentrated as described above.

Spin infection was performed with 8 µg/mL polybrene at 2,000 rpm at 37°C for 30 min. Afterward, cells were replated in fresh media in 6-well plates. After selection with 1 µg/ml puromycin (Sigma) for 48 hours, transduced cells were counted and collected for gene expression analysis. In parallel, cells were plated at a density of 20,000 cells per well in 150 µL media containing 1 µg/ml puromycin in 96 well plates, followed by treatment with Quizartinib sequentially diluted 2-fold for a total of 9 concentrations plus vehicle control (DMSO) for 24h.

#### **2.2.17. AML Xenograft Model**

6-to-10-week-old NOD.Cg-Prkdc<sup>scid</sup>Il2rg<sup>tm1Wjl</sup>/SzJ (NSG) mice were purchased from the Translational Animal Research Center at the University Medical Center, Mainz. For *in vivo* experiments they were injected via tail vein using 30Gx1/2" syringes with  $5 \times 10^6$  MV411 cells, diluted in 250 µL of PBS. The solution containing MV411 cells was kept on ice and re-suspended prior to injection. Animals were randomized into the following treatment groups: vehicle (25% DMSO, 25% PEG400, and 50% PBS), MI-503 (50 mg/kg; intraperitoneal (IP), twice daily), Quizartinib (10 mg/kg; oral (PO), once daily) or combination of both drugs.

The stock solution containing MI-503 was prepared the following way: for injecting 6 mice twice a day for 14 days 225 µg of MI-503 was dissolved in 9.375 mL of DMSO and for injecting 12 mice – 890 µg of MI-503 was dissolved in 37.083 mL of DMSO. Then the solution was aliquoted to Eppendorf tubes (330 µL per tube). Prior to injection either 315 µL (6 mice) or 630 µL (12 mice) of DMSO stock was mixed with 315 µL/630 µL of PEG400 and 630 µL/1260 µL of PBS, respectively. As a vehicle control, DMSO solution without MI-503 was dissolved the same way in PEG400 and PBS. For preparing the stock solution containing Quizartinib for injecting 6 mice 18.48 mg of drug was dissolved in 18.48 mL of 22% 2-hydroxyl-beta-cyclodextrin, diluted with distilled water, and for injecting 12 mice 65 mg of Quizartinib was dissolved in 65 mL of 22% 2-hydroxyl-beta-cyclodextrin. Each animal was injected with 200 µL of solution, containing either drug or vehicle.

For assessment of leukemia burden, the mice were sacrificed after 14 days of drug treatment. The bone marrow cells were obtained by serial mashing the femur, tibia and fibula bones and re-suspending them in ice-cold PBS containing 2% FBS. Collected bone marrow cells were singled using a 40 µm sterile cell strainer. Next, bone marrow cells were centrifuged for 5 minutes at 1500 rpm at 4°C, re-suspended in 10 mL of Red Blood Cells lysis buffer (RBC buffer) and kept on ice for 10 min. The lysis was stopped by adding 20-40 mL of DMEM containing FBS to the cells. Then cells were filtered through the cell strainer again, centrifuged for 5 minutes at 1500 rpm at 4°C and re-suspended in PBS. For evaluation of leukemia burden in bone marrow, the cells were stained with anti-human CD45-FITC antibody and the number of hCD45-positive cells was determined by flow cytometry.

For survival analysis, treatment was initiated on day 12 after transplantation and continued until day 45 with a 2-day treatment break to allow partial recovery from local irritation at the injection sites. Moribund animals were sacrificed when they displayed signs of terminal leukemic disease such as reduced motility, hunch-backed position and ruffled coat. All mouse experiments were approved by the National Investigation Office Rheinland-Pfalz.

### **2.2.18. Data Analysis and Statistical Methods**

Statistics were calculated using Prism, Version 7 software (GraphPad). Student's t-test was used to assess significance in *in vitro* assays, and the Kaplan-Meier Log-Rank was used for survival analysis. P-values < 0.05 were considered significant with \*, P < 0.05; \*\*, P < 0.005; \*\*\*,

$P < 0.0005$ . All *in vitro* experiments were performed in at least two independent experiments, each performed in three technical replicates.

### 3. Results

#### 3.1. Menin-MLL inhibition exerts anti-proliferative effects in *MLL*-rearranged and *NPM1*<sup>mut</sup> leukemia cells

As previously published data showed that Menin-MLL interaction has a dependency in *MLL*-r and *NPM1*<sup>mut</sup> leukemias<sup>75</sup>, at first, I confirmed the selective inhibitory effects of Menin-MLL inhibitors on leukemia cell proliferation. For this, I used a selection of *MLL*-r and *NPM1*<sup>mut</sup> human and murine leukemia cells with and without activating *FLT3* mutations (*MLL*-r: MOLM13 [*FLT3*-ITD]; MV411 [*FLT3*-ITD], OCI-AML2 [wildtype (wt) *FLT3*]; murine *Mll-Af9* [wt *Flt3*]; *NPM1*<sup>mut</sup>: OCI-AML3 [wt *FLT3*], murine *Npm1*<sup>CA/+Flt3<sup>ITD/+</sup>). I treated cells with the small inhibitory molecule MI-503 in a dose-dependent manner with the highest concentration of 2.5  $\mu$ M, versus vehicle control (DMSO). Cell viability was assessed by DAPI staining using flow cytometry and was evaluated on days 4, 7 and 11 (Figure 3.1 A-C). The half-maximum inhibitory concentration (IC<sub>50</sub>) defined as the concentration of the compound, at which 50% of the cells are dead, was calculated as the mean of 3 independent experiments (Figure 3.1 D-E).</sup>

In accordance with previous reports that the drug response to the Menin-MLL inhibitors takes longer<sup>29,75</sup>, I observed a profound dose-dependent reduction on cell proliferation in all *MLL*-r and *NPM1*<sup>mut</sup> cells at days 7 and 11, but not at day 4. Leukemia cells lacking an *MLL*-r or an *NPM1* mutation showed only minor responses to very high concentrations of the drug (human APL cell lines: NB4; HL-60; murine *Hoxa9-Meis1*-transformed cells) with IC<sub>50</sub> values > 1500 nM (Figure 3.1 D-E).

---

\*Most of the results contained in this thesis were published (in modified form)<sup>118</sup>.

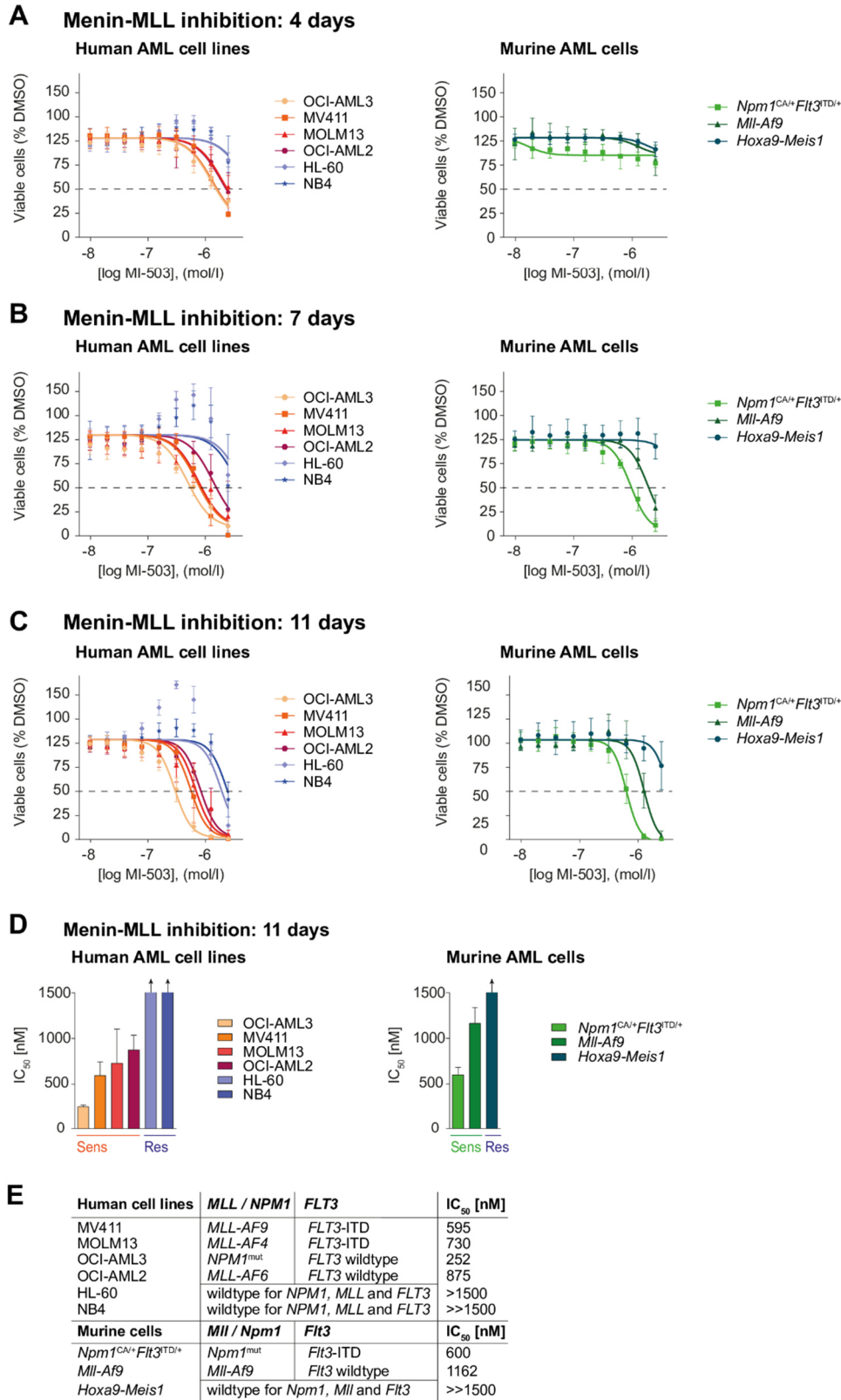


Figure 3.1. A-C) Dose-response curves from cell-viability assays after 4 (A), 7 (B) and 11 (C) days of treatment with MI-503 in human (left) and murine (right) leukemia cells. Viable (DAPI-negative) cells were assessed by flow cytometry. D) IC<sub>50</sub> values for 11 days of treatment with MI-503 for human (left) and murine (right) AML cells. E) Summary of IC<sub>50</sub> values (MI-503), *MLL*-rearrangement, *NPM1* and *FLT3* mutation status in AML cells assessed in this study<sup>118</sup>.

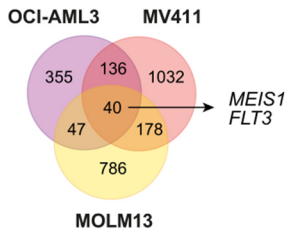
### 3.2. *MEIS1* and *FLT3* transcription is uniformly suppressed upon Menin-MLL inhibition in *MLL*-rearranged and *NPM1*<sup>mut</sup> leukemia

To assess global transcriptional changes upon Menin-MLL inhibition in *NPM1*<sup>mut</sup> and *MLL*-r leukemia cells, the RNA sequencing (RNA-seq) following MI-503 [2.5  $\mu$ M] treatment in OCI-AML3, MOLM13, and MV411 cell lines was performed and analyzed. Gene expression was assessed after 4 days of treatment in OCI-AML3 and MOLM13 cells and after 3 days in MV411 as these exhibited an earlier anti-proliferative response to the treatment. In the *MLL*-r *FLT3*-ITD positive leukemia cells, 1051 (MOLM13) and 1386 (MV411) genes were downregulated by at least 2-fold (adjusted p-value < 0.05; Figure 3.2 A). Many of the most profoundly downregulated genes were known *MLL*-target genes, including *MEIS1*, *PBX3*, *JMJD1C*, and *MEF2C*. As hypothesized, *FLT3* expression was also found to be dramatically suppressed (Figure 3.2 B). In the *NPM1*<sup>mut</sup> OCI-AML3 cells MI-503 led to downregulation of 578 genes including *MEIS1*, *PBX3*, and *FLT3* using the same thresholds (Figure 3.2 A-B). It is interesting to note that in contrast with the previously published Menin-MLL inhibitor MI-2-2<sup>64</sup>, *HOXA/B* genes were not uniformly repressed in these cells (Figure 3.2 C). 40 genes were significantly downregulated in both, *NPM1*<sup>mut</sup> and *MLL*-r leukemia cells and included *MEIS1* and *FLT3* (Figure 3.2 A; Appendix Table 7.1).

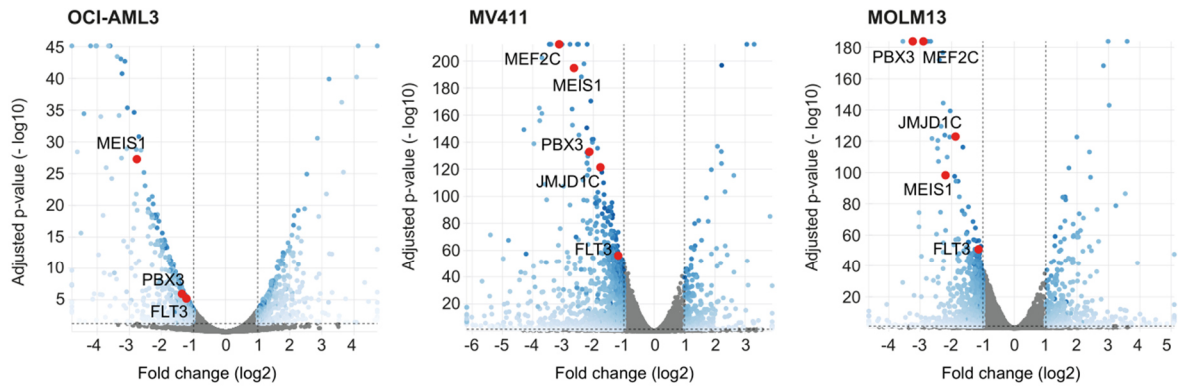
Using qPCR, I confirmed *MEIS1* and *FLT3* to be uniformly downregulated upon Menin-MLL inhibition in all other *NPM1*<sup>mut</sup> and *MLL*-r leukemia cells following MI-503 treatment for 4 days (Figure 3.2 D). Dramatic suppression of *FLT3* in MV411 cells known to harbor a hemizygous *FLT3*-ITD mutation (with no remaining *FLT3* wild type copy) indicated that Menin-MLL inhibition also suppresses the mutated *FLT3*-ITD transcript. qPCR with individually designed ITD-specific primers confirmed this finding in MOLM13 and MV411 cells (Figure 3.2 E).

These data validate previous findings that pharmacological disruption of the Menin-MLL complex significantly downregulates *MEIS1* expression, which is of particular interest as it is an important leukemogenic factor. Moreover, Menin-MLL inhibition also downregulates the expression of wild type *FLT3* and mutant *FLT3*-ITD in *NPM1*<sup>mut</sup> and *MLL*-r leukemias.

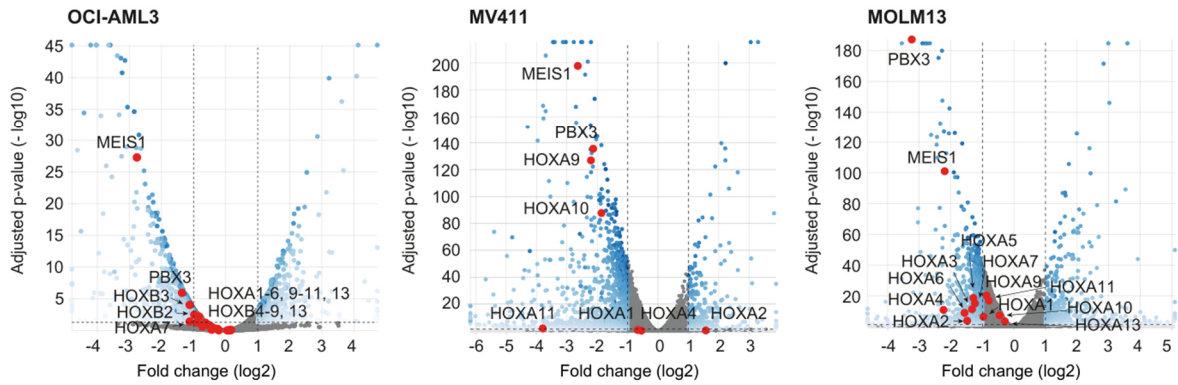
### A Downregulated genes



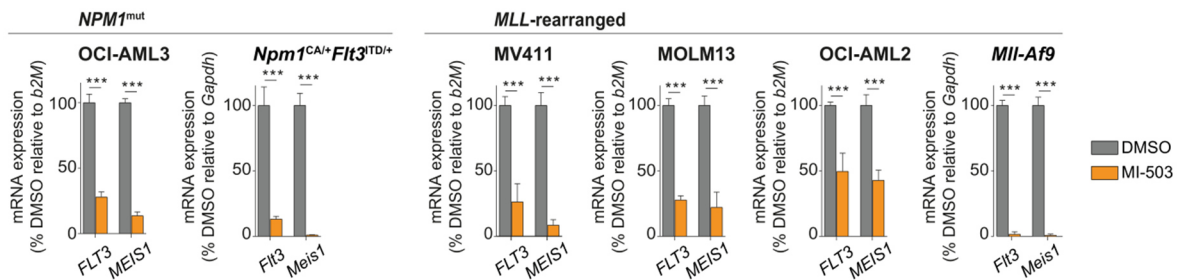
### B Downregulated MLL target genes



### C HOX genes expression



### D Gene expression



### E Gene expression

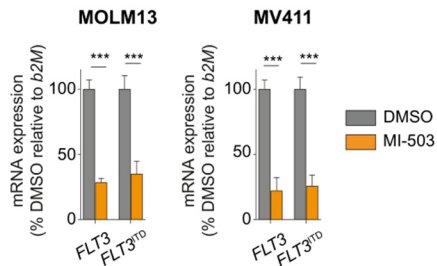


Figure 3.2. A) Venn diagram showing downregulated genes identified by RNA-seq (>2-fold decrease,

adjusted p-value < 0.05), in OCI-AML3, MOLM13 and MV411 cells upon MI-503 treatment (2.5  $\mu$ M) compared to the DMSO control. B)-C) Volcano plots of RNA-seq data obtained from OCI-AML3, MOLM13 and MV411 cells treated with MI-503 (2.5  $\mu$ M). *FLT3*, selected MLL-fusion targets (B) and *HOX* genes (C) are labeled. D) *FLT3* and *MEIS1* mRNA expression in human and murine leukemia cells following four days of MI-503 treatment (2.5  $\mu$ M), as assessed by qRT-PCR. E) *FLT3* and *FLT3*-ITD mRNA expression in MOLM13 and MV411 cells following four days of MI-503 treatment (2.5  $\mu$ M), as assessed by qRT-PCR. Individually designed primers that bind to both non-mutant and *FLT3*-ITD or specifically to *FLT3*-ITD sequences were used<sup>118</sup>.

### **3.3. Pharmaceutical disruption of the Menin-MLL complex decreases its binding to the *MEIS1* gene locus and is associated with downregulation of *FLT3* protein expression**

Next, I elucidated whether observed downregulation of *MEIS1* gene expression might be associated with abrogated binding of both Menin and MLL protein to *MEIS1* gene locus upon pharmacological inhibition of Menin-MLL interaction. Previous studies showed the most abundant binding of both Menin and MLL within *MEIS1* in the gene body, including exons 2 to 6 (chromosome 2: 66664820 – 66674278) and less binding in the promoter region and the start site of transcription<sup>33,34</sup>. This binding pattern was validated in human *MLL*-rearranged MV411 and MOLM13 as well as in murine *Npm1*<sup>CA/+</sup>*Flt3*<sup>ITD/+</sup> cells and the consequences of MI-503 treatment [2.5  $\mu$ M] for 4 days were assessed by using chromatin immunoprecipitation (ChIP) followed by qPCR. Inhibition of Menin-MLL interaction significantly reduced the binding of both Menin and MLL at specific sites within the *MEIS1* gene that show the most abundant binding compared to promoter and TSS sites (Figure 3.3 A-B). As a negative control, primers specific to *SOX2* gene were used, and no significant binding of Menin and MLL to this sequence upon MI-503 and DMSO treatment was proven. These results are consistent with the assumption that Menin-MLL is required for *MEIS1* expression.

Next, I assessed whether Menin-MLL inhibition has an effect on *FLT3* protein expression in human and murine *NPM1*<sup>mut</sup> and *MLL*-r leukemia cells. For this, I performed flow cytometry using antibodies that recognize an extracellular *FLT3* epitope to assess *FLT3* protein expression in human and murine *NPM1*<sup>mut</sup> and *MLL*-r leukemia cells upon 7 days of MI-503 treatment. MV411 cells were treated for 4 days as they show an earlier anti-proliferative response to the treatment. In fact, *FLT3* protein expression was also significantly reduced in all *NPM1*<sup>mut</sup> and *MLL*-r leukemias upon inhibition of Menin-MLL interaction (Figure 3.3 C).

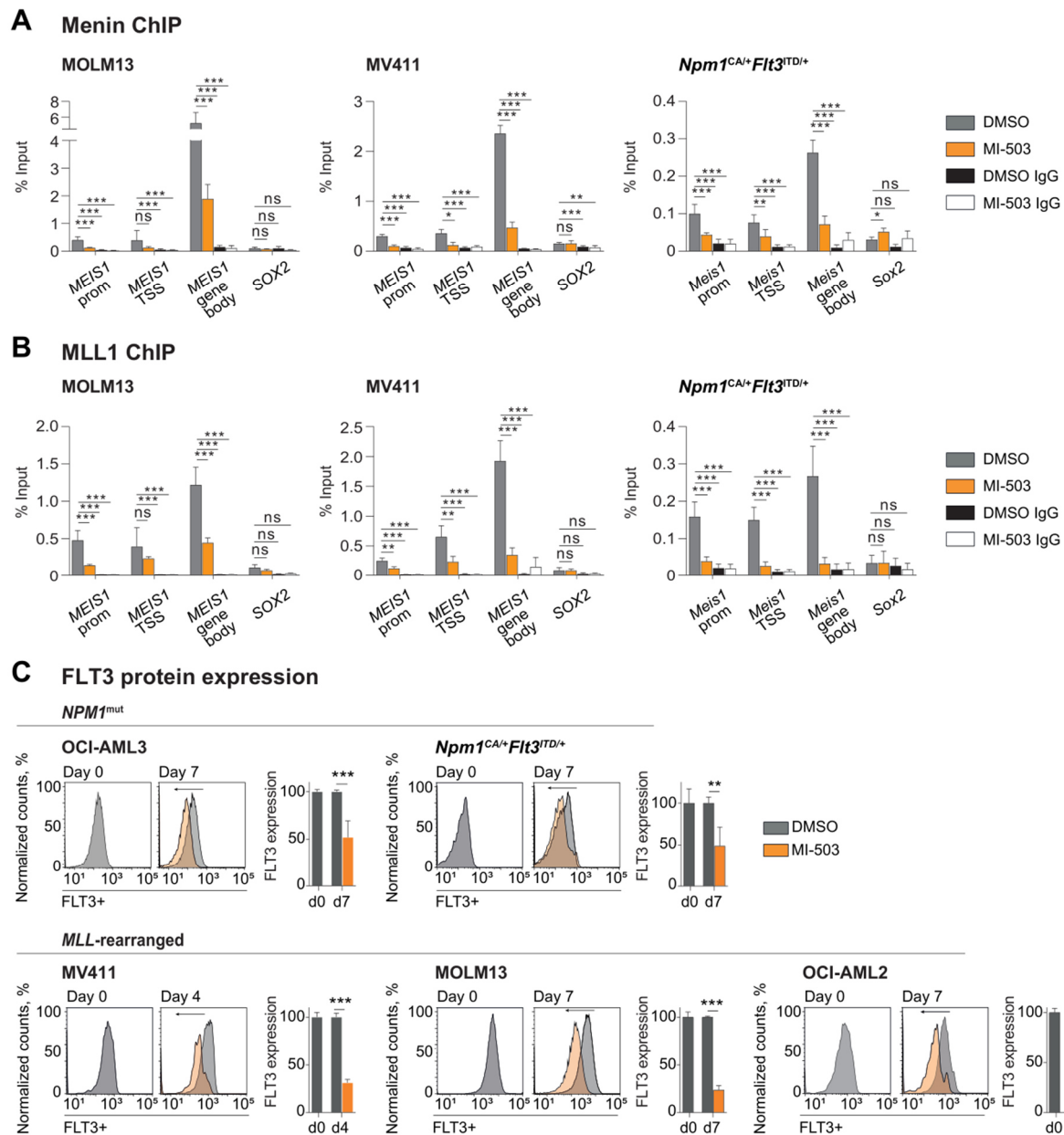


Figure 3.3. A-B) ChIP using antibodies against Menin (A) or MLL (B) and IgG as negative control followed by qPCR detecting a sequence within the *MEIS1* promoter, TSS and gene body regions or *SOX2* as negative control. Cells were treated with MI-503 (2.5  $\mu$ M) or vehicle control for 4 days. C) FLT3 protein expression assessed by flow cytometry in human and murine *NPM1*<sup>mut</sup> and *MLL*-rearranged AML cells following MI-503 treatment (2.5  $\mu$ M for four or 7 days as indicated). Representative histograms of three independent experiments are shown<sup>118</sup>.

These data imply that that pharmacological Menin-MLL inhibition causes a uniform decrease of Menin and MLL binding to *MEIS1* gene and it downregulates FLT3 protein expression in *NPM1*<sup>mut</sup> and *MLL*-r leukemias.

### 3.4. FLT3 inhibitors have anti-leukemic activity against *MLL-r* or *NPM1*<sup>mut</sup> leukemias that harbor a concurrent *FLT3*-ITD

The data presented above indicate that mutant *FLT3* expression can be targeted via Menin-MLL inhibition in *MLL-r* and *NPM1*<sup>mut</sup> leukemias. Therefore, I sought to assess the effects of combining Menin-MLL inhibition with direct FLT3 kinase inhibitors that have been shown to be highly active against *FLT3* mutant AML. First, I determined IC<sub>50</sub> values of the specific and potent FLT3 inhibitors Quizartinib, Crenolanib, Gilteritinib, and Ponatinib in human *MLL-r* *FLT3*-ITD-positive MOLM13 and MV411 leukemia cell lines after 48 hours of treatment. Both cell lines were highly sensitive to the FLT3 inhibitors (Figure 3.4 A-B). Consistent with published data, Quizartinib was the most potent inhibitor and highly selective against *FLT3*-ITD-positive leukemias with IC<sub>50</sub> values within the sub-nanomolar range, whereas AML cells without *FLT3* mutation were unaffected (Figure 3.4 C-D, I).

Next, I assessed FLT3 inhibition in the murine *Npm1*<sup>CA/+</sup>*Flt3*<sup>ITD/+</sup> leukemia cells known to harbor an F692L point mutation (“gatekeeper mutation”) that mediates resistance to most FLT3 inhibitors<sup>119</sup>. In accordance with published data, the cells showed hardly any response to Quizartinib, and the IC<sub>50</sub> values of Ponatinib, Crenolanib and Gilteritinib, were shifted to higher concentrations compared to the values determined from the MOLM13 and MV411 cells lacking the F692L mutation. Murine *Hoxa9-Meis1*-transformed cells without a *Flt3* mutation were not affected by FLT3 inhibition (Figure 3.4 E-I). As the multi-tyrosine kinase inhibitor Ponatinib showed the lowest IC<sub>50</sub> (48nM, 48h) among the different compounds, I used this inhibitor for the treatment of the murine *Npm1*<sup>CA/+</sup>*Flt3*<sup>ITD/+</sup> leukemias and validated the results with higher doses of the more specific drug Gilteritinib. Quizartinib was chosen for experiments in the human *MLL-r* *FLT3*-ITD-positive cells and Ponatinib in the murine *Npm1*<sup>CA/+</sup>*Flt3*<sup>ITD/+</sup> cells.

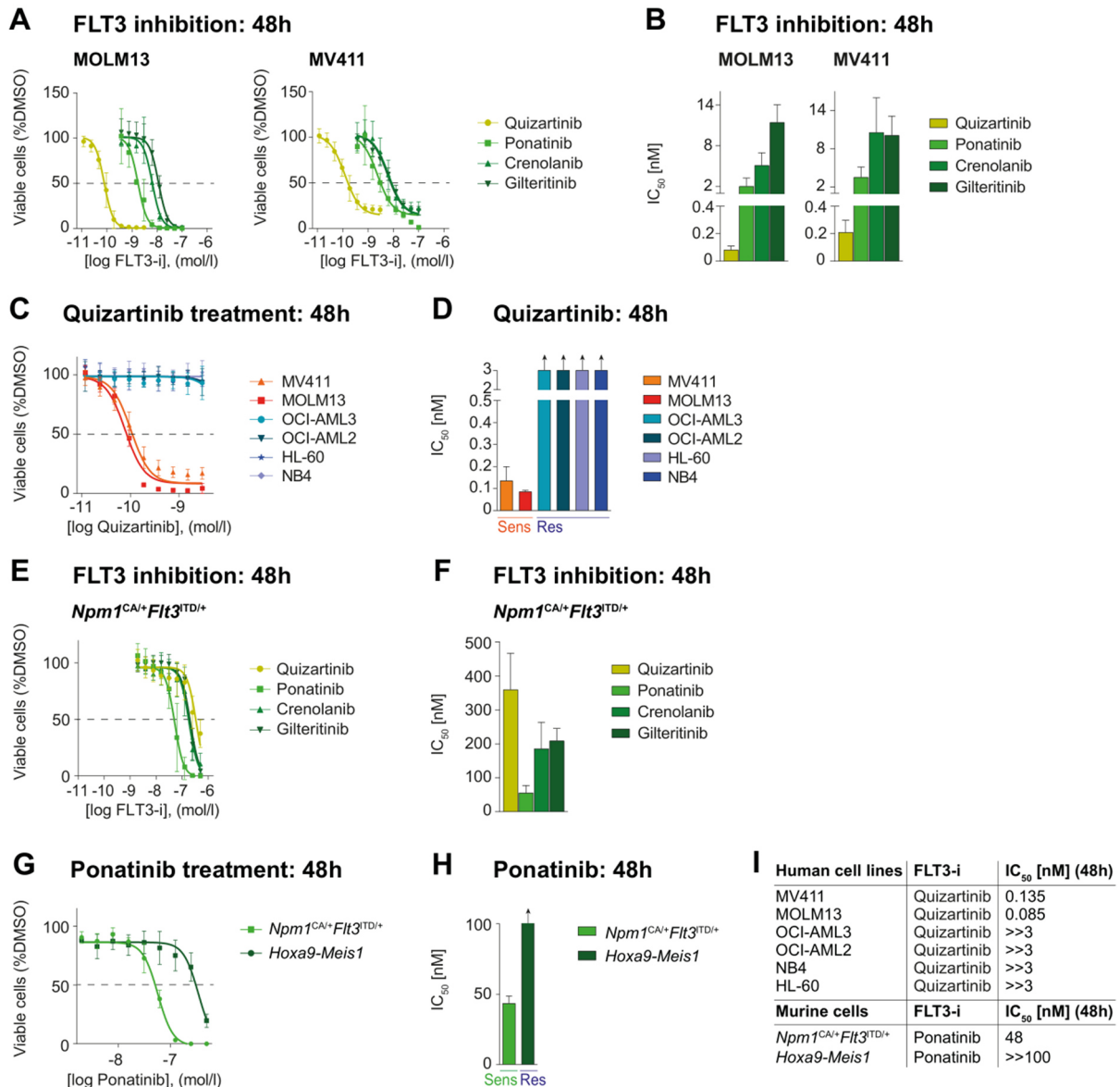


Figure 3.4. A) Dose-response curves from cell-viability assays after 48h of treatment with various FLT3 inhibitors in MOLM13 (left) and MV411 (right) cells. B) IC<sub>50</sub> values after 48h of treatment with various FLT3 inhibitors in MOLM13 (left) and MV411 (right). C) Dose-response curves from cell-viability assays after 48h of treatment with Quizartinib in *FLT3*-ITD-positive and *FLT3* wildtype human leukemia cell lines. D) Quizartinib IC<sub>50</sub> values in *FLT3*-ITD-positive MOLM13, MV411 and *FLT3* wild type OCI-AML2, OCI-AML3, HL-60 and NB4 human leukemia cell lines. E) Dose-response curves from cell-viability assays after 48h treatment with various FLT3 inhibitors in murine *Npm1<sup>CA/+</sup>Flt3<sup>ITD/+</sup>* cells. F) Dose-response curves from cell-viability assays after 48h treatment with various FLT3 inhibitors in murine *Npm1<sup>CA/+</sup>Flt3<sup>ITD/+</sup>* cells. G) Dose-response curves from cell-viability assays after 48h of treatment with Ponatinib in murine *Npm1<sup>CA/+</sup>Flt3<sup>ITD/+</sup>* and *Hoxa9-Meis1*-transformed cells. H) Ponatinib IC<sub>50</sub> concentrations in murine *Npm1<sup>CA/+</sup>Flt3<sup>ITD/+</sup>* and *Hoxa9-Meis1*-transformed cells after 48h of treatment. I) Table summarizing FLT3 inhibitor IC<sub>50</sub> concentrations in human and murine leukemias assessed in this study<sup>118</sup>.

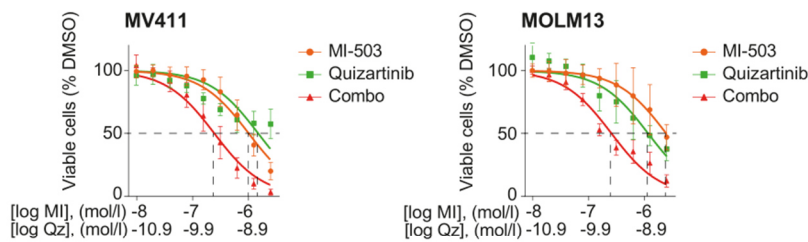
### 3.5. Combined Menin-MLL and FLT3 inhibition has synergistic activity against *MLL-r* or *NPM1<sup>mut</sup>* leukemias that harbor a concurrent *FLT3-ITD*

As the next step combined Menin-MLL and FLT3 inhibition in the human *MLL-r FLT3-ITD* MV411 and MOLM13 cells and the murine *Npm1<sup>CA/+</sup>Flt3<sup>ITD/+</sup>* leukemia cells was assessed (Figure 3.5 A-B). As single-drug treatment with Menin-MLL inhibitors impedes proliferation with a latency of several days<sup>29,75</sup> and single drug FLT3 inhibition induces a more rapid cytotoxic response *in vitro*, I pre-treated the leukemia cells for 2 (MV411) or 3 days (MOLM13, murine *Npm1<sup>CA/+</sup>Flt3<sup>ITD/+</sup>* cells), with MI-503, respectively, and then added the FLT3 inhibitor for additional 24 hours (combination treatment). The combined treatment was compared with single-drug treatment and vehicle control. Dual Menin-MLL and FLT3 inhibition resulted in dramatically enhanced inhibition of proliferation compared to single-drug treatment in all assessed leukemias (Figure 3.5 A-C).

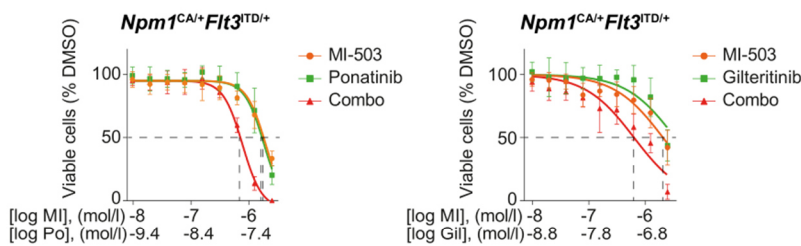
Next, I assessed if the treatment effects of combined treatment were synergistic by using the CompuSyn software tool based on Chou-Talalay method based algorithm<sup>114</sup>, and found a synergism for all of the evaluated leukemias, human MOLM13 and MV411 and murine *Npm1<sup>CA/+</sup>Flt3<sup>ITD/+</sup>* cells (Figure 3.5 D-E). Human and murine AML cells without *MLL-r*, *NPM1<sup>mut</sup>*, or *FLT3* mutation (HL-60, NB4, and *Hoxa9-Meis1*-transformed cells) that served as negative controls were not affected by single drug or combinatorial treatment (Figure 3.5 F).

These findings reveal synergistic anti-leukemic activity of combined Menin-MLL and FLT3 inhibition in *MLL-r* and *NPM1<sup>mut</sup> FLT3-ITD* leukemia cells.

### A Combined Menin-MLL / FLT3 inhibition

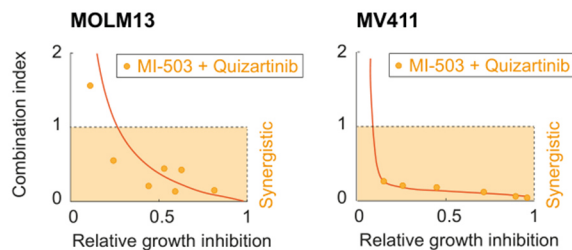


### B Combined Menin-MLL / FLT3 inhibition

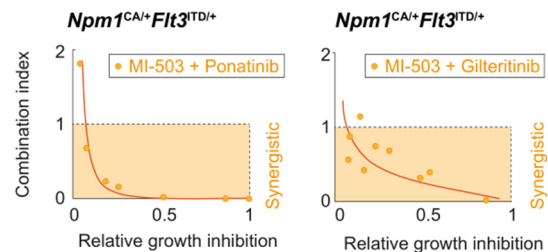


Human cell lines	IC <sub>50</sub> (MI-503) [nM]	IC <sub>50</sub> (Quizartinib) [nM]	IC <sub>50</sub> (MI-503 x Quizartinib) [nM]
MV411	1010	1.2	244.3 x 0.3
MOLM13	2444	1.4	255.5 x 0.3
Murine cells	IC <sub>50</sub> (MI-503) [nM]	IC <sub>50</sub> (Ponatinib) [nM]	IC <sub>50</sub> (MI-503 x Ponatinib) [nM]
<i>Npm1</i> <sup>CA+/+</sup> <i>FIt3</i> <sup>ITD/+</sup>	1989	86	674 x 27
Murine cells	IC <sub>50</sub> (MI-503) [nM]	IC <sub>50</sub> (Gilteritinib) [nM]	IC <sub>50</sub> (MI-503 x Gilteritinib) [nM]
<i>Npm1</i> <sup>CA+/+</sup> <i>FIt3</i> <sup>ITD/+</sup>	2202	362.8	631.1 x 101

### D Drug synergism



### E Drug synergism



### F Combined Menin-MLL / FLT3 inhibition

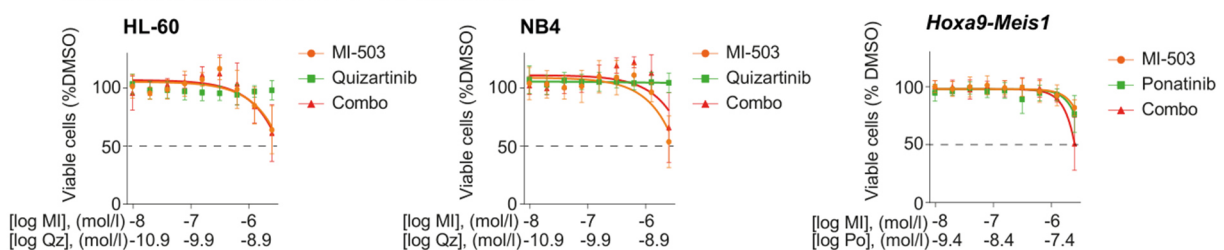


Figure 3.5. A) Dose-response curves from cell viability assays of MV411 and MOLM13 cells comparing MI-503 (MI, 3 days for MV411 and 4 days for MOLM13 cells), Quizartinib (Qz, 24h), and combinatorial MI-503 (3 or 4 days) and Quizartinib (24h) treatment. Dashed lines indicate IC<sub>50</sub> values. B) Dose-response curves from cell viability assays of *Npm1*<sup>CA+/+</sup>*FIt3*<sup>ITD/+</sup> comparing MI-503 (MI, 4 days), Ponatinib (Po, 24h, left) or Gilteritinib (Gil, 24h, right) or with their combination (4 days MI-503, 24h Ponatinib or Gilteritinib). Dashed lines indicate IC<sub>50</sub> values. C) Summary of IC<sub>50</sub> values comparing MI-503 (2.5 μM, 4 days for MOLM13 and 3 days for MV411 cells) and Quizartinib (3 nM, 24h) in human MOLM13 and MV411 cells or MI-503 (2.5 μM, 4 days) and Ponatinib (100 nM, 24h) or Gilteritinib (400 nM, 24h) in murine *Npm1*<sup>CA+/+</sup>*FIt3*<sup>ITD/+</sup> cells. D) Isobolograms corresponding to dose-response curves of MOLM13 and MV411 cells treated with MI-503 (4 days for MOLM13 and 3 days for MV411), Quizartinib (24h) and their

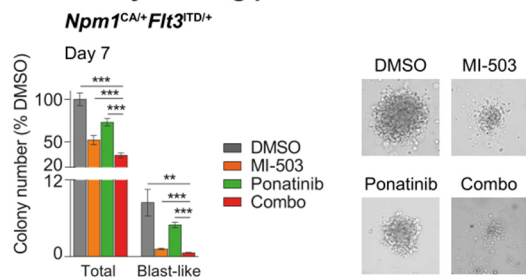
combination. Combination indices (CI) $<1$  indicate synergism. CI values were calculated using the CompuSyn software tool basing on the Chou-Talalay algorithm. E) Isobologram corresponding to the dose-response curve of murine *Npm1*<sup>CA/+</sup>*Flt3*<sup>ITD/+</sup> cells treated with MI-503 (4 days), Ponatinib (24h) or Gilteritinib (24h) and their combination as shown in Figure 2G. F) Dose-response curves from cell viability assays of human HL-60 (left), NB4 (middle) and murine *Hoxa9–Meis1*-transformed (right) cells comparing MI-503 (MI, 4 days), FLT3 inhibition (Quizartinib: Qz, 24h, Ponatinib: Po, 24h), and combinatorial MI-503 and Quizartinib/Ponatinib treatment. Dashed lines indicate IC<sub>50</sub> values. Error bars represent SD of three independent experiments, each performed in three technical replicates<sup>118</sup>.

To assess how combined Menin-MLL and FLT3 inhibition affects the colony-forming potential, I treated murine *Npm1*<sup>CA/+</sup>*Flt3*<sup>ITD/+</sup> leukemia cells with MI-503 and Ponatinib in methylcellulose for 7 days. Combinatorial treatment showed significantly better suppression of total and blast-colony formation compared to single-drug treatment or vehicle control (Figure 3.6 A). I observed that the FLT3 inhibitor Quizartinib did not consistently suppress blast colony formation compared to the vehicle control, whereas Menin-MLL inhibition dramatically inhibited blast colony formation (Figure 3.6 A). It is of interest to note that combinatorial Menin-MLL and FLT3 inhibition resulted in significantly more pronounced inhibition of blast colony formation than Menin inhibition alone in murine *Npm1*<sup>CA/+</sup>*Flt3*<sup>ITD/+</sup> leukemia cells.

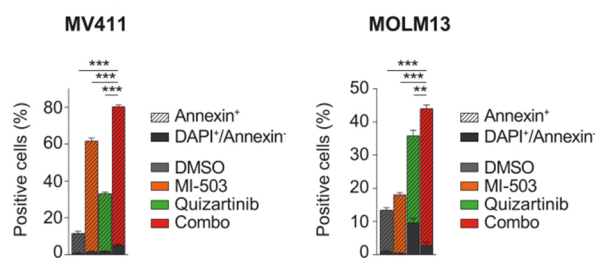
The enhanced killing of *MLL-r FLT3*-ITD-positive and the *Npm1*<sup>CA/+</sup>*Flt3*<sup>ITD/+</sup> leukemia cells was associated with significantly enhanced induction of apoptosis compared to single-drug or vehicle treatment (Figure 3.6 B-C). As Menin-MLL inhibitors are known to inhibit proliferation in *MLL-r* and *NPM1*<sup>mut</sup> leukemias with a latency of several days, I was wondering if early-onset induction of differentiation may also contribute to the quick killing effect of the combination treatment. Therefore, I assessed cell morphology in all 3 cell types at the time when efficient inhibition of proliferation was noted with combination treatment (3 and 4 days of Menin-MLL inhibition, respectively, and 24h of FLT3 inhibition). The mild to moderate myelo-monocytic differentiation observed at this early time point (Figure 3.6 D) indicates that apoptosis induction might be the main mechanism of the anti-leukemic activity of the combination treatment.

These data indicate that combined Menin-MLL and FLT3 inhibition enhances apoptosis induction compared to single-drug treatment of *NPM1*<sup>mut</sup> and *MLL-r* leukemias with *FLT3*-ITD and significantly depletes blast-colony forming potential in murine *Npm1*<sup>CA/+</sup>*Flt3*<sup>ITD/+</sup> leukemia cells.

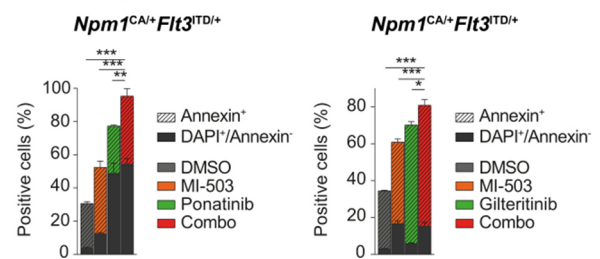
### A Colony-forming potential



### B Apoptosis



### C Apoptosis



### D Morphological changes

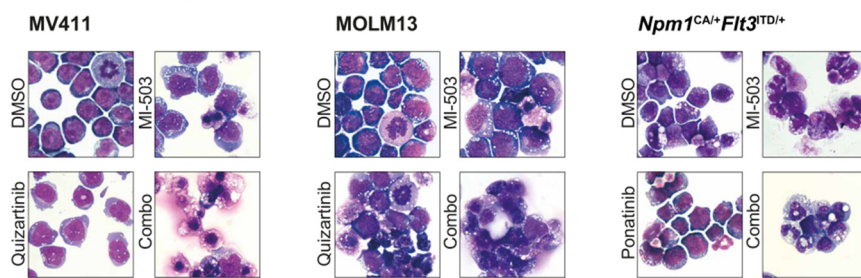


Figure 3.6. A) Effect of MI-503 (2.5  $\mu$ M), Ponatinib (100 nM) and combinatorial treatment (2.5  $\mu$ M and 100 nM) on total and blast-like colony numbers in murine *Npm1<sup>CA/+</sup>Flt3<sup>ITD/+</sup>* cells, normalized to DMSO. B-C) Percentage of apoptotic (Annexin V) and dead (DAPI) cells after single and combinatorial treatment with MI-503 (2.5  $\mu$ M) and Quizartinib (3 nM) in human cell lines (B) or MI-503 (2.5  $\mu$ M) and Ponatinib (100 nM) or Gilteritinib (400 nM) in murine cells (C). D) Giemsa-stained cytopins showing human MV411, MOLM13 and murine *Npm1<sup>CA/+</sup>Flt3<sup>ITD/+</sup>* cells after single and combinatorial treatment with MI-503 (2.5  $\mu$ M, 4 days and 3 days for MV411) and FLT3 inhibitor (Quizartinib: 3 nM, 24h, and Ponatinib: 100 nM, 24h) or their combination (d4/24h and d3/24h for MV411, respectively). Error bars represent SD of three independent experiments, each performed in three technical replicates<sup>118</sup>.

## 3.6. Menin-MLL inhibition enhances FLT3 inhibitor mediated abrogation of phosphorylated FLT3

To characterize the effects of combined Menin-MLL and FLT3 inhibition in more detail, I first assessed *MEIS1* and *FLT3* gene expression upon combinatorial drug treatment. As described above, Menin-MLL inhibition alone or in combination with an FLT3 inhibitor suppressed *MEIS1* and *FLT3* transcription in both *MLL-r FLT3-ITD* positive and the *Npm1<sup>CA/+</sup>Flt3<sup>ITD/+</sup>* leukemias. As expected, downregulation of *MEIS1* and *FLT3* gene expression was not significant with single inhibition of FLT3 phosphorylation. In fact, *FLT3* transcription was

even upregulated in MV411 and *Npm1<sup>CA/+</sup>Flt3<sup>ITD/+</sup>* with single FLT3 inhibition, which is consistent with previous reports<sup>108,120,121</sup> (Figure 3.7 A).

These transcriptional changes translated into similar changes on the protein level as assessed by immunoblotting. While total FLT3 protein expression was reduced with Menin-MLL or combination treatment, single-drug FLT3 inhibition caused no change (MOLM13) or upregulation (MV411) of total FLT3 protein levels (Figure 3.7 B). Assessment of FLT3 receptor phosphorylation (pFLT3; activated FLT3) in these cell lines showed a strong reduction in pFLT3 following its direct inhibition by Quizartinib and was also mildly reduced following Menin-MLL inhibition, the latter most likely reflecting the decreased total FLT3 protein level (Figure 3.7 B). Combinatorial drug treatment caused an even more pronounced reduction of pFLT3 compared to single-drug treatment as assessed in the human *MLL-r FLT3-ITD* positive leukemias by immunoblotting (Figure 3.7 B).

Similar results were obtained when pFLT3 expression was assessed by flow cytometry in the human *MLL-r FLT3-ITD* and the murine *Npm1<sup>CA/+</sup>Flt3<sup>ITD/+</sup>* leukemia cells, in which combination treatment abrogated pFLT3 levels significantly more than single-drug or vehicle treatment (Figure 3.7 C). In order to validate that the pFLT3 protein levels measured with the antibody are specific to pFLT3 and do not reflect changes in total FLT3, I tested pFLT3 antibody upon FLT3 ligand (FLT3L) stimulation of human MOLM13 and MV411 cells as well as murine *Npm1<sup>CA/+</sup>Flt3<sup>ITD/+</sup>* cells (Figure 3.7 D). After FLT3L stimulation (100ng/ml, 15min), the average percentage of pFLT3-positive cells was doubled in MOLM13 cells, and also significantly increased in murine *Npm1<sup>CA/+</sup>Flt3<sup>ITD/+</sup>* cells. MV411 cells did only show a very mild increase in pFLT3 levels, which is consistent with published data<sup>122-125</sup> and most likely a consequence of the hemizygously mutated FLT3 receptor with ongoing autophosphorylation that might be difficult to be further increased.

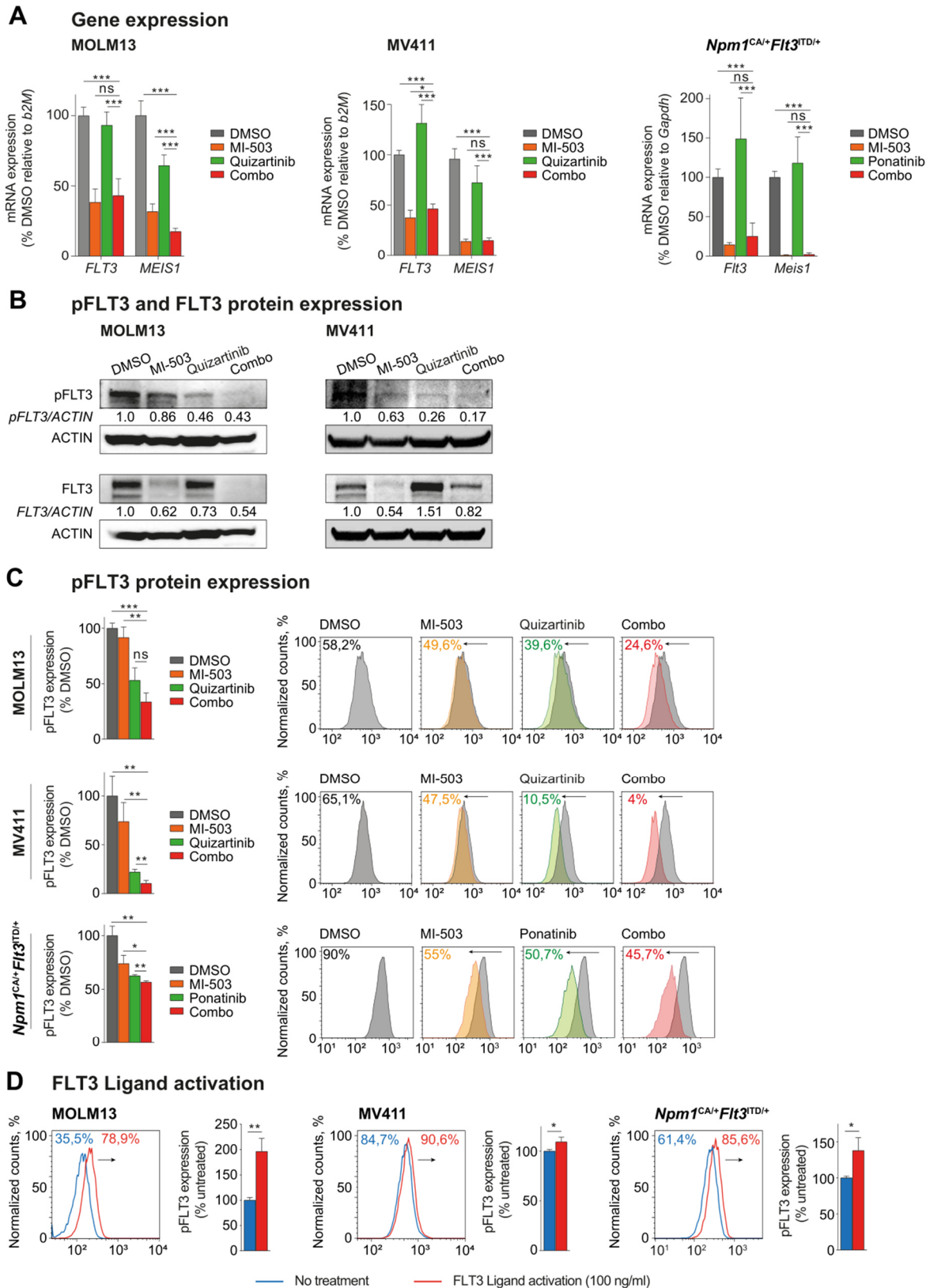


Figure 3.7. A) *FLT3* and *MEIS1* mRNA expression in human MOLM13 (left) and MV411 (middle) and murine *Npm1<sup>CA/+</sup>Flt3<sup>ITD/+</sup>* (right) leukemia cells following single or combinatorial treatment with MI-503 (2.5  $\mu$ M, 4 days for MOLM13 and *Npm1<sup>CA/+</sup>Flt3<sup>ITD/+</sup>* cells and 3 days for MV411 cells) and FLT3 inhibitors (Quizartinib: 3 nM and Ponatinib: 100 nM, 24 hours) as assessed by qRT-PCR. Bar graphs represent the mean with SD of three independent experiments, each performed in technical triplicates. B)

Immunoblotting of FLT3 and phosphorylated (p)FLT3 in MOLM13 cells (left) and MV411 cells (right) upon treatment with 2.5  $\mu$ M of MI-503 (for 3 and 4 days in MV411 and MOLM13, respectively), Quizartinib (3 nM, 24h) or their combination. One representative blot of three independent experiments is shown. Numbers indicate the DMSO-normalized quantification of western blot signals, relative to the loading control, performed by densitometry using the ImageJ software tool. C) pFLT3 protein expression in human MOLM13, MV411 and murine *Npm1<sup>CA/+</sup>Flt3<sup>ITD/+</sup>* cells following treatment with MI-503 (2.5  $\mu$ M, 4 days for MOLM13 and *Npm1<sup>CA/+</sup>Flt3<sup>ITD/+</sup>* cells and 3 days for MV411 cells), FLT3 inhibitor (Quizartinib: 3 nM and Ponatinib: 100 nM, 24h) or their combination, as assessed by flow cytometry. One representative histogram of three independent experiments is shown. The colored numbers in the flow histograms indicate the percentage of pFLT3-positive cells, respectively. D) pFLT3 protein expression in MOLM13, MV411 and murine *Npm1<sup>CA/+</sup>Flt3<sup>ITD/+</sup>* cells with or without previous stimulation with FLT3 ligand (100 ng/ml, 15 min), assessed by flow cytometry. For each cell model, one representative histogram of three independent experiments is shown. Bar graphs represent three independent experiments with pFLT3 expression normalized to the non-stimulated (untreated) control<sup>118</sup>.

### 3.7. Combined Menin-MLL and FLT3 inhibition suppress pFLT3 downstream signaling pathways

Next, I assessed by immunoblotting if there is an enhanced reduction of phosphorylation of the FLT3 downstream signaling proteins, such as STAT5 (pSTAT5) and ERK1/2 (pERK1/2) upon combined Menin-MLL and FLT3 inhibition compared to the single-drug treatment. Similar to pFLT3, I observed reduced phosphorylation of both proteins with single-drug treatment that was even more pronounced with combinatorial treatment for pERK1/2 in MV411 and MOLM13 and pSTAT5 in MV411 cells, whereas the dramatic reduction of pSTAT5 observed with Quizartinib in MOLM13 was not further reduced (Figure 3.8 A-B).

The levels of phosphorylated downstream signaling proteins pSTAT5 and pERK1/2 were also assessed by flow cytometry. Again, the decrease of FLT3 downstream signaling proteins pSTAT5 and pERK1/2 was more pronounced after combinatorial treatment compared to single-drug treatment in MV411 cells and murine leukemia cells as assessed by flow cytometry, while Quizartinib and combinatorial treatment showed a similar reduction of pSTAT5 in MOLM13 cells (Figure 3.8 C-D).

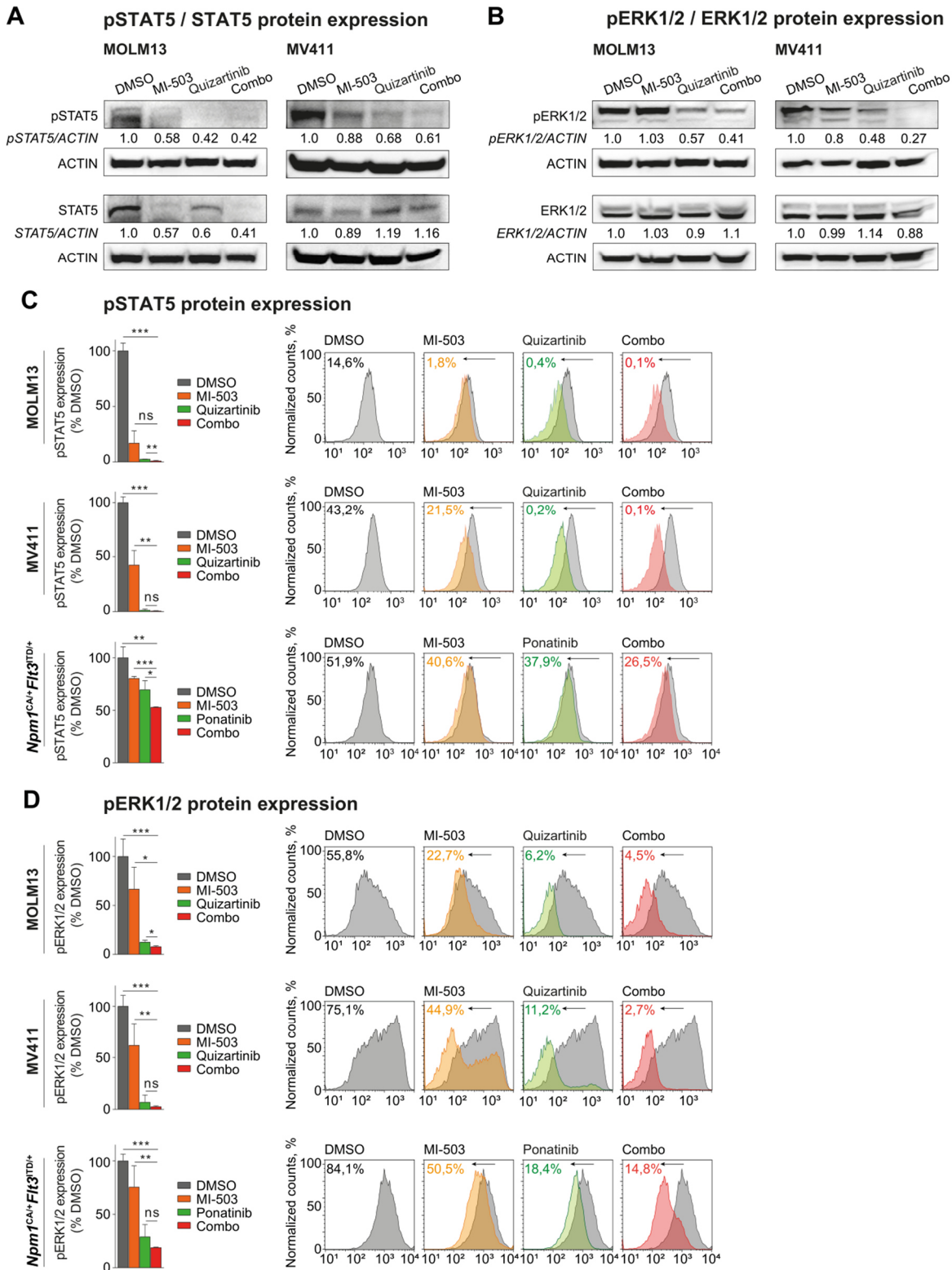


Figure 3.8. A-B) Immunoblotting of STAT5 and phosphorylated (p)STAT5 (A) and ERK1/2 and (p)ERK1/2 (B) in MOLM13 cells (left) and MV411 cells (right) upon treatment with 2.5  $\mu$ M of MI-503 (for 3 and 4 days in MV411 and MOLM13, respectively), Quizartinib (3 nM, 24h) or their combination. One representative blot of three independent experiments is shown. Numbers indicate the DMSO-normalized quantification of western blot signals, relative to the loading control, performed by densitometry using the ImageJ software tool. C-D) pSTAT5 (C) and pERK1/2 (D) protein expression in human MOLM13, MV411 and murine *Npm1<sup>CA/+</sup>Flt3<sup>TD/+</sup>* cells following treatment with MI-503 (2.5  $\mu$ M, 4

days for MOLM13 and *Npm1<sup>CA/+</sup>Flt3<sup>TD/+</sup>* cells and 3 days for MV411 cells), FLT3 inhibitor (Quizartinib: 3 nM and Ponatinib: 100 nM, 24h) or their combination, as assessed by flow cytometry. Bar graphs represent the mean of three independent experiments. Error bars represent SD. One representative histogram of three independent experiments is shown. The colored numbers in the flow histograms indicate the percentage of pFLT3-positive cells, respectively<sup>118</sup>.

To explore the global transcriptional consequences of the enhanced reduction of pFLT3 I performed RNA-seq analysis in the MV411 cells and compared combinatorial versus single-drug or vehicle treatment. Gene set enrichment analysis (GSEA) revealed that the genes downregulated with combinatorial treatment were significantly enriched for target genes of the FLT3 activated transcription factor STAT5A (Figure 3.9 A). When comparing the expression levels of STAT5A target genes between the different treatment groups in more detail, I found most of these genes to be moderately suppressed by single-drug treatment with either Menin-MLL or FLT3 inhibitors. The combinatorial treatment further reduced the expression levels of these genes more efficiently (Figure 3.9 B).

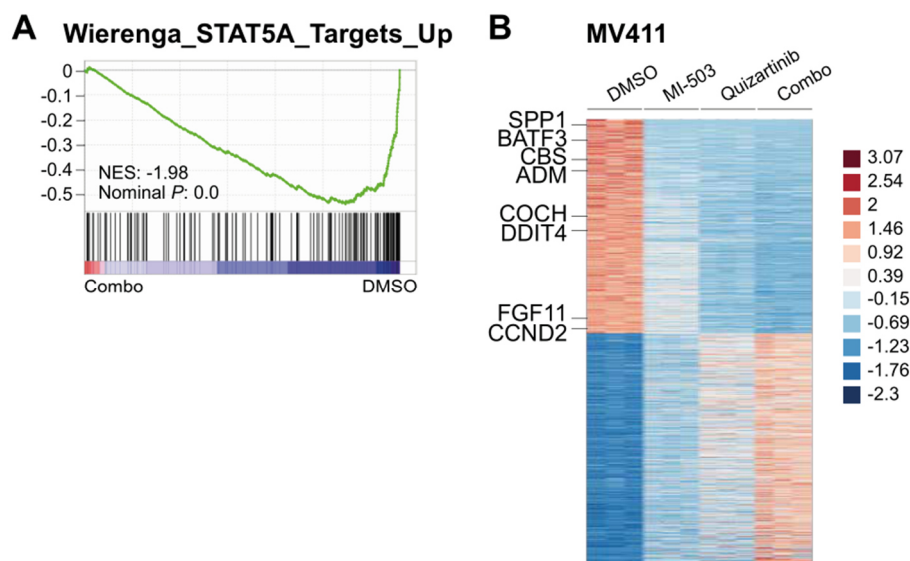


Figure 3.9. A) Gene set enrichment analysis (GSEA) of gene expression changes in MV411 cells treated with combined MI-503 (2.5  $\mu$ M, 3 days) and Quizartinib (3 nM, 24h) compared to STAT5A targets. B) Heatmap of differentially expressed genes (log2-fold change >1 and <-1, respectively, and adjusted p-value <0.05) in MV411 cells following single and combinatorial treatment with MI-503 (2.5  $\mu$ M, 3 days) and Quizartinib (3 nM, 24h). Target genes of STAT5A are indicated<sup>118</sup>.

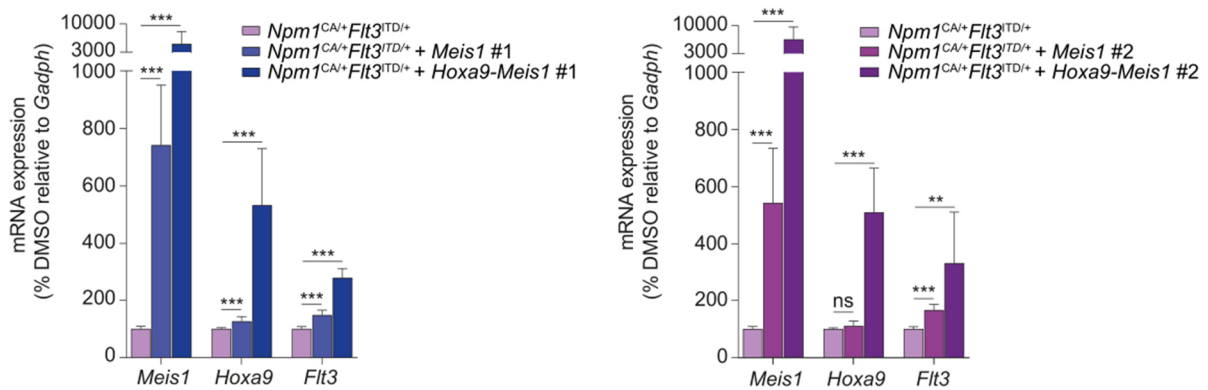
### 3.8. Ectopic *Meis1* and *Hoxa9* expression partially rescues the anti-proliferative effect of Menin-MLL and FLT3 inhibition

As *FLT3* is a reported MEIS1 and HOXA9 transcriptional and potential binding target<sup>73,97,98</sup>, I next assessed the effect of ectopic expression of *Meis1* and *Hoxa9-Meis1* on *Flt3* expression in *Npm1<sup>CA/+</sup>Flt3<sup>ITD/+</sup>* murine leukemia cells. *Npm1<sup>CA/+</sup>Flt3<sup>ITD/+</sup>-Meis1* and *Npm1<sup>CA/+</sup>Flt3<sup>ITD/+</sup>-Hoxa9-Meis1* cells were each obtained from 2 different clones after retroviral transduction (clone #1 and #2).

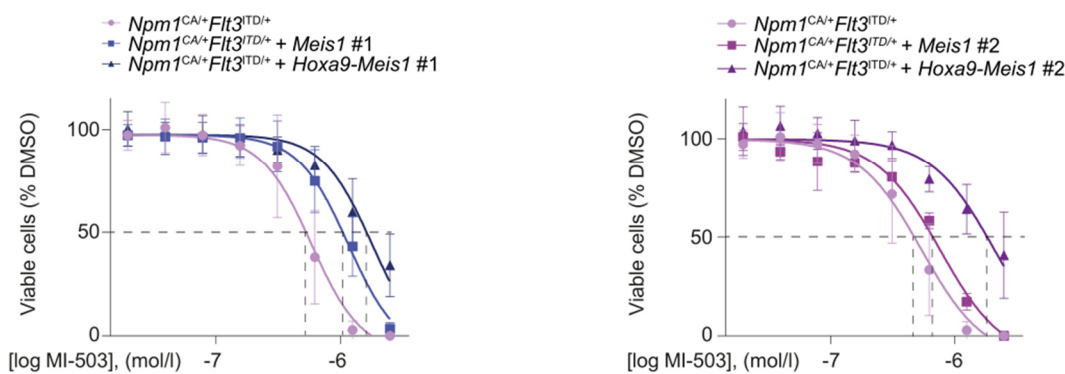
At first, I assessed the transcription of *Meis1* and *Hoxa9* in transduced cells. The *Meis1* expression was elevated by 6.6- and 5.8-fold compared to the controls in clone #1 and #2 of *Npm1<sup>CA/+</sup>Flt3<sup>ITD/+</sup>-Meis1* cells, respectively (Figure 3.10 A). While expression of *Meis1* in *Npm1<sup>CA/+</sup>Flt3<sup>ITD/+</sup>-Hoxa9-Meis1* cells was increased by 45- and 69-fold, *Hoxa9* expression was elevated by 5- and 4.5-fold, clone #1 and #2 correspondingly (Figure 3.10 A). Of interest, both ectopic expression of *Meis1* and *Hoxa9-Meis1* also led to a substantial increase of endogenous *Flt3* expression by 1.5- and 2.8-fold, respectively (Figure 3.10 A).

Next, I evaluated the rescued effect of ectopic *Meis1* and *Hoxa9-Meis1* expression upon Menin-MLL inhibition alone or in combination with FLT3 inhibition compared to controls. For this, I treated transduced *Npm1<sup>CA/+</sup>Flt3<sup>ITD/+</sup>-Meis1* and *Npm1<sup>CA/+</sup>Flt3<sup>ITD/+</sup>-Hoxa9-Meis1* cells as well as native *Npm1<sup>CA/+</sup>Flt3<sup>ITD/+</sup>* cells with either MI-503 for 11 days or pre-treated them with MI-503 for 3 days and then added Ponatinib additionally for another 3 days (Figure 3.10 B-C). As a result, ectopic expression of *Meis1* and *Hoxa9-Meis1* partially rescued the *Npm1<sup>CA/+</sup>Flt3<sup>ITD/+</sup>* cells not only from the antiproliferative activity of the Menin-MLL inhibitor (Figure 3.10 B) but also from the combinatorial treatment (Figure 3.10 C).

## A Ectopic *Meis1* and *Hoxa9* gene expression



## B Menin-MLL inhibition: 11 days



## C Combined Menin-MLL / FLT3 inhibition

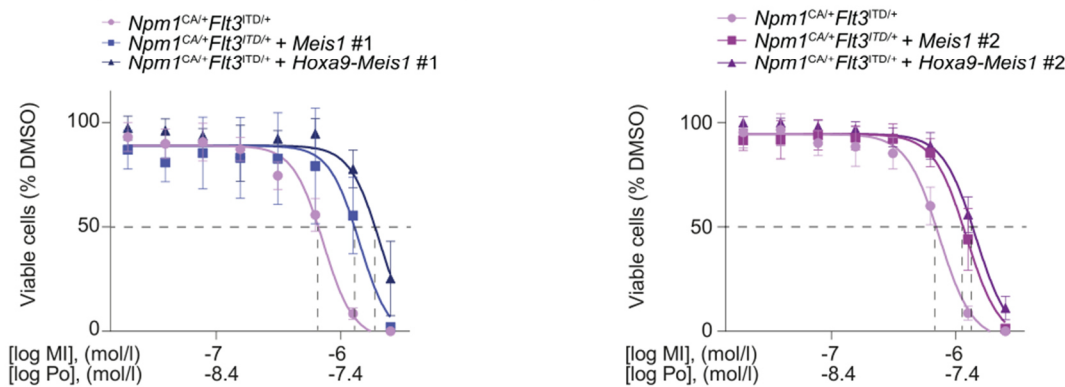


Figure 3.10. A) Relative mRNA expression of *Meis1*, *Hoxa9* and *Flt3* in murine *Npm1<sup>CA/+</sup>Flt3<sup>ITD/+</sup>* cells ectopically expressing *Meis1* or both *Meis1* and *Hoxa9*, normalized to cells with just endogenous *Meis1* and *Hoxa9* expression. The bars show the averaged results from three different experiments with either clone #1 (left) or clone #2 (right), all performed in triplicates. Error bars represent SD. B) Dose-response curves from cell viability assays after 11 days of MI-503 treatment comparing *Npm1<sup>CA/+</sup>Flt3<sup>ITD/+</sup>* cells versus *Npm1<sup>CA/+</sup>Flt3<sup>ITD/+</sup>* cells overexpressing *Meis1* or *Meis1-Hoxa9* (clone #1 – left, clone #2 – right). Dashed lines indicate the shift of IC<sub>50</sub> values. C) Dose-response curves from cell viability assays after combinatorial treatment with MI-503 (MI, 6 days) and Ponatinib (Po, 72h) comparing *Npm1<sup>CA/+</sup>Flt3<sup>ITD/+</sup>* cells versus *Npm1<sup>CA/+</sup>Flt3<sup>ITD/+</sup>* cells overexpressing *Meis1* or *Meis1-Hoxa9* (clone #1 – left, clone #2 – right). Dashed lines indicate the shift of IC<sub>50</sub> values<sup>118</sup>.

Then, I assessed the effect of *Meis1* and *Hoxa9-Meis1* ectopic expression on *Flt3* gene expression in the transduced cells compared to the native cells following combined Menin-MLL and FLT3 inhibition. I observed that downregulation of *Flt3* gene expression observed in native *Npm1<sup>CA/+</sup>Flt3<sup>ITD/+</sup>* murine leukemia cells was partially rescued in the context of *Meis1* and *Hoxa9-Meis1* ectopic expression (Figure 3.11 A). I also analyzed the impact of *Meis1* or *Hoxa9-Meis1* ectopic expression on colony-formation potential upon combined Menin-MLL and FLT3 inhibition. For this, I treated *Npm1<sup>CA/+</sup>Flt3<sup>ITD/+</sup>-Meis1* and *Npm1<sup>CA/+</sup>Flt3<sup>ITD/+</sup>-Hoxa9-Meis1* cells with MI-503 and Ponatinib in methylcellulose for 7 days and found that both scenarios rescued the distortion of colony formation (Figure 3.11 B).

These results support the concept that the MEIS1 transcription factor drives *FLT3* expression in these leukemias.

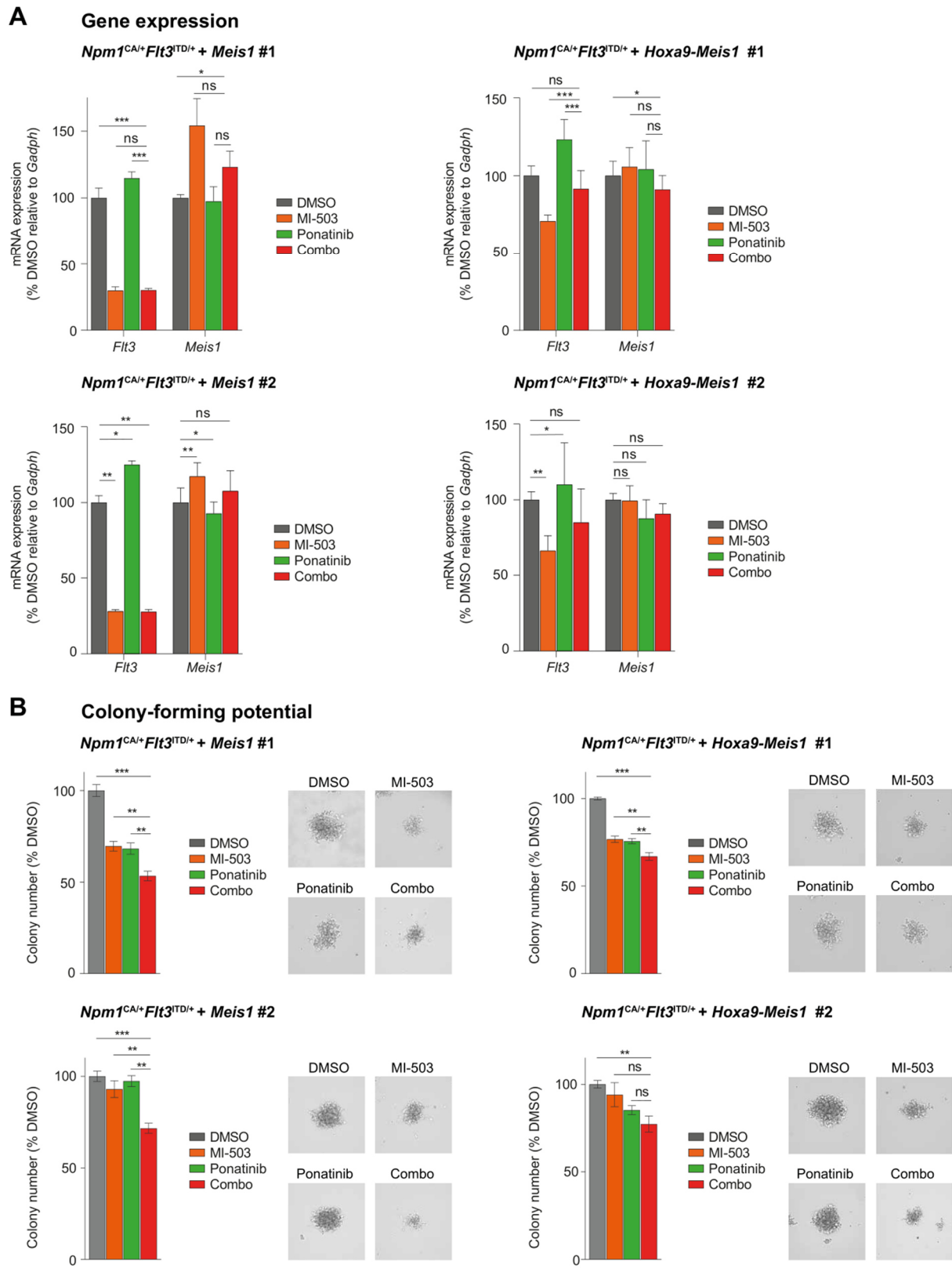


Figure 3.11. A) Relative mRNA expression of Flt3 and Meis1 in murine *Npm1<sup>CAI/+</sup>Flt3<sup>ITD/+</sup>* cells ectopically expressing *Meis1* or both *Meis1* and *Hoxa9*, following MI-503 (2.5  $\mu$ M, 4 days), Ponatinib (100 nM, 24h) and combinatorial treatment. B) Effects of MI-503 (2.5  $\mu$ M), Ponatinib (100 nM) and combinatorial treatment (2.5  $\mu$ M and 100 nM) on blast colony-forming units in murine *Npm1<sup>CAI/+</sup>Flt3<sup>ITD/+</sup>* cells ectopically expressing *Meis1* or both *Meis1* and *Hoxa9* (clone #1, upper panel, and clone #2, lower panel), normalized to DMSO and assessed on day 7 of treatment. Bar graphs represent the mean and standard

deviation of 3 (A) and 2 (B) independent experiments, each performed in 3 replicates. Representative photos of two independent experiments are shown.

### 3.9. Synergistic anti-leukemic activity of combined Menin/FLT3 inhibition is confirmed with the more selective next-generation Menin-MLL inhibitor VTP50496

To confirm the effects of pharmacological Menin-MLL inhibition using MI-503, I performed knock-down of *MEN1* in MOLM13 and MV411 cells using two small-hairpin (sh)RNAs. 48h after lentiviral transduction, *MEIS1* and *FLT3* gene expression was downregulated in a *MEN1* suppression-dependent manner. Importantly, *MEN1* knockdown consistently sensitized the *MLL-r* AML cells to pharmacological FLT3 inhibition, thereby phenocopying the effects observed with MI-503 (Figure 3.12 A-B).

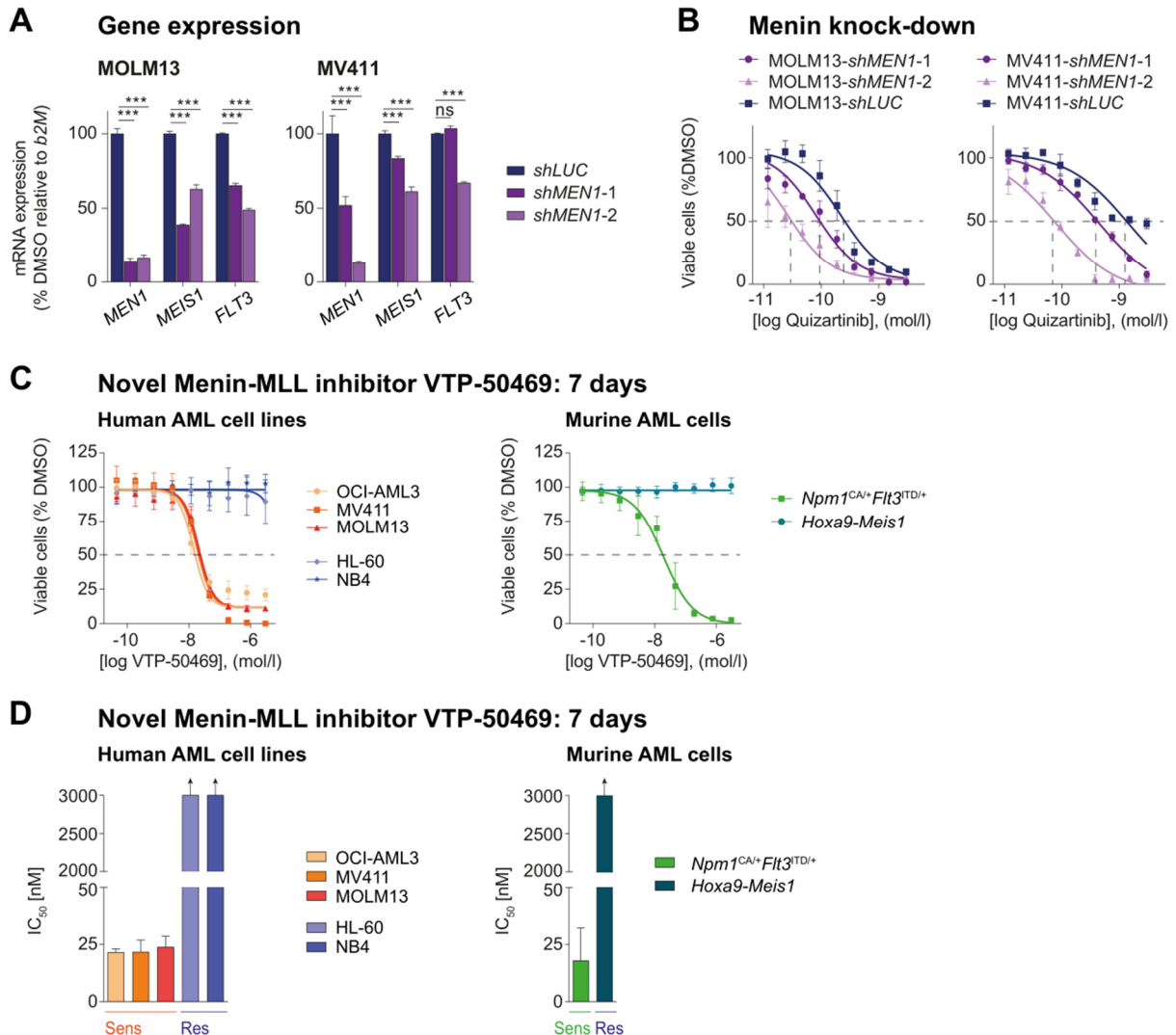


Figure 3.12. A) Dose-response curves of MOLM13 and MV411 cells treated with Quizartinib for 24h, comparing cells transduced with shRNAs against *MEN1* with control-transduced cells (shLUC). B) mRNA

expression levels of *MEN1*, *MEIS1* and *FLT3* in MOLM13 and MV411 cells with *MEN1* knockdown or control-transduced cells, assessed 48h after transduction. C) Dose-response curves from cell-viability assays after 7 days of treatment with VTP-50469 in human (left) and murine (right) leukemia cells. Viable (DAPI-negative) cells were assessed by flow cytometry. D) Human (left) and murine (right) AML cells were treated for 7 days with VTP-50469. Viable (DAPI-negative) cells were assessed by flow cytometry and IC<sub>50</sub> values were graphically calculated using GraphPad Prism<sup>118</sup>.

I also used one of the two next-generation drugs, which have recently entered clinical trials and yet are publicly unavailable, – selective and orally bioavailable Menin-MLL inhibitor, VTP-50469<sup>33,34</sup>. It became accessible to our laboratory and therefore, I used this compound to validate independently the drug effects observed with MI-503 in basic *in vitro* experiments. First, I confirmed selective growth inhibition of VTP-50469 on *MLL-r* and *NPM1<sup>mut</sup>* leukemia cells (Figure 3.12 C-D).

Next, I assessed its combination with the FLT3 inhibitors Quizartinib and Gilteritinib in the human *MLL-r* and Ponatinib and Gilteritinib in the murine *Npm1<sup>CA/+</sup>Flt3<sup>ITD/+</sup>* leukemia cells. Therefore, the leukemia cells were pre-treated for 2 days (MV411), 3 days (MOLM13) or 5 days (murine *Npm1<sup>CA/+</sup>Flt3<sup>ITD/+</sup>* cells), with VTP-50469, respectively, and then added the FLT3 inhibitor (Quizartinib and Gilteritinib to human AML cells or Ponatinib and Gilteritinib to murine AML cells) for additional 24 hours (combination treatment). VTP-50469 combined with all different FLT3 inhibitors resulted in synergistic inhibition of cell proliferation compared to single-drug treatment (Figure 3.13 A-F). Human and murine AML cells without *MLL-r*, *NPM1<sup>mut</sup>*, or *FLT3* mutation (NB4 and *Hoxa9-Meis1*-transformed cells) that served as negative controls were not affected by single-drug or combinatorial treatment (Figure 3.13 G-H).

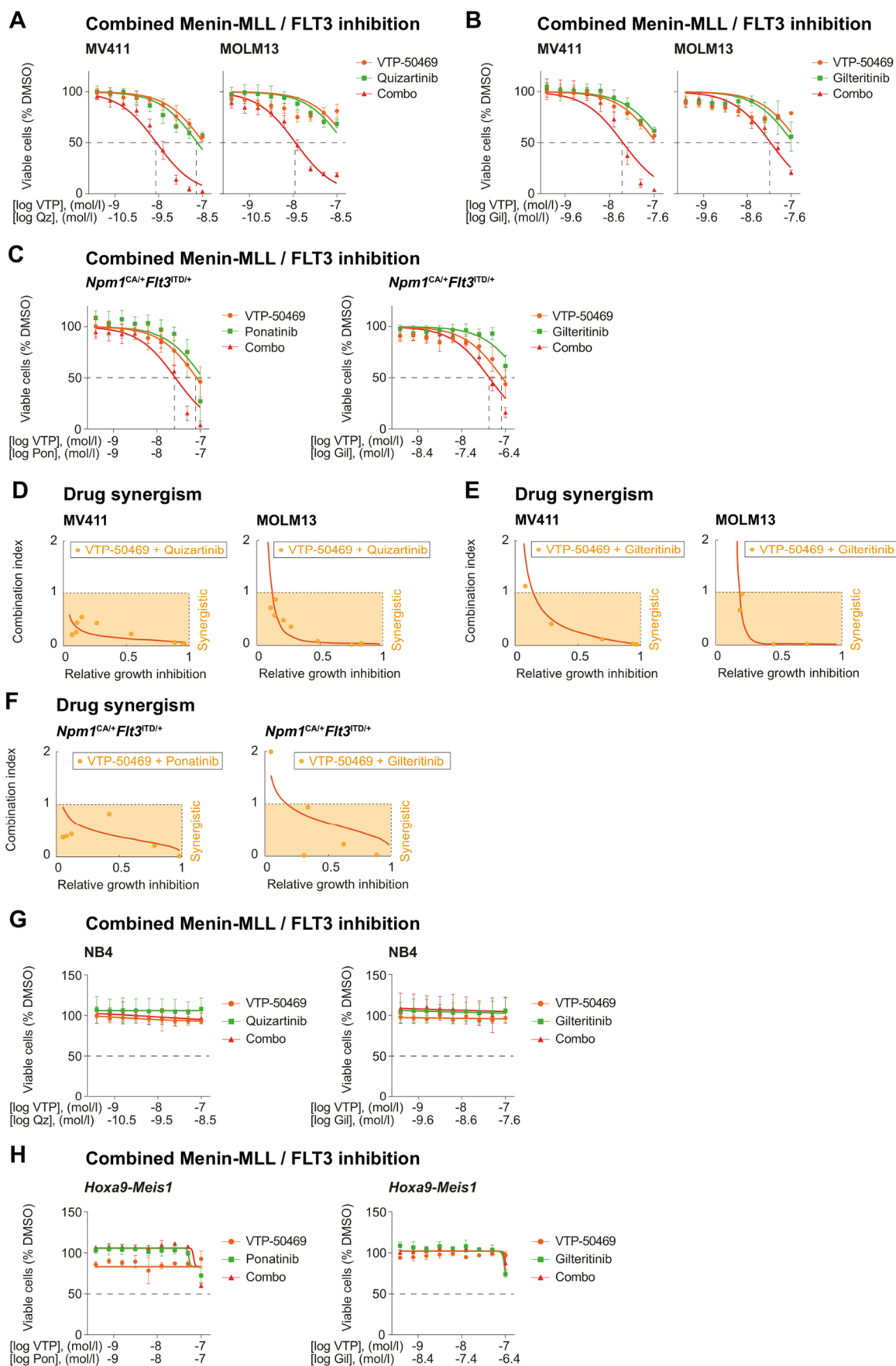


Figure 3.13. A-B) Dose-response curves from cell viability assays of MV411 and MOLM13 cells comparing VTP-50469 (VTP, 3 days for MV411 and 4 days for MOLM13 cells), Quizartinib (Qz, 24h, A), Gilteritinib

(Gil, 24h, B) and combinatorial VTP-50469 (3 or 4 days) and FLT3 inhibition (24h) treatment. Dashed lines indicate IC<sub>50</sub> values. C) Dose-response curves from cell viability assays of *Npm1*<sup>CA/+</sup>*Flt3*<sup>ITD/+</sup> comparing VTP-50469 (VTP, 6 days), Ponatinib (Po, 24h, left) or Gilteritinib (Gil, 24h, right) with their combination (6 days VTP50469, 24h FLT3 inhibition). Dashed lines indicate IC<sub>50</sub> values. D-E) Isobolograms corresponding to dose-response curves of MOLM13 and MV411 cells treated with VTP-50469 (4 days for MOLM13 and 3 days for MV411), Quizartinib (24h, D) or Gilteritinib (24h, E) and their combination. Combination indices (CI)<1 indicate synergism. CI values were calculated using the CompuSyn software tool basing on the Chou-Talalay algorithm. F) Isobologram corresponding to the dose-response curve of murine *Npm1*<sup>CA/+</sup>*Flt3*<sup>ITD/+</sup> cells treated with VTP-50469 (6 days), Ponatinib or Gilteritinib (24h) and their combination. G) Dose-response curves from cell viability assays of NB4 cells comparing VTP-50469 (VTP, 4 days), Quizartinib (Qz, 24h, left panel) and Gilteritinib (Gil, 24h, right panel), and combinatorial VTP-50469 (4 days) and FLT3-inhibitor (24h) treatment. Dashed lines indicate IC<sub>50</sub> values. H) Dose-response curves from cell viability assays of Hoxa9-Meis1-transduced murine cells comparing VTP-50469 (VTP, 6 days), Ponatinib (Po, 24h, left panel), Gilteritinib (Gil, 24h, right panel) and combinatorial VTP-50469 (6 days) and FLT3-i (24h) treatment. Dashed lines indicate IC<sub>50</sub> values<sup>118</sup>.

Similar to MI-503, *MEIS1* and *FLT3* gene expression was significantly downregulated with VTP-50469 treatment as well as when combined with FLT3 inhibitors (Figure 3.14 A). Next, I evaluated FLT3 and pFLT3 protein expression in MV411 and MOLM13 leukemia cells following combined VTP-50469 and Quizartinib treatment. In a like manner to MI-503, I observed prominent abrogation of total FLT3 upon VTP-50469 treatment in both cell lines, which possibly reflects the transcriptional suppression of *FLT3* via Menin-MLL inhibition. Combined treatment resulted in more pronounced abrogation of pFLT3 protein levels than each of the single-drug treatments alone, supporting my previous results (Figure 3.14 A-B). These results confirm previous findings and show a possible translational application of VTP-50469 in a combination with FLT3 inhibitors.

In summary, *MEN1* knockdown, as well as treatment with selective inhibitor VTP-50496 followed by pharmacological FLT3 inhibition, displayed similar anti-leukemic effects as those observed with MI-503. These results support the concept of synergistic anti-leukemic activity of combined Menin-MLL and FLT3 inhibition in *MLL-r* and *NPM1*<sup>mut</sup> *FLT3*-ITD leukemia.

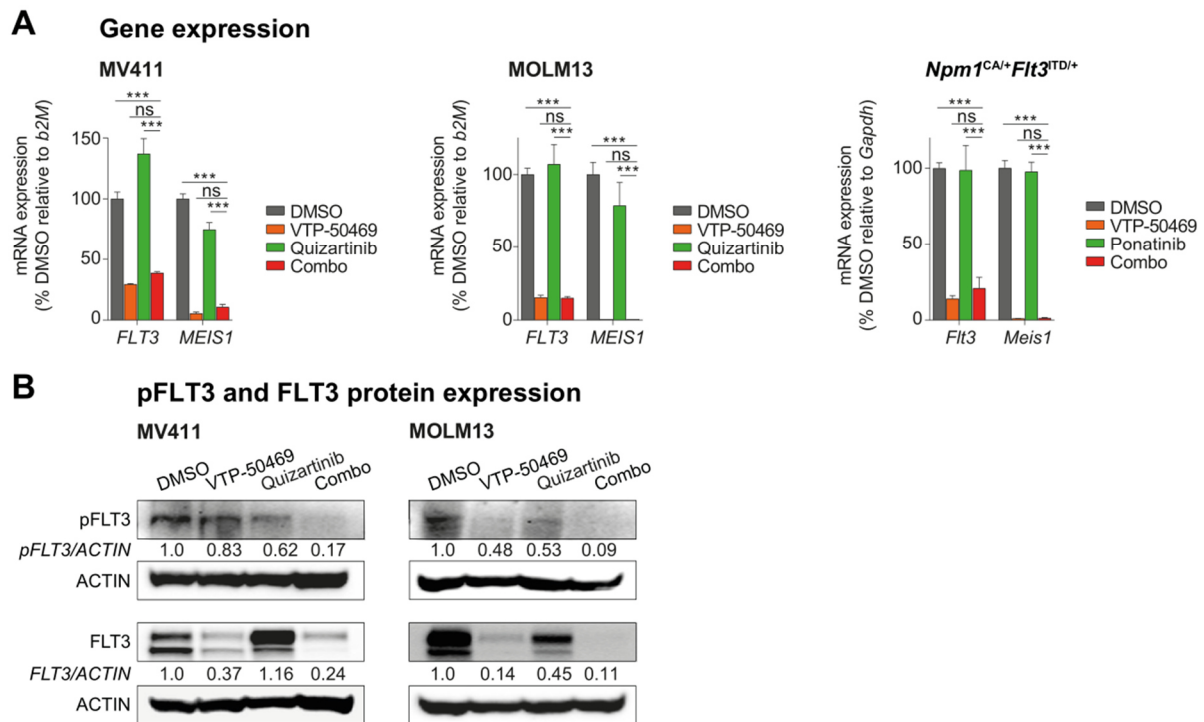


Figure 3.14. A) *FLT3* and *MEIS1* mRNA expression in human MV411 (left), MOLM13 (middle) and murine *Npm1<sup>CAI/+</sup>Flt3<sup>ITD/+</sup>* (right) leukemia cells following single or combinatorial treatment with VTP-50469 (100 nM, 4 days for MOLM13 and *Npm1<sup>CAI/+</sup>Flt3<sup>ITD/+</sup>* cells and 3 days for MV411 cells) and FLT3 inhibitors (Quizartinib: 3 nM and Ponatinib: 100 nM, 24h) as assessed by qRT-PCR. Bar graphs represent the mean with SD of three independent experiments, each performed in technical triplicates. B) Immunoblotting of FLT3 and phosphorylated (p)FLT3 in MV411 cells (left) and MOLM13 cells (right) upon treatment with VTP-50469 (100 nM for 3 and 4 days in MV411 and MOLM-13, respectively) Quizartinib (3 nM, 24h) or their combination. Numbers indicate the DMSO-normalized quantification of western blot signals, relative to the loading control, performed by densitometry using the ImageJ software tool<sup>118</sup>.

### 3.10. Combinatorial treatment suppresses primary *NPM1<sup>mut</sup>FLT3<sup>ITD</sup>* AML patient cells *in vitro*

To investigate combinatorial Menin-MLL and FLT3 inhibitor treatment in primary AML patient samples, I used a previously described co-culture assay<sup>75</sup> that allowed me to maintain and treat these leukemia cells in serum-free medium with cytokines on a (HS27) stromal cell layer *in vitro* (Figure 3.15 A). 5 *de novo* *NPM1<sup>mut</sup>FLT3-ITD* AML patient samples were treated for 7 days with DMSO, MI-503 [2  $\mu$ M], Quizartinib [6 nM], or the combination. All 5 samples showed significantly enhanced reduction of cell numbers with combinatorial treatment compared to single-drug treatment. In all samples, MI-503 and Quizartinib also reduced the number of viable cells significantly compared to the cells exposed to the drug vehicle (Figure 3.15 B-C).

To control for potential non-specific drug toxicity, I also treated 2 primary AML patient samples lacking an *NPM1*<sup>mut</sup>, *MLL-r*, or an *FLT3*-ITD. It is of interest to note, that in both samples the viable cell number was not significantly affected by either single-drug or combinatorial treatment (Figure 3.15 D). I also treated 4 of the 5 primary *NPM1*<sup>mut</sup> *FLT3*-ITD samples with DMSO, MI-503 [2.5 μM], Quizartinib [3 nM], or the combination in methylcellulose for 12 days. Similar to the proliferation assays, the blast-colony formation was most significantly reduced with the drug combination versus other treatment groups (Figure 3.15 E).

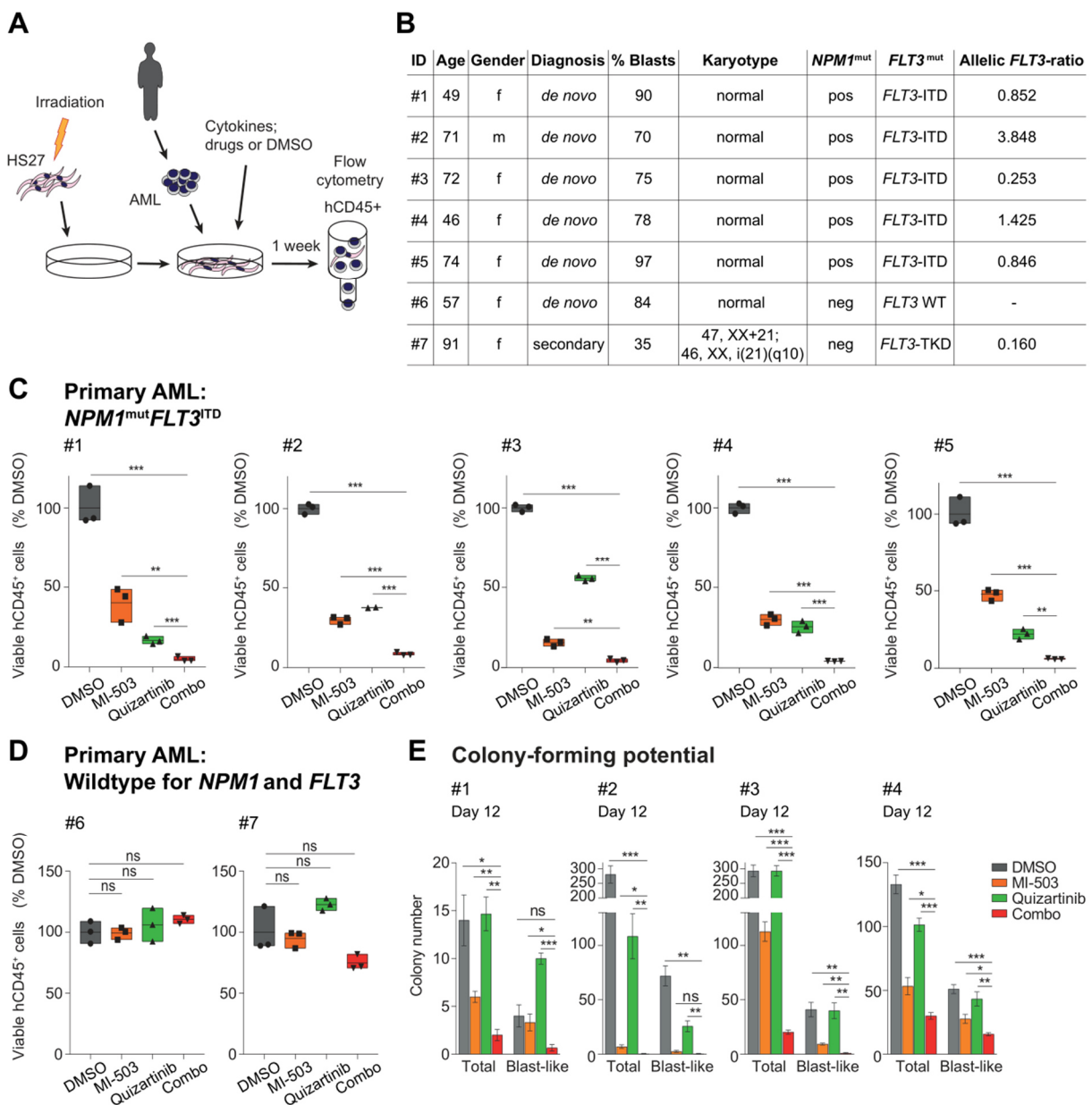


Figure 3.15. A) Schematic of the human stromal cell co-culture assay for maintaining primary AML patient blasts. B) Summary of patient characteristics for the samples used in C-E. C-D) Viable cell numbers of de novo AML samples treated in co-culture for seven days with DMSO, MI-503 (2 μM), Quizartinib (6 nM) or combinatorial MI-503 and Quizartinib. C) Five independent samples of

de novo *NPM1*<sup>mut</sup>*FLT3*<sup>ITD</sup> AML. D) Two independent samples of *de novo* AML, wildtype for *NPM1*, *FLT3*, and *MLL*. Depicted are DAPI-negative, human CD45-positive cell numbers as assessed by flow cytometry. E) Effect of MI-503 (2.5  $\mu$ M), Quizartinib (3 nM) and combinatorial treatment (2.5  $\mu$ M and 3 nM) on total and blast-like colony-forming units in primary patient sample cells<sup>118</sup>.

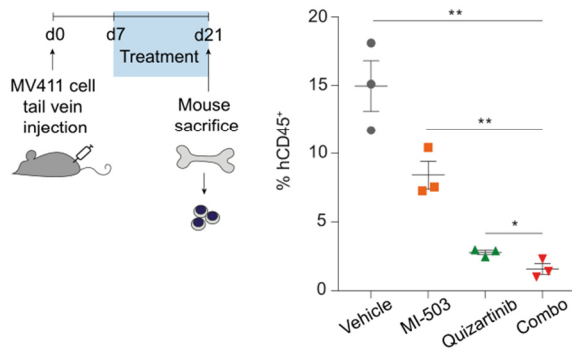
These results from primary *NPM1*<sup>mut</sup> *FLT3*-ITD AML patient samples further support that combinatorial Menin-MLL and FLT3 inhibition might be considered as a potential therapeutic opportunity for *FLT3*-mutated *NPM1*<sup>mut</sup> leukemia.

### **3.11. Combined *in vivo* treatment significantly prolongs survival of *MLL*-r *FLT3*-ITD positive leukemic mice**

Next, I sought to explore the therapeutic potential of combined Menin-MLL and FLT3 inhibition *in vivo*. First, I assessed the effects of these drugs on leukemic burden using a disseminated human MV411 xenotransplantation model. For this purpose, MV411 cells were transplanted into NSG mice via tail-vein injection and then randomly divided into 4 groups receiving MI-503, Quizartinib, the combination, or vehicle control treatment. The treatment was started 1 week after transplantation (d7) and the animals were sacrificed after 14 days of treatment. Leukemia burden, as defined by the percentage of bone marrow cells expressing human CD45, was significantly reduced within the animal group treated with the combination versus all other groups (vehicle: 15%, MI-503: 8%, Quizartinib: 3%, combo: 1.5%; p-value < 0.05 for combo vs. other groups; Figure 3.16 A).

In a separate experiment, I assessed survival in the disseminated MV411 xenograft leukemia model. Drug treatment was initiated on day 12 after transplantation and continued until day 45. Combinatorial MI-503 and Quizartinib treatment resulted in a highly significant survival advantage for the drug combination treatment compared to single-drug or vehicle-treated animals (Hazard-ratios for death: 0.15 and 0.35; 95% confidence interval: 0.02845-0.8061 and 0.0285-0.8783, p=0.0269 and p=0.0350 for combo vs. MI-503 and combo vs. Quizartinib, respectively) (Figure 3.16 B).

**A Bone marrow engraftment:  
Xenograft model of MLL leukemia**



**B Overall survival:  
Xenograft model of MLL leukemia**

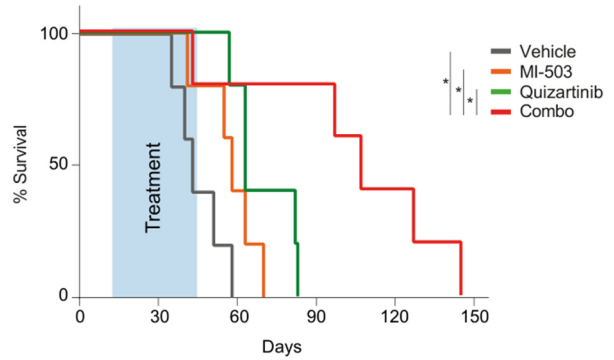


Figure 3.16. A) Left: Experimental setup for the treatment of MV411-derived leukemic xenograft mice. Right: Percentage of human CD45-positive cells in the bone marrow of leukemic mice after treatment with drug vehicles, MI-503 (50 mg/kg; bid IP), Quizartinib (10 mg/kg; PO; once daily), or combined MI-503 and Quizartinib. B) Kaplan-Meier survival analysis of MV411-derived leukemic xenograft mice treated with drug vehicles, MI-503 (50 mg/kg; bid IP), Quizartinib (10 mg/kg; PO; once daily), or combinatorial MI-503 and Quizartinib (n=5 mice/group). The treatment period is displayed in blue. The Log-rank (Mantel-Cox) test was used to calculate p-values.

In summary, these data confirm that the combination of Menin-MLL and FLT3 inhibition substantially improves survival of mice with *MLL-r FLT3-ITD* positive leukemia compared to single-drug or vehicle-treated animals and supports this therapeutic concept as a synergistic approach against these leukemias.

## 4. Discussion

### 4.1. A necessity of combined treatment against AML

Intensive chemotherapy remains the backbone of curative treatment for patients suffering from AML<sup>9</sup>. However, this aggressive therapy can induce long-term remissions in only about half of the patients with *NPM1*<sup>mut</sup> AML and one-third of the patients with *MLL*-r AML<sup>12</sup>. An explanation for these relatively unsatisfactory survival rates is older age at diagnosis, the comorbidities and the presence of concurrent poor prognostic disease markers, such as the *FLT3*-ITD mutations<sup>89,105,126</sup>. These mutations are associated with treatment failure, relapse, and death<sup>85</sup>, and also represent important therapeutic targets. *FLT3* inhibitors were shown to increase survival rates in *de novo* as well as in relapsed or refractory AML<sup>110,111,127</sup> and potent, highly selective second-generation *FLT3* inhibitors can induce high response rates as single agents. However, without further consolidating treatment almost all patients relapse and ultimately succumb to their disease<sup>110,111</sup>.

There are several explanations why single-drug *FLT3* inhibition stays limited in its utilization. One of them is drug resistance to *FLT3* inhibitors, which can be detected in patients with *de novo* AML (primary resistance) or with secondary AML (acquired resistance) after initial treatment<sup>127</sup>. Mechanisms of resistance are heterogeneous, where primary resistance might be explained by differences in patient metabolism and genetic variation. It also can be caused by binding of *FLT3* inhibitors to unspecific proteins in plasma, inability of drugs to access the leukemic cells in bone marrow, persistent activation of *FLT3* downstream pathways and many other reasons<sup>127-129</sup>. Acquired resistance commonly develops due to new mutations (secondary mutations) within the *FLT3* gene or independent activation of *FLT3* downstream pathways in response to primary treatment with *FLT3* inhibitors<sup>127,130,131</sup>. Primary and acquired resistance to *FLT3* inhibitors remains a therapeutic challenge, and various research groups are working on understanding its mechanism in order to develop an improved treatment<sup>132</sup>.

Single-drug treatment might be limited because of other possible reasons as well. It is known that AML is commonly driven by multiple oncogenic mechanisms and not by a single *FLT3* mutation. Recent deep sequencing efforts found a median number of 5 and at least 2 genetic driver events to be present per AML case<sup>10</sup>. During AML evolution new various mutations may be acquired at a later time point, and some of them will act as active drivers in

disease progression<sup>10,11,133</sup>. These second mutations can be independent of initial mutations in AML or just appear downstream of the initial mutation. Emerged subclones with a new set of mutations can be resistant to the initial treatment, which makes therapy inefficient.

It is still debatable whether *FLT3*-ITD is considered an initial driver mutation or a secondary event. In general, *FLT3* mutations are believed to occur relatively late in leukemogenesis and may not be present in the founding leukemic clone of various AMLs<sup>134,135</sup>. However, this point is complicated by the fact that other studies demonstrated *FLT3* mutations to be present in leukemia stem cells (LSCs) of some AMLs<sup>136,137</sup>. For instance, it has been demonstrated that the knock-in of only *FLT3*-ITD in mice induced myeloproliferative neoplasm, but not leukemia, while being combined with another mutation *Nup98-HoxD13* (*NHD13*) resulted in leukemia progression<sup>138</sup>. As there is definitive evidence on when *FLT3*-ITD appears during leukemogenesis, it remains an open question what the specific mechanism behind detected resistance to *FLT3* inhibitors is. One of the possible scenarios is that *FLT3* inhibitors target the dominant *FLT3* mutant AML blast population but potentially not the AML founding clone, which also can be a *FLT3* wild type clone, from which relapse may originate<sup>139</sup>. Another possibility includes the acquisition of new driver mutations independent of the *FLT3*-ITD pathway after initial treatment of patients with *FLT3* inhibitors.

Due to the biologic heterogeneity of AML, it is generally not believed to be cured by single drug treatment<sup>140</sup>. On the other hand, the assumption of possible resistance to a single drug proposes a potential in combining *FLT3* inhibitors either with conventional treatment or with other inhibitors.

Here, I developed a synergistic treatment regimen that combines Menin-MLL and *FLT3* inhibitors to target leukemogenic gene expression in *NPM1*<sup>mut</sup> or *MLL*-r leukemia as well as activating *FLT3* mutations. The development of this approach was based on the previous findings that inhibition of the Menin-MLL interaction reverses leukemogenic gene expression in *NPM1*<sup>mut</sup> AML including the most pronounced *MEIS1* transcription factor and its putative transcriptional target gene *FLT3*<sup>75</sup>. Worth to mention, *MEIS1* has been shown to maintain stem cell self-renewal properties<sup>98,141</sup>. Furthermore, progenitors immortalized by co-expression of *MEIS1* and *HOXA9* transcription factors displayed characteristics of the leukemia-initiating stem cells, where *MEIS1* was proposed to maintain the survival of leukemic progenitors by activating HSC-specific genes such as *FLT3* and *CD34*<sup>98,141,142</sup>.

In a detailed assessment, I could also demonstrate that both, wild type and mutant *FLT3* transcript levels were consistently downregulated in response to MI-503 in *NPM1*<sup>mut</sup> and *MLL-r* AML models. Moreover, it has been shown that some of the mutations like the ones targeting signaling pathways and epigenetic regulators are mutually exclusive<sup>10</sup>, as mutations in the same pathway might not provide a survival advantage to the cell or the presence of both of them can have a negative effect on their selection<sup>143</sup>. Therefore, the concept of targeting different leukemic driver pathways by combining inhibition of Menin-MLL complex and FLT3 phosphorylation is of particular therapeutic interest as it also may apply enhanced pressure on mutant FLT3 targeting.

#### **4.2. Potential and limitations of combined Menin-MLL and FLT3 inhibition**

My data show a translational potential of combined Menin-MLL and FLT3 inhibition, yet some questions considering clinical efficiency remain unreciprocated as just human trials can reveal the possible application of proposed treatment in the future. Here, I show that Menin-MLL inhibition alone downregulates expression of both *FLT3* wild type and *FLT3*-ITD, as well as combined Menin-MLL and FLT3 inhibition downregulates pFLT3 and its downstream signaling. As FLT3 is known to participate in the regulation of stem and progenitor cell proliferation, overlapping toxicity of two drugs both targeting FLT3 might lead to the malfunctioning of patient bone marrow or even cause a myeloablation. Such a side effect can be observed in some cancer treatments<sup>144</sup>.

On the other hand, even though FLT3 inhibitors showed an obvious apoptotic effect *in vitro*, FLT3 inhibitors in clinical trials in contrast-induced differentiation over apoptosis<sup>145</sup>. Therefore, the combination of Menin-MLL with FLT3 inhibitors might theoretically cause differentiation syndrome (DS), which was previously described for patients with acute promyelocytic leukemia (APL) undergoing ATRA treatment<sup>146</sup>. The causes of DS are still unclear, but it might be associated with cytokine release from the differentiated myeloid cells<sup>147</sup>. In order to address these questions, more detailed studies, including human trials, have to be conducted in the future.

Another concern includes the possibility that FLT3 mutations might appear as a secondary event during leukemogenesis and therefore it would be interesting to clarify whether the combined Menin-MLL and FLT3 inhibition can eradicate more primitive leukemia cells.

Some previous studies defined leukemia-initiating cells as the ones, which can give rise to blast-like colonies and stay during serial replating<sup>148,149</sup>. Therefore, to address this question, I evaluated the effects of the Menin-MLL and FLT3 inhibition in colony-forming assays on 4 of the 5 primary AML patient samples harboring *NPM1* and *FLT3*-ITD mutations (subject #5 did not form colonies), as well as in the murine *Npm1<sup>CA/+</sup>Flt3<sup>ITD/+</sup>* AML cells in methylcellulose *in vitro* (compare chapter 3.5 and 3.10). It is of interest to note, that the FLT3 inhibitor Quizartinib either slightly suppressed blast colony formation or did not suppress it at all compared to the vehicle control, whereas Menin-MLL inhibition alone and especially combined with FLT3 inhibition dramatically abrogated blast colony formation together with replating capacity in all assessed human and murine AML samples. The mechanisms behind this observation remain to be determined in detailed *in vivo* studies assessing single and combined drug effects on the leukemia-initiating fraction in these leukemia subtypes.

Still, these results hint at the potential of combined treatment to target immature leukemia-initiating clones. In order to answer this question fully, further investigation is required with detailed engraftment studies to determine the presence or absence of *FLT3* mutations in leukemia stem cells (LSCs) and dosing experiments with the newly developed Menin-MLL inhibitors that have been shown to eradicate disease in animal models<sup>33,102</sup>.

On the other hand, it is possible that the selection of cells, whose proliferation is independent of the FLT3 mutant pathway, might develop resistance to FLT3 inhibitors<sup>139</sup>. Nevertheless, my data suggest that combined Menin-MLL and FLT3 inhibition may overcome resistance to a single-drug FLT3 inhibition, but only clinical trials will provide more definitive answers to these questions. Moreover, further characterization of dependency of Menin-MLL interaction in leukemia cells resistant to FLT3 inhibition should be performed.

Other alternatives in combination with Menin-MLL inhibition treatment also need to be evaluated in the future. In this work, *BCL2* was among the most depressed transcripts upon Menin-MLL inhibition, correlating with previously published data showing the direct binding of the MLL-fusion complex to *BCL2* gene<sup>150</sup>. As *BCL2* inhibitors have emerged as very effective treatment of AML<sup>151</sup>, combined Menin-MLL and *BCL2* inhibition constitutes another possible synergistic treatment strategy, which warrants further investigation.

### 4.3. Regulation of *FLT3* gene transcription

As *FLT3* is a transcriptional target gene of *MEIS1*<sup>53,63</sup>, *FLT3* downregulation upon Menin-MLL inhibition is therefore likely a result of the dramatically suppressed *MEIS1* expression. I also observed a decreased binding of Menin and MLL proteins to the *MEIS1* gene locus upon Menin-MLL inhibition, supporting the concept that disruption of the Menin-MLL complex shows a dramatic effect on *FLT3* expression, most probably via *MEIS1*.

Moreover, the ectopic expression of *Meis1* alone or together with *Hoxa9* in *Npm1*<sup>CA/+</sup>*Flt3*<sup>ITD/+</sup> leukemia cells showed an elevated level of the *Flt3* transcript. Furthermore, the anti-proliferative effect of the Menin-MLL inhibition alone or in a combination with the *FLT3* inhibitor was partially rescued upon *Meis1* and *Hoxa9* ectopic expression. However, the lack of complete restoration indicates additional alternative ways of *FLT3* gene regulation. *FLT3* expression may also be co-regulated by the transcription factors *PBX3*, *MYB*, or the CCAAT/enhancer-binding protein *C/EBPα* – known regulators of *FLT3*<sup>73,152</sup>. Interestingly, according to our RNA-seq data, Menin-MLL inhibition downregulates *PBX3* expression, but shows no effect on *MYB* and *C/EBPα* expression.

Therefore, Menin-MLL inhibitors are particularly attractive combination partners for inhibiting *FLT3*. They allow the effective targeting of a core leukemogenic gene expression program driven by *NPM1* mutations or MLL-fusions, including the transcription factors *MEIS1* and *PBX3*<sup>54,73,74</sup>, which play a role in *FLT3* gene expression. Our assessment of blast colony formation upon drug treatment is consistent with the view that Menin-MLL inhibition targets immature leukemia-initiating cells, most likely via suppression of the self-renewal associated *MEIS1*- and *PBX3*-driven gene expression.

### 4.4. *FLT3* targeting as the main mechanism behind Menin-MLL and *FLT3* synergism

To discover the potential mechanism behind the observed synergism of combined Menin-MLL and *FLT3* inhibition, I hypothesized it might function as a result of enhanced targeting of activated *FLT3* tyrosine receptor. Based on my results, I suggest that the Menin-MLL inhibitor targets *FLT3* gene expression, most likely via suppressing expression of the *MEIS1* transcription factor, therefore targeting *FLT3* on a transcriptional level, while the *FLT3* inhibitor blocks *FLT3* phosphorylation on a protein level. In order to confirm that the synergistic effects I observed with MI-503 and Quizartinib are not drug-dependent, I used the next-generation

Menin-MLL inhibitor VTP-50469 and the FLT3 inhibitor Gilteritinib. Even though Quizartinib is 10-fold more selective for targeting FLT3 than c-KIT<sup>153</sup>, I wanted to eliminate potential inhibition of c-KIT as the main mechanism of synergism considering that c-KIT also plays an important role in leukemogenesis<sup>154,155</sup>. Therefore, I used Gilteritinib, which is 800-fold more potent for targeting FLT3 over c-KIT and it was already approved for the treatment of relapsed/refractory *FLT3*-ITD AML in combination with standard chemotherapy in the U.S. and Europe<sup>111,156</sup>.

I have shown a decrease of FLT3 protein expression upon Menin-MLL inhibition by 2 independent methods, a flow cytometry-based assessment of FLT3 cell surface expression and immunoblotting. The reduction of FLT3 protein upon Menin-MLL inhibition most probably can be explained by transcriptional downregulation of *FLT3* gene expression after exposure to Menin-MLL inhibitors. I also observed an upregulation of FLT3 protein expression upon single-drug FLT3 inhibition in MV411 cells and no change in MOLM13 cells, while treatment with Menin-MLL or combinatorial treatment decreased the level of total FLT3 dramatically in both cell lines. This finding supports previously published data, showing an elevated expression of the FLT3 receptor tyrosine kinase in response to their inhibition by small molecules in MV411 cells and no change or slight downregulation of total FLT3 protein expression in MOLM13 cells<sup>157,158</sup>. I have also shown that the increased expression of FLT3 can be reversed with the addition of the Menin-MLL inhibitor. This finding suggests that the combination with Menin-MLL inhibitors may contribute to enhanced activity of FLT3 inhibitors, however, future studies are needed in order to determine if this concept may help to prevent or overcome resistance to FLT3 inhibition. Reduced total FLT3 levels were also associated with less pFLT3 that I observed upon Menin-MLL inhibition.

Altogether, this may explain the superior reduction of pFLT3 that I observed with the combination treatment compared to direct inhibition of pFLT3 with the FLT3 inhibitor or Menin-MLL inhibition alone.

#### **4.5. Role of STAT5 and ERK1/2 in AML**

As pFLT3 was dramatically abrogated upon combined Menin-MLL and FLT3 inhibition, I hypothesized that FLT3 downstream signaling might also be inhibited. To test this, I looked in more detail at JAK/STAT5 and RAS/ERK pathways, which are normally activated by ligand-

stimulated wildtype FLT3, and are also getting constitutively activated by FLT3-ITD during leukemogenesis<sup>90</sup>.

STAT5, represented by two homologous proteins STAT5A and STAT5B, plays an important role in the self-renewal and maintenance of hematopoietic stem and progenitor cells in normal hematopoiesis<sup>159</sup>, and its aberrant activation can potentially contribute to leukemia development<sup>160</sup>. Therefore, the pharmacological targeting of the STAT5 pathway represents a potential strategy for leukemia treatment<sup>161,162</sup>. As phosphorylation of STAT5 is commonly regulated via JAK tyrosine kinase activity, several JAK inhibitors have been clinically tested and one of them has already been approved by the FDA for treating myeloproliferative neoplasms<sup>163</sup>. Interestingly, even though several inhibitors targeting STAT5 have also been developed, none of them have been approved yet, and the number of clinical trials with STAT5 inhibitors is in general very limited<sup>164</sup>. Considering that FLT3-ITD can directly activate STAT5 in a JAK-independent manner<sup>165</sup>, it is of particular interest to directly target activated (phosphorylated) STAT5 in *FLT3*<sup>mut</sup> AML.

In this work, I showed that Menin-MLL inhibition downregulates both total STAT5 and activated pSTAT5 protein expression (Figure 3.8). While downregulation of pSTAT5 can be explained by its dependency on pFLT3 expression, which is also downregulated upon Menin-MLL inhibition, future studies are needed to assess how Menin-MLL inhibition influences total STAT5 expression. I also observed a decrease of pSTAT5 upon FLT3 inhibition, which is consistent with previously published data<sup>166</sup>. The combination of Menin-MLL and FLT3 inhibitors downregulated pSTAT5 protein expression in MV411 the most compared to the single-drug treatments, while the prominent abrogation of pSTAT5 upon Quizartinib treatment in MOLM13 was not further reduced in a combination with Menin-MLL inhibition.

Of note, the more pronounced decrease of pFLT3 upon combinatorial Menin-MLL and FLT3 inhibition also resulted in significantly enhanced suppression of STAT5A target genes in MV411 cells, such as *SPP1*, *BATF3*, *CBS*, *ADM*, *COCH*, *DDIT4*, *FGF11*, and *CCND2* (Figure 3.9). As STAT5A contributes to leukemia maintenance and is an important downstream mediator of activating *FLT3* mutations<sup>92,95,161</sup>, the synergistic anti-leukemic activity of combined Menin-MLL and FLT3 inhibition is likely caused by its enhanced on-target activity against FLT3 signaling.

These findings are of particular interest, as combined Menin-MLL and FLT3 inhibition might serve as an alternative way of targeting the STAT5 pathway, given the fact that high levels of pSTAT5 protein expression have been reported to represent a poor prognostic indicator in

newly diagnosed AML patients<sup>167</sup>. Moreover, considering the finding that Menin-MLL inhibition alone decreased STAT5 and pSTAT5 protein expression, it might be interesting to assess a potential combination of Menin-MLL and JAK inhibitors in future projects.

In this study, I demonstrated that another FLT3 downstream pathway – the RAS/ERK pathway – is affected by combined Menin-MLL and FLT3 inhibition. Impaired regulation of this pathway is important, as it has been shown to participate in abnormal cell proliferation, eventually leading to leukemia development<sup>168</sup>. Moreover, the aberrantly activated RAS/ERK pathway was reported to have an impact on the development of drug resistance in response to chemotherapy<sup>169</sup>. ERK1/2 regulates the activity of various substrates, including transcription factors, which can influence the expression of other genes responsible for proliferation and apoptosis<sup>169</sup>. Therefore, activated ERK1/2 is an important target in cancer treatment, and even though ERK inhibitors are actively being tested for treating solid tumors, there are just a few ERK inhibitors that undergo clinical trials for AML treatment<sup>170</sup>.

In our work, I observed that Quizartinib decreases pERK1/2 protein expression (Figure 3.8), which supports previously published data<sup>166</sup>. Interestingly, I also detected a slight decrease in pERK1/2 upon Menin-MLL inhibition assessed by flow cytometry, which might also reflect the decrease in pFLT3 protein level. The most pronounced decrease of pERK1/2 was observed upon combined Menin-MLL and FLT3 inhibition in both MOLM13 and MV411 cell lines (Figure 3.8). This finding can be potentially explained by enhanced inhibition of pFLT3 upon combined Menin-MLL and FLT3 inhibition, and therefore, supports our hypothesis that combined treatment affects the pFLT3 downstream pathways. Furthermore, BCL-2 expression has been shown to be regulated via the ERK1/2 pathway<sup>168</sup>. Considering that Menin-MLL inhibition downregulates the expression of the *BCL2* gene, and it also potentially might affect BCL-2 on the protein level, it would be interesting to investigate a potential combination of Menin-MLL and BCL-2 inhibitors in the future.

#### **4.6. The relation of Menin-MLL inhibition and *HOX* gene expression**

*MLL*-rearranged and *NPM1*<sup>mut</sup> AML subtypes are characterized by dysregulation of *HOX* gene expression, important for their self-renewal. Interestingly, *HOX* expression in AML is restricted to specific genes in the *HOXA* or *HOXB* loci, which is nearly identical to the expression signature of normal hematopoietic stem/progenitor cells (HSPCs) along with the expression of

*MEIS1* and *PBX3* genes<sup>171</sup>. The development of the first Menin-MLL inhibitors such as MI-2, MI-3<sup>28</sup>, and MI-2-2<sup>64</sup> showed an anti-leukemic effect with downregulation of *HOX* and *MEIS1* genes. However, despite previous results with these inhibitors, I observed that the HOX transcription factors were only moderately suppressed (*MLL-r* and murine *Npm1*<sup>CA/+</sup>*FIt3*<sup>ITD/+</sup>) or unchanged (human *NPM1*<sup>mut</sup> OCI-AML3) upon treatment with the later-developed Menin-MLL inhibitor – MI-503. This is consistent with findings from recent studies assessing novel and even more selective Menin-MLL inhibitors, such as VTP-50469 and MI-3454, that downregulated the expression of some MLL-fusion target genes, including *MEIS1* and *PBX3*, in all human and murine leukemia models<sup>33,34,102</sup>. Whereas, *HOX* gene expression was less sensitive to Menin-MLL inhibition in the same leukemia models<sup>33,34</sup>. These findings are also in line with the observation that MLL-fusion occupancy was not globally displaced from chromatin upon pharmacological inhibition of Menin-MLL interaction as well as knockdown of *MEN1*, and it rather was lost only on a subset of genes, including *MEIS1*, *MEF2C* and *JMJD1C* loci, but not *HOXA*<sup>33</sup>. Of note, Menin-MLL inhibition caused a global loss of Menin binding to chromatin<sup>33</sup>.

Considering the known dependencies of *MLL-r* and *NPM1*<sup>mut</sup> leukemia subtypes on *HOX* expression and their sensitivity to Menin-MLL inhibition, which does not affect *HOX* gene expression uniformly, the exact mechanism behind the different responses at those specific loci remains unclear. It has been shown that the two novel Menin-MLL inhibitors dramatically suppress a core transcriptional program which includes *MEIS1*<sup>33,34,102</sup>. Additionally, another study has shown that mice being transduced with cells overexpressing *Hoxa9* and *Meis1* resulted in a more aggressive AML leading to shorter overall survival compared to the mice having cells overexpressing just *Hoxa9*<sup>172</sup>. Together these data give a hint that *MEIS1* may play one of the key roles in those leukemia subtypes by promoting the expression of genes associated with HSC and LSC cells, including *FLT3*<sup>98,141</sup>. It will be also interesting to see in future studies if a strong anti-leukemic effect observed upon Menin-MLL inhibition can be correlated with a consistent and dramatic downregulation of *MEIS1* expression. It is still unclear why *HOX* expression, important for maintaining *MLL-r* and *NPM1*<sup>mut</sup> leukemias, is not as sensitive to Menin-MLL inhibition as *MEIS1* expression. Speculating about the potential link between *MEIS1* and *HOX* transcription factors in *MLL-r* and *NPM1*<sup>mut</sup> leukemias, it has been suggested that other *HOX* transcription factors might be critically dependent on their co-factor *MEIS1* in promoting leukemogenesis<sup>171</sup>. However, this hypothesis has to be validated in future studies. Therefore,

targeting MEIS1 represents a very appealing therapy in AML, even though it is currently undruggable.

#### 4.7. Model of combined Menin-MLL and FLT3 inhibition

Here, I propose a model of how Menin-MLL and FLT3 inhibition synergizes to target leukemic cells (Figure 4.1). The Menin-MLL inhibitor blocks the interaction between these proteins, leading to decreased binding of both Menin and MLL protein to the *MEIS1* gene, and also causes its downregulation. As *MEIS1* is one of the transcription factors known to play a role in the regulation of *FLT3* gene expression, inhibition of Menin-MLL interaction downregulates *FLT3* gene expression via *MEIS1*. As a consequence, decreased levels of total FLT3 protein as well as its active form, pFLT3, are observed. Additionally, FLT3 inhibitors, known for blocking the phosphorylation of FLT3, decrease the level of pFLT3 as well. Therefore, when Menin-MLL and FLT3 inhibitors are combined, they enhance abrogation of pFLT3 and, as a result, downregulate the downstream pathway of pFLT3 by decreasing pSTAT5 and pERK1/2 proteins and STAT5A-dependent gene expression. All this leads to synergistically decreased leukemia cell proliferation and leukemic gene expression.

Therefore, these data show that combined Menin-MLL and FLT3 inhibition may represent a novel and promising therapeutic strategy for patients with *NPM1*<sup>mut</sup> or *MLL-r* leukemia and concurrent *FLT3* mutation.

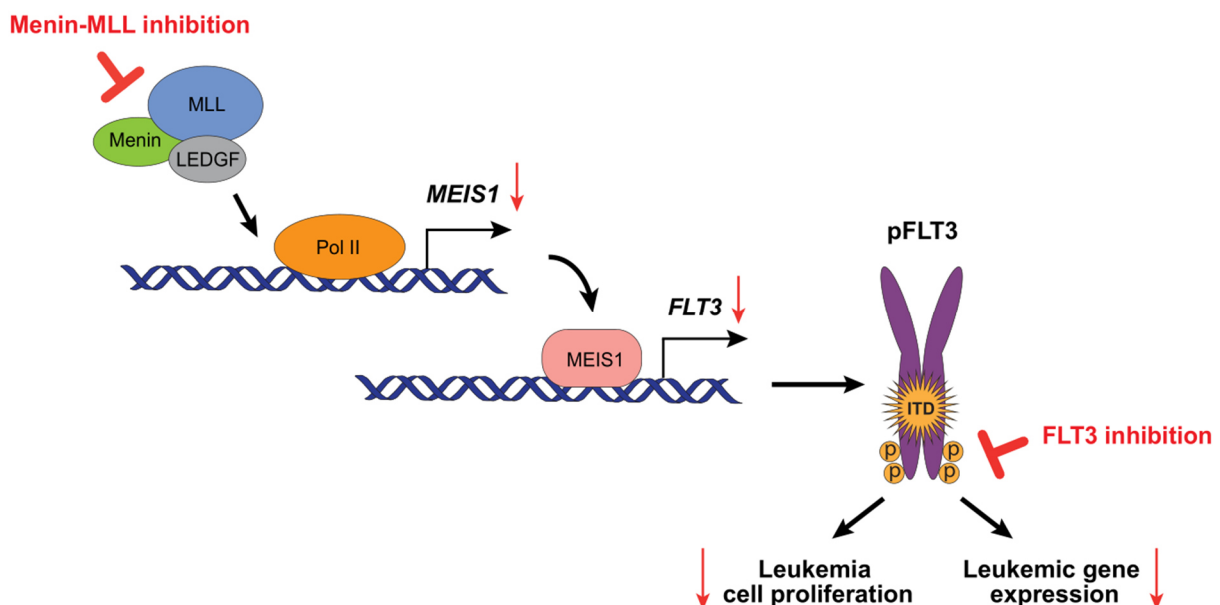


Figure 4.1. Schematic of the proposed mechanism of Menin-MLL and FLT3 inhibition.

## 5. References

1. Short NJ, Rytting ME, Cortes JE. Acute myeloid leukaemia. *Lancet* 2018;392:593-606.
2. Dohner H, Weisdorf DJ, Bloomfield CD. Acute Myeloid Leukemia. *N Engl J Med* 2015;373:1136-52.
3. Vardiman JW, Thiele J, Arber DA, et al. The 2008 revision of the World Health Organization (WHO) classification of myeloid neoplasms and acute leukemia: rationale and important changes. *Blood* 2009;114:937-51.
4. Arber DA, Orazi A, Hasserjian R, et al. The 2016 revision to the World Health Organization classification of myeloid neoplasms and acute leukemia. *Blood* 2016;127:2391-405.
5. Juliusson G, Antunovic P, Derolf A, et al. Age and acute myeloid leukemia: real world data on decision to treat and outcomes from the Swedish Acute Leukemia Registry. *Blood* 2009;113:4179-87.
6. Yamamoto JF, Goodman MT. Patterns of leukemia incidence in the United States by subtype and demographic characteristics, 1997-2002. *Cancer Causes Control* 2008;19:379-90.
7. De Kouchkovsky I, Abdul-Hay M. 'Acute myeloid leukemia: a comprehensive review and 2016 update'. *Blood Cancer J* 2016;6:e441.
8. Bennett JM, Catovsky D, Daniel MT, et al. Proposals for the classification of the acute leukaemias. French-American-British (FAB) co-operative group. *Br J Haematol* 1976;33:451-8.
9. Dohner H, Estey E, Grimwade D, et al. Diagnosis and management of AML in adults: 2017 ELN recommendations from an international expert panel. *Blood* 2017;129:424-47.
10. Cancer Genome Atlas Research N, Ley TJ, Miller C, et al. Genomic and epigenomic landscapes of adult de novo acute myeloid leukemia. *N Engl J Med* 2013;368:2059-74.
11. Kronke J, Bullinger L, Teleanu V, et al. Clonal evolution in relapsed NPM1-mutated acute myeloid leukemia. *Blood* 2013;122:100-8.
12. Papaemmanuil E, Gerstung M, Bullinger L, et al. Genomic Classification and Prognosis in Acute Myeloid Leukemia. *N Engl J Med* 2016;374:2209-21.
13. Tyner JW, Tognon CE, Bottomly D, et al. Functional genomic landscape of acute myeloid leukaemia. *Nature* 2018;562:526-31.
14. Chen SJ, Shen Y, Chen Z. A panoramic view of acute myeloid leukemia. *Nat Genet* 2013;45:586-7.
15. Bullinger L, Dohner K, Dohner H. Genomics of Acute Myeloid Leukemia Diagnosis and Pathways. *J Clin Oncol* 2017;35:934-46.
16. Dohner H, Estey EH, Amadori S, et al. Diagnosis and management of acute myeloid leukemia in adults: recommendations from an international expert panel, on behalf of the European LeukemiaNet. *Blood* 2010;115:453-74.
17. Dohner K, Schlenk RF, Habdank M, et al. Mutant nucleophosmin (NPM1) predicts favorable prognosis in younger adults with acute myeloid leukemia and normal cytogenetics: interaction with other gene mutations. *Blood* 2005;106:3740-6.
18. Green CL, Evans CM, Zhao L, et al. The prognostic significance of IDH2 mutations in AML depends on the location of the mutation. *Blood* 2011;118:409-12.

19. Marinello J, Delcuratolo M, Capranico G. Anthracyclines as Topoisomerase II Poisons: From Early Studies to New Perspectives. *Int J Mol Sci* 2018;19.
20. Rechkoblit O, Johnson RE, Buku A, Prakash L, Prakash S, Aggarwal AK. Structural insights into mutagenicity of anticancer nucleoside analog cytarabine during replication by DNA polymerase  $\epsilon$ . *Sci Rep* 2019;9:16400.
21. Schiller GJ. Evolving treatment strategies in patients with high-risk acute myeloid leukemia. *Leuk Lymphoma* 2014;55:2438-48.
22. Dombret H, Gardin C. An update of current treatments for adult acute myeloid leukemia. *Blood* 2016;127:53-61.
23. Winer ES, Stone RM. Novel therapy in Acute myeloid leukemia (AML): moving toward targeted approaches. *Ther Adv Hematol* 2019;10:2040620719860645.
24. Richard-Carpentier G, DiNardo CD. Single-agent and combination biologics in acute myeloid leukemia. *Hematology Am Soc Hematol Educ Program* 2019;2019:548-56.
25. Wouters BJ, Delwel R. Epigenetics and approaches to targeted epigenetic therapy in acute myeloid leukemia. *Blood* 2016;127:42-52.
26. Bewersdorf JP, Shallis R, Stahl M, Zeidan AM. Epigenetic therapy combinations in acute myeloid leukemia: what are the options? *Ther Adv Hematol* 2019;10:2040620718816698.
27. Stone RM, Mandrekar SJ, Sanford BL, et al. Midostaurin plus Chemotherapy for Acute Myeloid Leukemia with a FLT3 Mutation. *N Engl J Med* 2017;377:454-64.
28. Grembecka J, He S, Shi A, et al. Menin-MLL inhibitors reverse oncogenic activity of MLL fusion proteins in leukemia. *Nat Chem Biol* 2012;8:277-84.
29. Borkin D, He S, Miao H, et al. Pharmacologic inhibition of the Menin-MLL interaction blocks progression of MLL leukemia in vivo. *Cancer Cell* 2015;27:589-602.
30. Borkin D, Klossowski S, Pollock J, et al. Complexity of Blocking Bivalent Protein-Protein Interactions: Development of a Highly Potent Inhibitor of the Menin-Mixed-Lineage Leukemia Interaction. *J Med Chem* 2018;61:4832-50.
31. Borkin D, Pollock J, Kempinska K, et al. Property Focused Structure-Based Optimization of Small Molecule Inhibitors of the Protein-Protein Interaction between Menin and Mixed Lineage Leukemia (MLL). *J Med Chem* 2016;59:892-913.
32. He S, Malik B, Borkin D, et al. Menin-MLL inhibitors block oncogenic transformation by MLL-fusion proteins in a fusion partner-independent manner. *Leukemia* 2016;30:508-13.
33. Krivtsov AV, Evans K, Gadrey JY, et al. A Menin-MLL Inhibitor Induces Specific Chromatin Changes and Eradicates Disease in Models of MLL-Rearranged Leukemia. *Cancer Cell* 2019;36:660-73 e11.
34. Uckelmann HJ, Kim SM, Wong EM, et al. Therapeutic targeting of preleukemia cells in a mouse model of NPM1 mutant acute myeloid leukemia. *Science* 2020;367:586-90.
35. Barski A, Cuddapah S, Cui K, et al. High-resolution profiling of histone methylations in the human genome. *Cell* 2007;129:823-37.
36. Heintzman ND, Stuart RK, Hon G, et al. Distinct and predictive chromatin signatures of transcriptional promoters and enhancers in the human genome. *Nat Genet* 2007;39:311-8.
37. Schuettengruber B, Martinez AM, Iovino N, Cavalli G. Trithorax group proteins: switching genes on and keeping them active. *Nat Rev Mol Cell Biol* 2011;12:799-814.

38. Yang W, Ernst P. Distinct functions of histone H3, lysine 4 methyltransferases in normal and malignant hematopoiesis. *Curr Opin Hematol* 2017;24:322-8.
39. Yokoyama A, Cleary ML. Menin critically links MLL proteins with LEDGF on cancer-associated target genes. *Cancer Cell* 2008;14:36-46.
40. Yokoyama A, Somerville TC, Smith KS, Rozenblatt-Rosen O, Meyerson M, Cleary ML. The menin tumor suppressor protein is an essential oncogenic cofactor for MLL-associated leukemogenesis. *Cell* 2005;123:207-18.
41. Chen YX, Yan J, Keeshan K, et al. The tumor suppressor menin regulates hematopoiesis and myeloid transformation by influencing Hox gene expression. *Proc Natl Acad Sci U S A* 2006;103:1018-23.
42. Milne TA, Hughes CM, Lloyd R, et al. Menin and MLL cooperatively regulate expression of cyclin-dependent kinase inhibitors. *Proc Natl Acad Sci U S A* 2005;102:749-54.
43. El Ashkar S, Schwaller J, Pieters T, et al. LEDGF/p75 is dispensable for hematopoiesis but essential for MLL-rearranged leukemogenesis. *Blood* 2018;131:95-107.
44. Zhu L, Li Q, Wong SH, et al. ASH1L Links Histone H3 Lysine 36 Dimethylation to MLL Leukemia. *Cancer Discov* 2016;6:770-83.
45. Thirman MJ. Paradoxical Effects of MLL Paralogs in MLL-Rearranged Leukemia. *Cancer Cell* 2017;31:729-31.
46. Yang W, Ernst P. SET/MLL family proteins in hematopoiesis and leukemia. *Int J Hematol* 2017;105:7-16.
47. Ernst P, Wang J, Korsmeyer SJ. The role of MLL in hematopoiesis and leukemia. *Curr Opin Hematol* 2002;9:282-7.
48. Meyer C, Burmeister T, Groger D, et al. The MLL recombinome of acute leukemias in 2017. *Leukemia* 2018;32:273-84.
49. Marschalek R. Systematic Classification of Mixed-Lineage Leukemia Fusion Partners Predicts Additional Cancer Pathways. *Ann Lab Med* 2016;36:85-100.
50. Krivtsov AV, Armstrong SA. MLL translocations, histone modifications and leukaemia stem-cell development. *Nat Rev Cancer* 2007;7:823-33.
51. Slany RK. The molecular biology of mixed lineage leukemia. *Haematologica* 2009;94:984-93.
52. Armstrong SA, Staunton JE, Silverman LB, et al. MLL translocations specify a distinct gene expression profile that distinguishes a unique leukemia. *Nat Genet* 2002;30:41-7.
53. Brown FC, Still E, Koche RP, et al. MEF2C Phosphorylation Is Required for Chemotherapy Resistance in Acute Myeloid Leukemia. *Cancer Discov* 2018;8:478-97.
54. Guo H, Chu Y, Wang L, et al. PBX3 is essential for leukemia stem cell maintenance in MLL-rearranged leukemia. *Int J Cancer* 2017;141:324-35.
55. Placke T, Faber K, Nonami A, et al. Requirement for CDK6 in MLL-rearranged acute myeloid leukemia. *Blood* 2014;124:13-23.
56. Chan AKN, Chen CW. Rewiring the Epigenetic Networks in MLL-Rearranged Leukemias: Epigenetic Dysregulation and Pharmacological Interventions. *Front Cell Dev Biol* 2019;7:81.

57. Shen C, Jo SY, Liao C, Hess JL, Nikolovska-Coleska Z. Targeting recruitment of disruptor of telomeric silencing 1-like (DOT1L): characterizing the interactions between DOT1L and mixed lineage leukemia (MLL) fusion proteins. *J Biol Chem* 2013;288:30585-96.
58. Okada Y, Feng Q, Lin Y, et al. hDOT1L links histone methylation to leukemogenesis. *Cell* 2005;121:167-78.
59. Schubeler D, MacAlpine DM, Scalzo D, et al. The histone modification pattern of active genes revealed through genome-wide chromatin analysis of a higher eukaryote. *Genes Dev* 2004;18:1263-71.
60. Deshpande AJ, Deshpande A, Sinha AU, et al. AF10 regulates progressive H3K79 methylation and HOX gene expression in diverse AML subtypes. *Cancer Cell* 2014;26:896-908.
61. Chen Y, Anastassiadis K, Kranz A, et al. MLL2, Not MLL1, Plays a Major Role in Sustaining MLL-Rearranged Acute Myeloid Leukemia. *Cancer Cell* 2017;31:755-70 e6.
62. Tang G, Lu X, Wang SA, et al. Homozygous inv(11)(q21q23) and MLL gene rearrangement in two patients with myeloid neoplasms. *Int J Clin Exp Pathol* 2014;7:3196-201.
63. Mishra BP, Zaffuto KM, Artinger EL, et al. The histone methyltransferase activity of MLL1 is dispensable for hematopoiesis and leukemogenesis. *Cell Rep* 2014;7:1239-47.
64. Shi A, Murai MJ, He S, et al. Structural insights into inhibition of the bivalent menin-MLL interaction by small molecules in leukemia. *Blood* 2012;120:4461-9.
65. Falini B, Mecucci C, Tiacci E, et al. Cytoplasmic nucleophosmin in acute myelogenous leukemia with a normal karyotype. *N Engl J Med* 2005;352:254-66.
66. Borer RA, Lehner CF, Eppenberger HM, Nigg EA. Major nucleolar proteins shuttle between nucleus and cytoplasm. *Cell* 1989;56:379-90.
67. Savkur RS, Olson MO. Preferential cleavage in pre-ribosomal RNA by protein B23 endoribonuclease. *Nucleic Acids Res* 1998;26:4508-15.
68. Maggi LB, Jr., Kuchenruether M, Dadey DY, et al. Nucleophosmin serves as a rate-limiting nuclear export chaperone for the Mammalian ribosome. *Mol Cell Biol* 2008;28:7050-65.
69. Wang W, Budhu A, Forgues M, Wang XW. Temporal and spatial control of nucleophosmin by the Ran-Crm1 complex in centrosome duplication. *Nat Cell Biol* 2005;7:823-30.
70. Box JK, Paquet N, Adams MN, et al. Nucleophosmin: from structure and function to disease development. *BMC Mol Biol* 2016;17:19.
71. Federici L, Falini B. Nucleophosmin mutations in acute myeloid leukemia: a tale of protein unfolding and mislocalization. *Protein Sci* 2013;22:545-56.
72. Verhaak RG, Goudswaard CS, van Putten W, et al. Mutations in nucleophosmin (NPM1) in acute myeloid leukemia (AML): association with other gene abnormalities and previously established gene expression signatures and their favorable prognostic significance. *Blood* 2005;106:3747-54.
73. Garcia-Cuellar MP, Steger J, Fuller E, Hetzner K, Slany RK. Pbx3 and Meis1 cooperate through multiple mechanisms to support Hox-induced murine leukemia. *Haematologica* 2015;100:905-13.

74. Li Z, Chen P, Su R, et al. PBX3 and MEIS1 Cooperate in Hematopoietic Cells to Drive Acute Myeloid Leukemias Characterized by a Core Transcriptome of the MLL-Rearranged Disease. *Cancer Res* 2016;76:619-29.
75. Kuhn MW, Song E, Feng Z, et al. Targeting Chromatin Regulators Inhibits Leukemogenic Gene Expression in NPM1 Mutant Leukemia. *Cancer Discov* 2016;6:1166-81.
76. Adolfsson J, Mansson R, Buza-Vidas N, et al. Identification of Flt3+ lympho-myeloid stem cells lacking erythro-megakaryocytic potential a revised road map for adult blood lineage commitment. *Cell* 2005;121:295-306.
77. Verstraete K, Savvides SN. Extracellular assembly and activation principles of oncogenic class III receptor tyrosine kinases. *Nat Rev Cancer* 2012;12:753-66.
78. Levis M, Small D. FLT3: ITDoes matter in leukemia. *Leukemia* 2003;17:1738-52.
79. Kiyoi H, Ohno R, Ueda R, Saito H, Naoe T. Mechanism of constitutive activation of FLT3 with internal tandem duplication in the juxtamembrane domain. *Oncogene* 2002;21:2555-63.
80. Takahashi S. Downstream molecular pathways of FLT3 in the pathogenesis of acute myeloid leukemia: biology and therapeutic implications. *J Hematol Oncol* 2011;4:13.
81. Weis TM, Marini BL, Bixby DL, Perissinotti AJ. Clinical considerations for the use of FLT3 inhibitors in acute myeloid leukemia. *Crit Rev Oncol Hematol* 2019;141:125-38.
82. Pratz KW, Levis M. How I treat FLT3-mutated AML. *Blood* 2017;129:565-71.
83. Levis M. FLT3 mutations in acute myeloid leukemia: what is the best approach in 2013? *Hematology Am Soc Hematol Educ Program* 2013;2013:220-6.
84. Boddu P, Kantarjian H, Borthakur G, et al. Co-occurrence of FLT3-TKD and NPM1 mutations defines a highly favorable prognostic AML group. *Blood Adv* 2017;1:1546-50.
85. Kottaridis PD, Gale RE, Frew ME, et al. The presence of a FLT3 internal tandem duplication in patients with acute myeloid leukemia (AML) adds important prognostic information to cytogenetic risk group and response to the first cycle of chemotherapy: analysis of 854 patients from the United Kingdom Medical Research Council AML 10 and 12 trials. *Blood* 2001;98:1752-9.
86. Schnittger S, Bacher U, Haferlach C, Alpermann T, Kern W, Haferlach T. Diversity of the juxtamembrane and TKD1 mutations (exons 13-15) in the FLT3 gene with regards to mutant load, sequence, length, localization, and correlation with biological data. *Genes Chromosomes Cancer* 2012;51:910-24.
87. Whitman SP, Ruppert AS, Radmacher MD, et al. FLT3 D835/I836 mutations are associated with poor disease-free survival and a distinct gene-expression signature among younger adults with de novo cytogenetically normal acute myeloid leukemia lacking FLT3 internal tandem duplications. *Blood* 2008;111:1552-9.
88. Yamamoto Y, Kiyoi H, Nakano Y, et al. Activating mutation of D835 within the activation loop of FLT3 in human hematologic malignancies. *Blood* 2001;97:2434-9.
89. Gale RE, Green C, Allen C, et al. The impact of FLT3 internal tandem duplication mutant level, number, size, and interaction with NPM1 mutations in a large cohort of young adult patients with acute myeloid leukemia. *Blood* 2008;111:2776-84.
90. Stirewalt DL, Radich JP. The role of FLT3 in haematopoietic malignancies. *Nat Rev Cancer* 2003;3:650-65.

91. Hayakawa F, Towatari M, Kiyoi H, et al. Tandem-duplicated Flt3 constitutively activates STAT5 and MAP kinase and introduces autonomous cell growth in IL-3-dependent cell lines. *Oncogene* 2000;19:624-31.
92. Zhang S, Fukuda S, Lee Y, et al. Essential role of signal transducer and activator of transcription (Stat)5a but not Stat5b for Flt3-dependent signaling. *J Exp Med* 2000;192:719-28.
93. Choudhary C, Schwable J, Brandts C, et al. AML-associated Flt3 kinase domain mutations show signal transduction differences compared with Flt3 ITD mutations. *Blood* 2005;106:265-73.
94. Okada K, Nogami A, Ishida S, et al. FLT3-ITD induces expression of Pim kinases through STAT5 to confer resistance to the PI3K/Akt pathway inhibitors on leukemic cells by enhancing the mTORC1/Mcl-1 pathway. *Oncotarget* 2018;9:8870-86.
95. Spiekermann K, Bagrintseva K, Schwab R, Schmieja K, Hiddemann W. Overexpression and constitutive activation of FLT3 induces STAT5 activation in primary acute myeloid leukemia blast cells. *Clin Cancer Res* 2003;9:2140-50.
96. Wander SA, Levis MJ, Fathi AT. The evolving role of FLT3 inhibitors in acute myeloid leukemia: quizartinib and beyond. *Ther Adv Hematol* 2014;5:65-77.
97. Huang Y, Sitwala K, Bronstein J, et al. Identification and characterization of Hoxa9 binding sites in hematopoietic cells. *Blood* 2012;119:388-98.
98. Wang GG, Pasillas MP, Kamps MP. Meis1 programs transcription of FLT3 and cancer stem cell character, using a mechanism that requires interaction with Pbx and a novel function of the Meis1 C-terminus. *Blood* 2005;106:254-64.
99. Andersson AK, Ma J, Wang J, et al. The landscape of somatic mutations in infant MLL-rearranged acute lymphoblastic leukemias. *Nat Genet* 2015;47:330-7.
100. Kuhn MW, Bullinger L, Groschel S, et al. Genome-wide genotyping of acute myeloid leukemia with translocation t(9;11)(p22;q23) reveals novel recurrent genomic alterations. *Haematologica* 2014;99:e133-5.
101. Lavalley VP, Baccelli I, Kros J, et al. The transcriptomic landscape and directed chemical interrogation of MLL-rearranged acute myeloid leukemias. *Nat Genet* 2015;47:1030-7.
102. Klossowski S, Miao H, Kempinska K, et al. Menin inhibitor MI-3454 induces remission in MLL1-rearranged and NPM1-mutated models of leukemia. *J Clin Invest* 2020;130:981-97.
103. Linch DC, Hills RK, Burnett AK, Khwaja A, Gale RE. Impact of FLT3(ITD) mutant allele level on relapse risk in intermediate-risk acute myeloid leukemia. *Blood* 2014;124:273-6.
104. Schlenk RF, Kayser S, Bullinger L, et al. Differential impact of allelic ratio and insertion site in FLT3-ITD-positive AML with respect to allogeneic transplantation. *Blood* 2014;124:3441-9.
105. Pratcorona M, Brunet S, Nomdedeu J, et al. Favorable outcome of patients with acute myeloid leukemia harboring a low-allelic burden FLT3-ITD mutation and concomitant NPM1 mutation: relevance to post-remission therapy. *Blood* 2013;121:2734-8.
106. Short NJ, Kantarjian H, Ravandi F, Daver N. Emerging treatment paradigms with FLT3 inhibitors in acute myeloid leukemia. *Ther Adv Hematol* 2019;10:2040620719827310.
107. Larrosa-Garcia M, Baer MR. FLT3 Inhibitors in Acute Myeloid Leukemia: Current Status and Future Directions. *Mol Cancer Ther* 2017;16:991-1001.

108. Knapper S, Burnett AK, Littlewood T, et al. A phase 2 trial of the FLT3 inhibitor lestaurtinib (CEP701) as first-line treatment for older patients with acute myeloid leukemia not considered fit for intensive chemotherapy. *Blood* 2006;108:3262-70.
109. Stone RM. What FLT3 inhibitor holds the greatest promise? *Best Pract Res Clin Haematol* 2018;31:401-4.
110. Cortes JE, Khaled S, Martinelli G, et al. Quizartinib versus salvage chemotherapy in relapsed or refractory FLT3-ITD acute myeloid leukaemia (QuANTUM-R): a multicentre, randomised, controlled, open-label, phase 3 trial. *Lancet Oncol* 2019;20:984-97.
111. Perl AE, Martinelli G, Cortes JE, et al. Gilteritinib or Chemotherapy for Relapsed or Refractory FLT3-Mutated AML. *N Engl J Med* 2019;381:1728-40.
112. Smith CC. The growing landscape of FLT3 inhibition in AML. *Hematology Am Soc Hematol Educ Program* 2019;2019:539-47.
113. Castro F, Dirks WG, Fahrnich S, Hotz-Wagenblatt A, Pawlita M, Schmitt M. High-throughput SNP-based authentication of human cell lines. *Int J Cancer* 2013;132:308-14.
114. Chou TC. Theoretical basis, experimental design, and computerized simulation of synergism and antagonism in drug combination studies. *Pharmacol Rev* 2006;58:621-81.
115. Livak KJ, Schmittgen TD. Analysis of relative gene expression data using real-time quantitative PCR and the 2<sup>-</sup>(-Delta Delta C(T)) Method. *Methods* 2001;25:402-8.
116. Loven J, Orlando DA, Sigova AA, et al. Revisiting global gene expression analysis. *Cell* 2012;151:476-82.
117. Subramanian A, Tamayo P, Mootha VK, et al. Gene set enrichment analysis: a knowledge-based approach for interpreting genome-wide expression profiles. *Proc Natl Acad Sci U S A* 2005;102:15545-50.
118. Dzama MM, Steiner M, Rausch J, et al. Synergistic Targeting of FLT3 Mutations in AML via Combined Menin-MLL and FLT3 Inhibition. *Blood* 2020.
119. Dovey OM, Chen B, Mupo A, et al. Identification of a germline F692L drug resistance variant in cis with Flt3-internal tandem duplication in knock-in mice. *Haematologica* 2016;101:e328-31.
120. Jetani H, Garcia-Cadenas I, Nerreter T, et al. CAR T-cells targeting FLT3 have potent activity against FLT3(-)ITD(+) AML and act synergistically with the FLT3-inhibitor crenolanib. *Leukemia* 2018;32:1168-79.
121. Weisberg E, Ray A, Nelson E, et al. Reversible resistance induced by FLT3 inhibition: a novel resistance mechanism in mutant FLT3-expressing cells. *PLoS One* 2011;6:e25351.
122. Zheng R, Bailey E, Nguyen B, et al. Further activation of FLT3 mutants by FLT3 ligand. *Oncogene* 2011;30:4004-14.
123. Razumovskaya E, Masson K, Khan R, Bengtsson S, Ronnstrand L. Oncogenic Flt3 receptors display different specificity and kinetics of autophosphorylation. *Exp Hematol* 2009;37:979-89.
124. Moharram SA, Shah K, Khanum F, Ronnstrand L, Kazi JU. The ALK inhibitor AZD3463 effectively inhibits growth of sorafenib-resistant acute myeloid leukemia. *Blood Cancer J* 2019;9:5.

125. Kelly LM, Yu JC, Boulton CL, et al. CT53518, a novel selective FLT3 antagonist for the treatment of acute myelogenous leukemia (AML). *Cancer Cell* 2002;1:421-32.
126. Schlenk RF, Dohner K, Krauter J, et al. Mutations and treatment outcome in cytogenetically normal acute myeloid leukemia. *N Engl J Med* 2008;358:1909-18.
127. Daver N, Schlenk RF, Russell NH, Levis MJ. Targeting FLT3 mutations in AML: review of current knowledge and evidence. *Leukemia* 2019;33:299-312.
128. Chu SH, Small D. Mechanisms of resistance to FLT3 inhibitors. *Drug Resist Updat* 2009;12:8-16.
129. Siendones E, Barbarroja N, Torres LA, et al. Inhibition of Flt3-activating mutations does not prevent constitutive activation of ERK/Akt/STAT pathways in some AML cells: a possible cause for the limited effectiveness of monotherapy with small-molecule inhibitors. *Hematol Oncol* 2007;25:30-7.
130. Piloto O, Wright M, Brown P, Kim KT, Levis M, Small D. Prolonged exposure to FLT3 inhibitors leads to resistance via activation of parallel signaling pathways. *Blood* 2007;109:1643-52.
131. Daver N, Cortes J, Ravandi F, et al. Secondary mutations as mediators of resistance to targeted therapy in leukemia. *Blood* 2015;125:3236-45.
132. Lam SSY, Leung AYH. Overcoming Resistance to FLT3 Inhibitors in the Treatment of FLT3-Mutated AML. *Int J Mol Sci* 2020;21.
133. Shlush LI, Zandi S, Mitchell A, et al. Identification of pre-leukaemic haematopoietic stem cells in acute leukaemia. *Nature* 2014;506:328-33.
134. Jan M, Snyder TM, Corces-Zimmerman MR, et al. Clonal evolution of preleukemic hematopoietic stem cells precedes human acute myeloid leukemia. *Sci Transl Med* 2012;4:149ra18.
135. Welch JS, Ley TJ, Link DC, et al. The origin and evolution of mutations in acute myeloid leukemia. *Cell* 2012;150:264-78.
136. Levis M, Murphy KM, Pham R, et al. Internal tandem duplications of the FLT3 gene are present in leukemia stem cells. *Blood* 2005;106:673-80.
137. Al-Mawali A, Gillis D, Lewis I. Immunoprofiling of leukemic stem cells CD34+/CD38-/CD123+ delineate FLT3/ITD-positive clones. *J Hematol Oncol* 2016;9:61.
138. Greenblatt S, Li L, Slape C, et al. Knock-in of a FLT3/ITD mutation cooperates with a NUP98-HOXD13 fusion to generate acute myeloid leukemia in a mouse model. *Blood* 2012;119:2883-94.
139. McMahon CM, Ferng T, Canaani J, et al. Clonal Selection with RAS Pathway Activation Mediates Secondary Clinical Resistance to Selective FLT3 Inhibition in Acute Myeloid Leukemia. *Cancer Discov* 2019;9:1050-63.
140. Engert A, Balduini C, Brand A, et al. The European Hematology Association Roadmap for European Hematology Research: a consensus document. *Haematologica* 2016;101:115-208.
141. Argiropoulos B, Yung E, Humphries RK. Unraveling the crucial roles of Meis1 in leukemogenesis and normal hematopoiesis. *Genes Dev* 2007;21:2845-9.

142. Wang GG, Pasillas MP, Kamps MP. Persistent transactivation by meis1 replaces hox function in myeloid leukemogenesis models: evidence for co-occupancy of meis1-pbx and hox-pbx complexes on promoters of leukemia-associated genes. *Mol Cell Biol* 2006;26:3902-16.
143. Murati A, Brecqueville M, Devillier R, Mozziconacci MJ, Gelsi-Boyer V, Birnbaum D. Myeloid malignancies: mutations, models and management. *BMC Cancer* 2012;12:304.
144. Galanis A, Levis M. Inhibition of c-Kit by tyrosine kinase inhibitors. *Haematologica* 2015;100:e77-9.
145. Sexauer A, Perl A, Yang X, et al. Terminal myeloid differentiation in vivo is induced by FLT3 inhibition in FLT3/ITD AML. *Blood* 2012;120:4205-14.
146. Breccia M, Latagliata R, Carmosino I, et al. Clinical and biological features of acute promyelocytic leukemia patients developing retinoic acid syndrome during induction treatment with all-trans retinoic acid and idarubicin. *Haematologica* 2008;93:1918-20.
147. Sanz MA, Montesinos P. How we prevent and treat differentiation syndrome in patients with acute promyelocytic leukemia. *Blood* 2014;123:2777-82.
148. Will B, Vogler TO, Narayanagari S, et al. Minimal PU.1 reduction induces a preleukemic state and promotes development of acute myeloid leukemia. *Nat Med* 2015;21:1172-81.
149. Shankar DB, Cheng JC, Kinjo K, et al. The role of CREB as a proto-oncogene in hematopoiesis and in acute myeloid leukemia. *Cancer Cell* 2005;7:351-62.
150. Godfrey L, Kerry J, Thorne R, et al. MLL-AF4 binds directly to a BCL-2 specific enhancer and modulates H3K27 acetylation. *Exp Hematol* 2017;47:64-75.
151. Ramsey HE, Fischer MA, Lee T, et al. A Novel MCL1 Inhibitor Combined with Venetoclax Rescues Venetoclax-Resistant Acute Myelogenous Leukemia. *Cancer Discov* 2018;8:1566-81.
152. Volpe G, Walton DS, Del Pozzo W, et al. C/EBPalpha and MYB regulate FLT3 expression in AML. *Leukemia* 2013;27:1487-96.
153. Zarrinkar PP, Gunawardane RN, Cramer MD, et al. AC220 is a uniquely potent and selective inhibitor of FLT3 for the treatment of acute myeloid leukemia (AML). *Blood* 2009;114:2984-92.
154. Malaise M, Steinbach D, Corbacioglu S. Clinical implications of c-Kit mutations in acute myelogenous leukemia. *Curr Hematol Malig Rep* 2009;4:77-82.
155. Wichmann C, Quagliano-Lo Coco I, Yildiz O, et al. Activating c-KIT mutations confer oncogenic cooperativity and rescue RUNX1/ETO-induced DNA damage and apoptosis in human primary CD34+ hematopoietic progenitors. *Leukemia* 2015;29:279-89.
156. Mori M, Kaneko N, Ueno Y, et al. Gilteritinib, a FLT3/AXL inhibitor, shows antileukemic activity in mouse models of FLT3 mutated acute myeloid leukemia. *Invest New Drugs* 2017;35:556-65.
157. Wu H, Wang A, Qi Z, et al. Discovery of a highly potent FLT3 kinase inhibitor for FLT3-ITD-positive AML. *Leukemia* 2016;30:2112-6.
158. Reiter K, Polzer H, Krupka C, et al. Tyrosine kinase inhibition increases the cell surface localization of FLT3-ITD and enhances FLT3-directed immunotherapy of acute myeloid leukemia. *Leukemia* 2018;32:313-22.

159. Schepers H, van Gosliga D, Wierenga AT, Eggen BJ, Schuringa JJ, Vellenga E. STAT5 is required for long-term maintenance of normal and leukemic human stem/progenitor cells. *Blood* 2007;110:2880-8.
160. Benekli M, Baer MR, Baumann H, Wetzler M. Signal transducer and activator of transcription proteins in leukemias. *Blood* 2003;101:2940-54.
161. Wingelhofer B, Maurer B, Heyes EC, et al. Pharmacologic inhibition of STAT5 in acute myeloid leukemia. *Leukemia* 2018;32:1135-46.
162. Brachet-Botineau M, Polomski M, Neubauer HA, et al. Pharmacological Inhibition of Oncogenic STAT3 and STAT5 Signaling in Hematopoietic Cancers. *Cancers (Basel)* 2020;12.
163. Sapre M, Tremblay D, Wilck E, et al. Metabolic Effects of JAK1/2 Inhibition in Patients with Myeloproliferative Neoplasms. *Sci Rep* 2019;9:16609.
164. Loh CY, Arya A, Naema AF, Wong WF, Sethi G, Looi CY. Signal Transducer and Activator of Transcription (STATs) Proteins in Cancer and Inflammation: Functions and Therapeutic Implication. *Front Oncol* 2019;9:48.
165. Choudhary C, Brandts C, Schwable J, et al. Activation mechanisms of STAT5 by oncogenic Flt3-ITD. *Blood* 2007;110:370-4.
166. Gunawardane RN, Nepomuceno RR, Rooks AM, et al. Transient exposure to quizartinib mediates sustained inhibition of FLT3 signaling while specifically inducing apoptosis in FLT3-activated leukemia cells. *Mol Cancer Ther* 2013;12:438-47.
167. Brady A, Gibson S, Rybicki L, et al. Expression of phosphorylated signal transducer and activator of transcription 5 is associated with an increased risk of death in acute myeloid leukemia. *Eur J Haematol* 2012;89:288-93.
168. Steelman LS, Abrams SL, Whelan J, et al. Contributions of the Raf/MEK/ERK, PI3K/PTEN/Akt/mTOR and Jak/STAT pathways to leukemia. *Leukemia* 2008;22:686-707.
169. Steelman LS, Franklin RA, Abrams SL, et al. Roles of the Ras/Raf/MEK/ERK pathway in leukemia therapy. *Leukemia* 2011;25:1080-94.
170. Germann UA, Furey BF, Markland W, et al. Targeting the MAPK Signaling Pathway in Cancer: Promising Preclinical Activity with the Novel Selective ERK1/2 Inhibitor BVD-523 (Ulixertinib). *Mol Cancer Ther* 2017;16:2351-63.
171. Gundry MC, Goodell MA, Brunetti L. It's All About MEIs: Menin-MLL Inhibition Eradicates NPM1-Mutated and MLL-Rearranged Acute Leukemias in Mice. *Cancer Cell* 2020;37:267-9.
172. Mohr S, Doebele C, Comoglio F, et al. Hoxa9 and Meis1 Cooperatively Induce Addiction to Syk Signaling by Suppressing miR-146a in Acute Myeloid Leukemia. *Cancer Cell* 2017;31:549-62 e11.







## 7. Appendix

### 7.1. List of Abbreviations

<b>Abbreviation</b>	<b>Explanation</b>
°C	Degree Celsius
µg	Microgram
µl	Microliter
µm	Micrometer
µM	Micromolar
A/G	Immunoglobulin binding domains of both protein A and protein G
AF1Q	MLLT11 transcription factor 7 cofactor
AF4	AF4/FMR2 family member 1
AF6	Afadin, adherens junction formation factor
AF9	MLLT3 super elongation complex subunit
AF10	MLLT10 histone lysine methyltransferase DOT1L cofactor
AKT	A serine-threonine protein kinase
Allo-HSCT	Allogeneic hematopoietic stem cell transplantation
AML	Acute myeloid leukemia
APL	Acute promyelocytic leukemia
AR	Allelic ratio
ATP	Adenosine triphosphate
APC	Allophycocyanin
AraC	Cytosine arabinoside
ATRA	All-trans retinoic acid
β2M	β2 microglobulin
BCL-2	B-cell CLL/Lymphoma
BM	Bone marrow
bp	Base pairs
BSA	Bovine serum albumin
C/EBP-α	CCAAT enhancer binding protein alpha
CD	Cluster of differentiation
cDNA	Complementary DNA

ChIP	Chromatin Immunoprecipitation
CI	Combination index
c-Kit	A tyrosine-protein kinase, SCF receptor
C-terminal	Carboxy-terminal
CR	Complete remission
CSF1R	Colony stimulating factor 1 receptor
DAPI	4',6-diamidino-2-phenylindole
DMEM	Dulbecco's Modified Eagle's Medium
DMSO	Dimethyl sulfoxide
DNA	Deoxyribonucleic acid
DNMT	DNA methyltransferase
dNTP	Deoxynucleotide triphosphate
DOT1L	DOT1 Like Histone Lysine Methyltransferase
DPBS	Dulbecco's phosphate buffered saline
DS	Differentiation syndrome
ECL	Enhanced chemiluminescence
EDTA	Ethylenediaminetetraacetic acid
ENL	MLLT1 super elongation complex subunit
ELN	European LeukemiaNet
ELL	Elongation factor for RNA polymerase II
EPS15	Epidermal growth factor receptor pathway substrate 15
ERK1/2	Extracellular signal-regulated kinases 1 and 2
ERCC	External RNA control consortium
EZH2	Enhancer of Zeste 2 Polycomb Repressive Complex 2 Subunit
F	Forward
F692L	Substitution mutation in position 692, Phenylalanine (F) to Leucine (L)
FAB	French-American-British
FACS	Fluorescence-activated cell sorting
FBS	Fetal Bovine Serum
FDA	Federal Drug Association
FITC	Fluorescein isothiocyanate
FLT3	Fms related receptor tyrosine kinase 3

FLT3L	FLT3 ligand
GAPDH	Glyceraldehyde-3-phosphate dehydrogenase
G-CSF	Granulocyte colony-stimulating factor
GO	Gene Ontology
GSEA	Gene Set Enrichment Analysis
h	Hour(s)
H <sub>2</sub> O	Water
H3K4	4 <sup>th</sup> lysine residue of the histone H3 protein
H3K4me	Methylation at the 4 <sup>th</sup> lysine residue of the histone H3 protein
H3K79	79 <sup>th</sup> lysine residue of the histone H3 protein
H3K79me	Methylation at the 79 <sup>th</sup> lysine residue of the histone H3 protein
HEPES	4-(2-Hydroxyethyl)piperazine-1-ethanesulfonic acid
HOX	Homeobox
HOXA9	Homeobox protein Hox-A9
HRP	Horseradish peroxidase
HSC	Hematopoietic stem cells
IC <sub>50</sub>	The half maximal inhibitory concentration
ID	Identifier
IgG	Immunoglobulin G
IMDM	Iscove's Modified Dulbecco's Media
IL-3	Interleukin-3
IL-6	Interleukin-6
IP	Intraperitoneal
ITD	Internal tandem duplication
KCl	Potassium chloride
kDa	Kilodalton
KH <sub>2</sub> PO <sub>4</sub>	Potassium dihydrogenphosphate
LEDGF	Lens epithelium-derived growth factor
L-glu	L-glutamine
LiCl	Lithium chloride
LSC	Leukemic stem cells
M	Molar

MDS	Myelodysplastic syndrome
MEF2C	Myocyte Enhancer Factor 2C
MEIS1	Meis homeobox 1
Menin	Multiple endocrine neoplasia type 1
MEM-alpha	Minimum essential medium alpha
MES	2-(N-morpholino)ethanesulfonic acid
mg	Milligram
min	Minute(s)
ml	Milliliter
MLL	Histone-lysine N-methyltransferase 2A (KMT2A)
MLL-r	MLL-rearrangement/ MLL-rearranged
mM	Millimolar
MOPS	3-(N-morpholino)propanesulfonic acid
mRNA	Messenger RNA
MYB	MYB proto-oncogene, transcription factor
NaCl	Sodium chloride
Na <sub>2</sub> HPO <sub>4</sub>	Sodium hydrogenphosphate
NES	Normalized enrichment score
NGS	Next generation sequencing
NHD13	NUP98-HOXD13 fusion gene
nM	Nanomolar
NOS	Not otherwise specified
NPM1	Nucleophosmin 1
NSG	NOD.Cg-Prkdc <sup>scid</sup> Il2rg <sup>tm1Wjl</sup> / SzJ
O/N	Over night
OS	Overall survival
PBS	Phosphate-buffered saline
PBX3	Pre-B-cell leukemia transcription factor 3
PCR	Polymerase chain reaction
PEG	Polyethylene glycol
Pen	Penicillin
pERK1/2	Phosphorylated extracellular signal-regulated kinases 1 and 2

PI3K	Phosphoinositide 3-kinase
PO	Peroral
pSTAT5	Phosphorylated signal transducer and activator of transcription 5
PDGFR $\alpha/\beta$	Platelet derived growth factor receptor alpha and beta
PTD	Partial tandem duplication
RBC	Red Blood Cells lysis buffer
R	Reverse
RIPA	Radioimmunoprecipitation assay buffer
RNA	Ribonucleic acid
RNase	Ribonuclease
RNA-seq	RNA-sequencing
rpm	Revolutions per minute
RPMI	Roswell Park Memorial Institute cell culture medium
RT	Reverse transcriptase
SCF	Stem cell factor
SD	Standard deviation
SDS	Sodium dodecyl sulfate
SEC	Super elongation complex
shRNA	Short hairpin RNA
SOX2	(Sex determining region Y)-box 2
STAT5	Signal Transducer and Activator of Transcription 5
TBS	Tris-buffered saline
TBS-T	Tris-buffered saline with 0.1% Tween-20
TCGA	The Cancer Genome Atlas
TE	Tris-EDTA
TKD	Tyrosine kinase domain
TSS	Transcription start site
QRT-PCR	Quantitative real-time polymerase chain reaction
WBC	White blood cell
WHO	World Health Organization
WT	Wildtype

## 7.2. Table of common downregulated genes in MV411, MOLM13 and OCI-AML3

Genes	MV411		MOLM13		OCI-AML3	
	log2FC	p-value adj	log2FC	p-value adj	log2FC	p-value adj
<i>MEIS1</i>	-2.36487	2.09E-297	-2.19197	5.47E-99	-2.53756	0.00E+00
<i>ATF5</i>	-2.41757	1.41E-281	-0.93738	5.60E-19	-1.18624	1.60E-49
<i>GPT2</i>	-2.00330	2.25E-229	-1.00208	2.79E-28	-2.01887	0.00E+00
<i>PBX3</i>	-1.81533	7.28E-226	-3.23568	5.74E-264	-1.15466	1.17E-45
<i>SATB1</i>	-1.36293	6.75E-210	-1.19175	7.44E-47	-1.01670	2.30E-214
<i>SLC7A5</i>	-1.78214	2.23E-169	-1.14449	7.22E-39	-1.69952	0.00E+00
<i>MTHFD2</i>	-1.13216	6.08E-168	-0.86538	6.59E-24	-1.31142	0.00E+00
<i>BCAT1</i>	-1.91191	4.03E-133	-0.85047	8.65E-25	-1.79407	0.00E+00
<i>ASNS</i>	-1.33215	1.11E-123	-1.25057	4.17E-39	-2.51860	0.00E+00
<i>IGF2BP2</i>	-1.05154	6.83E-119	-0.99694	5.47E-34	-1.54497	0.00E+00
<i>TXNIP</i>	-0.95540	6.89E-117	-1.58361	3.70E-74	-1.97657	0.00E+00
<i>SLC38A1</i>	-3.26454	1.65E-109	-0.98926	6.15E-34	-1.89654	0.00E+00
<i>GARS</i>	-1.11169	1.24E-105	-0.95702	4.62E-31	-1.54590	0.00E+00
<i>TARS</i>	-0.85145	1.64E-86	-0.80063	3.33E-26	-1.09786	0.00E+00
<i>SATB2</i>	-1.00295	9.49E-85	-1.66102	2.98E-76	-1.55676	0.00E+00
<i>FLT3</i>	-0.87325	1.00E-84	-1.13944	1.45E-51	-1.04349	7.93E-116
<i>SULF2</i>	-1.86134	1.45E-81	-1.30911	1.06E-02	-3.63477	7.39E-278
<i>SLC7A1</i>	-0.83677	5.81E-80	-0.85481	2.75E-22	-1.19074	3.81E-208
<i>PCK2</i>	-1.28897	5.94E-76	-0.95642	2.49E-26	-1.63137	0.00E+00
<i>PSAT1</i>	-1.90124	1.34E-67	-1.17550	1.78E-39	-2.66920	0.00E+00
<i>CDKN1B</i>	-1.05442	1.91E-67	-0.81282	7.56E-22	-0.89500	1.15E-118
<i>SLC3A2</i>	-0.85361	1.66E-64	-0.85389	2.83E-21	-0.99190	5.02E-154
<i>SLC1A5</i>	-0.87339	4.17E-64	-1.05879	2.61E-41	-1.05222	1.99E-157
<i>LONP1</i>	-0.89205	5.38E-58	-1.11312	4.17E-40	-0.99391	1.01E-134
<i>ADM2</i>	-3.46261	1.19E-52	-1.31803	2.05E-12	-3.72816	1.60E-273
<i>RUNX2</i>	-0.82203	1.27E-47	-0.86659	8.14E-16	-1.26944	3.60E-187
<i>CBS</i>	-1.39785	5.64E-34	-1.50841	5.06E-53	-0.91825	7.68E-120
<i>SATB2-AS1</i>	-2.05896	2.63E-33	-6.26839	1.69E-08	-1.73161	3.23E-55
<i>CHAC1</i>	-1.90580	6.03E-26	-1.44823	1.50E-12	-4.06656	0.00E+00
<i>STC2</i>	-3.20910	4.00E-24	-1.25586	1.52E-25	-3.96461	0.00E+00
<i>DDIT4</i>	-1.38788	5.91E-18	-1.79179	3.63E-95	-2.62054	0.00E+00
<i>BATF3</i>	-2.09532	5.47E-17	-1.70854	2.49E-25	-1.19448	9.33E-84
<i>TUBE1</i>	-0.84576	9.91E-16	-0.96730	3.60E-19	-1.45193	2.05E-159
<i>MAMDC4</i>	-0.87105	5.55E-10	-1.60853	1.18E-10	-0.80032	3.75E-33
<i>RHBDL3</i>	-3.33817	1.19E-09	-1.90164	7.75E-03	-2.67341	9.88E-29
<i>HSH2D</i>	-1.14129	3.37E-09	-1.16973	6.05E-14	-1.50488	1.14E-32

<i>GPR65</i>	-0.90801	2.80E-08	-0.81415	6.95E-09	-1.38843	2.88E-112
<i>KCNG1</i>	-0.96572	7.27E-07	-0.91892	3.72E-05	-1.87986	1.36E-27
<i>DCHS1</i>	-1.09370	7.31E-05	-0.84827	7.23E-02	-1.20297	1.85E-70
<i>ULBP1</i>	-2.20173	1.38E-04	-1.36362	5.91E-13	-1.31598	9.15E-27







